

AD642102

AD



TECHNICAL REPORT ECOM-01377-F

BALLISTIC WINDS STUDY

BEST AVAILABLE COPY

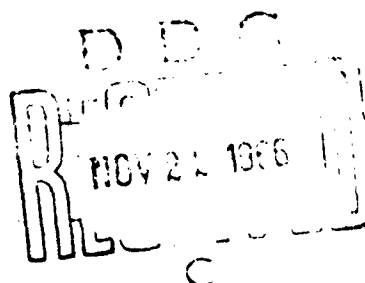
FINAL REPORT
REPORT NO. 4

By

FREDERICK P. OSTBY, JR.
JOSEPH P. PANDOLFO
KEITH W. VEIGAS
DAVID B. SPIEGLER

CLEARINGHOUSE	
FOR FEDERAL SCIENTIFIC AND TECHNICAL INFORMATION	
Hardcopy	Microfilm
\$3.00	\$0.65
147	pp

OCTOBER 1966



ECOM

UNITED STATES ARMY ELECTRONICS COMMAND • FORT MONMOUTH, N.J.

CONTRACT NO. DA 28-043 AMC-01377(E)

THE TRAVELERS RESEARCH CENTER, INC.
250 CONSTITUTION PLAZA, HARTFORD, CONNECTICUT 06103

DISTRIBUTION OF THIS DOCUMENT IS UNLIMITED

20040902001

October 1966

BALLISTIC WINDS STUDY

FINAL REPORT

1 June 1965 to 30 June 1966

Report No. 4

Contract No. DA-28-043-AMC-01377(E)

Project No. 1V0 25001-A-126-01

Prepared by

Frederick P. Ostby

Joseph P. Pandolfo

Keith W. Veigas

David B. Spiegler

THE TRAVELERS RESEARCH CENTER, INC.

250 Constitution Plaza

Hartford, Connecticut 06103

for

U.S. ARMY ELECTRONICS COMMAND

Fort Monmouth, N. J.

20164107
DISTRIBUTION OF THIS DOCUMENT IS UNLIMITED

ACKNOWLEDGMENTS

The authors wish to express their appreciation to Mr. Bernard Erickson, who supervised the entire data editing and error checking phase of the work and performed many of the subsequent calculations, and to Mrs. Ann Murphy and Messrs. G. Fisher and J. Welsh for their computer programming support. The cooperation and guidance of Messrs. M. Lowenthal, R. Bellucci, A. Barichivich, and J. Krieg, all of USASRDL, are also appreciated.

ABSTRACT

A three-dimensional objective analysis technique known as CRAM (Conditional Relaxation Analysis Method) was applied to investigate various properties of ballistic winds on a mesoscale in mountainous regions. From a 12-day sample of upper-air soundings taken 5 times a day at 2-hr intervals for 12 rawinsonde stations in the Ft. Huachuca region of southeastern Arizona, and artillery firings taken twice a day, CRAM analyses of temperature, density, and winds were performed for 10 atmospheric zones between the surface and 8,000 m using an IBM-7094.

It was determined that the CRAM technique produced fields which had the desirable features of map winds, i.e., the contour patterns were relatively smooth and varied slowly with time. The residual deflection errors which resulted were smaller for CRAM (75.2 m) than for a single station (Ft. Huachuca) near the firing range (85.1 m). It was also found that the time decay of ballistic winds in the firing area was smaller using CRAM than using the Ft. Huachuca observation, which implies that CRAM is a better tool with which to make a persistence forecast than a single station.

TABLE OF CONTENTS

<u>Section</u>	<u>Title</u>	<u>Page</u>
1.0	INTRODUCTION	1
2.0	DESIGN OF THE FIELD EXPERIMENT	3
3.0	DATA PROCESSING	6
3.1	Computation of Ballistic Quantities	6
3.1.1	Conventional Methods	6
3.1.2	Modified Methods	7
3.2	Preprocessing the Data	8
3.3	The CRAM Objective Analysis Procedure	10
3.3.1	The Analysis Grid	10
3.3.2	The Initial Guess	11
3.3.3	Correction Procedures (subroutines PCORR and TCORR)	12
3.3.4	Relaxation Methods	12
3.3.5	Smoothing (Subroutine SMOOTH)	14
3.3.6	Ballistic Computation	14
3.4	Production of Analyses by Application of CRAM	15
4.0	CALCULATION OF RESIDUAL ERRORS	27
4.1	Residual Errors Using CRAM and Ft. Huachuca Sounding	27
4.2	Comparison of Residual Errors	40
5.0	TIME VARIATIONS IN THE BALLISTIC WIND	64
5.1	Computation Procedure	64
5.1.1	Computations for Time Variability Studies	64
5.1.2	Input	65
5.1.3	Output	65
5.1.4	Computations	66
5.2	Time-variability as a Function of Lag	67
5.2.1	Variability of Line-10 Ballistic Winds	67
5.2.2	Comparison with Ft. Sill Experiment Results	70

<u>Section</u>	<u>Title</u>	<u>Page</u>
5.3	Spatial Distribution of Time-variability Parameters	73
5.3.1	Effects of Analysis Procedure on Computed rms Differences	73
5.3.2	Horizontal Distribution of Time Variability Parameters	73
5.3.3	Vertical Distribution of Time Variability Parameters	77
5.4	Hour-to-hour Range of Time Variability Parameters	81
6.0	SPATIAL VARIABILITY OF BALLISTIC WINDS	88
6.1	Areal Distribution of the rms Differences of Analyzed Ballistic Winds	88
6.2	A Comparison of Ballistic Winds Computed from Single Station and Analyzed Winds	89
6.3	Systematic Differences Between Single-station Ballistic Winds	89
6.4	Some Possible Orographic Effects for Low-level Ballistic Winds	90
6.5	Effect of Balloon Drift on Single-station Ballistic Wind Computations	91
7.0	WITHHELD DATA EXPERIMENT	105
8.0	PREDICTION EXPERIMENTS	109
8.1	Ballistic Wind Prediction	110
8.2	Artillery Corrections Based on Ballistic Wind Prediction Experiments	113
9.0	CONCLUSIONS AND RECOMMENDATIONS	124
10.0	REFERENCES	127
APPENDIX.	SYNOPTIC SITUATIONS FOR DAYS OF BALLISTIC WIND ANALYSES	129
DISTRIBUTION LIST		137

THIS DOCUMENT CONTAINED
BLANK PAGES THAT HAVE
BEEN DELETED

LIST OF ILLUSTRATIONS

<u>Figure</u>	<u>Title</u>	<u>Page</u>
2-1	Objective analysis grid showing observing stations	4
3-1	Zone-10 balloon displacements, 1400 MST, 25 January 1965	9
3-2	Ballistic wind analysis using CRAM: 0600 MST, 20 January 1965	17
3-3	Ballistic wind analysis using CRAM: 0800 MST, 20 January 1965	18
3-4	Ballistic wind analysis using CRAM: 1000 MST, 20 January 1965	19
3-5	Ballistic wind analysis using CRAM: 1200 MST, 20 January 1965	20
3-6	Ballistic wind analysis using CPAM: 1400 MST, 20 January 1965	21
3-7	Ballistic temperature and density analysis using CRAM: 0600 MST, 20 January 1965 (percent departure from Standard)	22
3-8	Ballistic temperature and density analysis using CRAM: 0800 MST, 20 January 1965 (percent departure from Standard)	23
3-9	Ballistic temperature and density analysis using CRAM: 1000 MST, 20 January 1965 (percent departure from Standard)	24
3-10	Ballistic temperature and density analysis using CRAM: 1200 MST, 20 January 1965 (percent departure from Standard)	25
3-11	Ballistic temperature and density analysis using CRAM: 1400 MST, 20 January 1965 (percent departure from Standard)	26
4-1	Range wind versus range error	62
4-2	Residual errors for artillery firings (Gun No. 1) based on CRAM and Ft. Huachuca (from Table 4-3)	63
5-1	Line-10 time variability, u-component	68
5-2	Line-10 time variability, v-component	69
5-3	Line-4 time variability, u-component	71
5-4	Line-4 time variability, v-component	72
5-5	Line-2 rms time differences, vector ($\tau = 2$)	74
5-6	Line-10 rms time differences, vector ($\tau = 2$)	75
5-7	Line-2 rms time differences, vector ($\tau = 8$)	76
5-8	Line-2 rms time differences, u-component ($\tau = 8$)	78
5-9	Line-2 rms time differences, v-component ($\tau = 8$)	79
5-10	Line-2 rms time differences, vector ($\tau = 2$)—based on selected grid points	80

<u>Figure</u>	<u>Title</u>	<u>Page</u>
5-11	Field-averaged time variability (vector), vertical profile	82
5-12	Field-averaged time variability (u-component), vertical profile	83
5-13	Single-station time variability (u-component), vertical profile	84
5-14	Field-averaged time variability (v-component), vertical profile	85
5-15	Single-station time variability (v-component), vertical profile	86
5-16	Range of variability for selected lags and lines, vector	87
6-1	Line-4 rms space differences, u-component (80 cases)	92
6-2	Line-4 rms space differences, v-component (80 cases)	93
6-3	Line-4 rms space differences, vector (80 cases)	94
6-4	Line-6 rms space differences, u-component (80 cases)	95
6-5	Line-6 rms space differences, v-component (80 cases)	96
6-6	Line-6 rms space differences, vector (80 cases)	97
6-7	Line-10 rms space differences, u-component (80 cases)	98
6-8	Line-10 rms space differences, v-component (80 cases)	99
6-9	Line-10 rms space differences, vector (80 cases)	100
6-10	Line-10 rms space differences, u- and v-components	101
6-11	Areas enclosing endpoints of balloon trajectories at Zone 10 for Benson (Areas A) and Tombstone (Areas B)	102
6-12	Line-2 rms space differences for selected grid points, u-component (80 cases)	103
6-13	Line-2 rms space differences for selected grid points, v-component (80 cases)	104
8-1	Ballistic wind prediction verification, Line 2	117
8-2	Ballistic wind prediction verification, Line 4	118
8-3	Ballistic wind prediction verification, Line 6	119
8-4	Ballistic wind prediction verification, Line 8	120
8-5	Ballistic wind prediction verification, Line 10	121
8-6	Vertical profile ballistic wind vector errors	122
8-7	Average residual deflection errors based on CRAM persistence	123

LIST OF TABLES

<u>Table</u>	<u>Title</u>	<u>Page</u>
2-1	Firing data	3
2-2	Meteorological stations in the Ft. Huachuca network	5
3-1	Zone structure and weighting factors for ballistic computations (maximum ordinate: 8,000 m)	7
4-1	Artillery corrections based on CRAM analysis	28
4-2	Artillery corrections based on Ft. Huachuca meteorological soundings	42
4-3	Comparison of residual errors using CRAM vs. single station (Ft. Huachuca), in meters	61
5-1	Distribution of wind differences computed by lag and terminal hour	64
7-1	Station observations used in withheld data experiments	106
7-2	Residual errors (in meters) using input data from single station (Ft. Huachuca) and CRAM analyses	107
8-1	Ballistic wind prediction experiment results using CRAM analyses	111
8-2	Residual deflection errors in meters using Line-10 ballistic winds for CRAM and Ft. Huachuca persistence and extrapolation	115
8-3	Average residual deflection errors (meters for prediction experiments	116

1.0 INTRODUCTION

In the general artillery firing problem it is necessary for the gunner to apply various corrections so that a round, or series of rounds, from his piece will come as near as possible to striking a preassigned target. There are two major factors in artillery correction problems. The first has to do mainly with characteristics of the weapon system being employed. These include projectile weight, powder temperature, muzzle velocity, and drift, and their investigation is essentially beyond the scope of this project. The second factor to be considered is the influence of the atmosphere through which the projectile travels. Of importance here are wind, temperature, and density. Although the method of registration (essentially a trial and error method of correcting subsequent shots based on results of previous ones, while firing a series of rounds) is possible in principle, it is not the most desirable tactically (the element of surprise may be of importance), practically (registration requires visual observation of the impact), or economically (it can be costly).

At present, the U.S. Army makes ballistic corrections for meteorological effects on an artillery projectile based on a single sounding method. An Artillery Metro Section launches a radiosonde and from the data computes a ballistic message which is provided to the gunner. This observation may be removed in both time and space from the projectile firing. Research results (Lowenthal, 1953, 1957) indicate that improved ballistic corrections can be obtained by use of multi-sounding data from which fields of wind, temperature, and density can be mapped. This so-called "map wind technique" has the desirable property that the analyzed fields are fairly smooth and slowly varying in time, and as such present a hopeful avenue for prognosis.

The objective of this program was to develop an automated objective analysis technique with emphasis on the mesoscale meteorological features to produce map winds, temperatures, and densities, which, when incorporated in an integrated metro message, would minimize the error from artillery firings made at the same time.

The research was to be conducted with a view toward providing the best possible answer to the following questions:

- (a) To what extent can artillery corrections be improved by using integrated map winds instead of a single sounding?

(b) How does mountainous terrain affect the variability of ballistic winds?

(c) What is the optimum placement and spacing of artillery metro sections in mountainous terrain?

(d) How often should soundings be made in mountainous terrain?

(e) How accurately, and for what duration, can map winds be forecast?

For this program, a field experiment was conducted at Ft. Huachuca in which multiple sounding data were taken concurrently with artillery firings for a number of days in January and February 1965. A detailed description of the field experiment is given in Section 2.0.

An analysis technique suited to the ballistic wind problem (called CRAM—Conditional Relaxation Analysis Method) was chosen as the primary investigatory tool. It is a technique that the contractor has had previous experience with and was extendable to three dimensions with relatively minor modifications. The technique is described in Section 3.0. The detailed program descriptions are contained in the supplement to this report.

While the advantages of map ballistic winds over single station ballistic winds, in principle, are readily apparent (cf. Lowenthal, 1953), an important evaluation criterion is how well a given technique performs when used for correcting actual artillery firings. This is discussed in Sections 4.0 and 7.0.

Questions concerning characteristics of the winds themselves, such as time and space variability and predictability, are discussed in Sections 5.0, 6.0, and 8.0.

2.0 DESIGN OF THE FIELD EXPERIMENT

Artillery firings were conducted at Ft. Huachuca, Arizona on 12 days during January and February, 1965 as part of this study. Two 8-inch howitzers were fired at 1000 MST and 1400 MST at targets approximately 14,500 m east-northeast from the gun locations. Each piece fired ten rounds alternately at one-minute intervals using fixed quadrant elevation angles and azimuths (see Table 2-1). Impact points were determined visually and the center-of-impact (CI) for the ten rounds from each piece was computed. The maximum ordinate of the projectiles was approximately 9700 m, or about 8200 m above the gun level.

Meteorological data were collected from a network of twelve rawinsonde stations surrounding the firing range (see Fig. 2-1). Soundings were taken 5 times a day at two-hour intervals beginning at 0600 MST, for even numbered days January 2-12, odd numbered days January 25-31, and even numbered days February 2-12, 1965. Thus, there were 16 days on which soundings were taken, or 80 observation times in all. The meteorological data were obtained using AN/GMD-1A equipment. The twelve meteorological stations for which rawinsonde data were collected are listed in Table 2-2.

The meteorological data were punched on cards and transferred to magnetic tape by the sponsoring agency using a Burroughs B-5000 Computer.

TABLE 2-1
FIRING DATA

Gun no.	Location*		Azimuth (mils)	Quadrant elev. (mils)
	Easting	Northing		
1	555472.8	3493987.7	1325.2	1114
2	555469.4	3494002.5	1322.8	1117

*Coordinates are based on the Universal Transverse Mercator Grid (Zone 12).

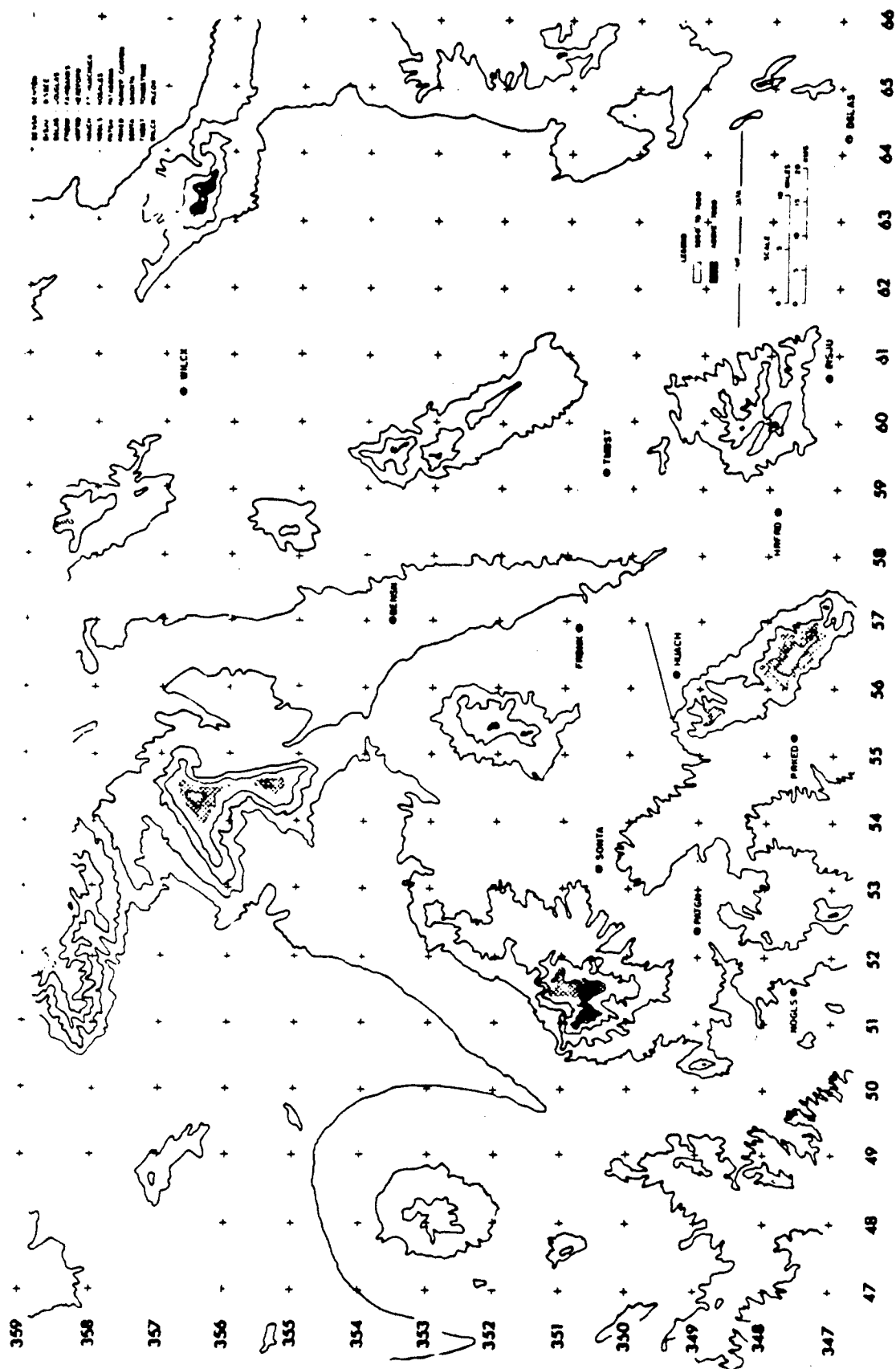


Fig. 2-1. Objective analysis grid showing observing stations. Grid units are based on the 10,000-m Universal Transverse Mercator Grid (Zone 12), with the last four digits of the grid numbers omitted.

TABLE 2-2
METEOROLOGICAL STATIONS IN THE FT. HUACHUCA NETWORK

Station	Easting(I)*	Northing(J)*	Elevation(m)
Benson	57.01	353.59	1083
Bisbee	60.68	347.01	1445
Douglas	64.10	346.82	1255
Fairbanks	56.81	350.92	1282
Hereford	58.62	347.72	1290
Ft. Huachuca	56.25	349.36	1433
Nogales	51.48	347.51	1190
Patagonia	52.40	348.95	1240
Parker Canyon	55.37	347.51	1685
Sonoita	53.29	350.41	1480
Tombstone	59.26	350.38	1450
Wilcox	60.49	356.73	1275

*Grid coordinates are based on the 10,000-meter Universal Transverse Mercator Grid (Zone 12).

3.0 DATA PROCESSING

The meteorological data described in the previous section needed considerable editing, error checking, calculation of additional variables, etc., before objective analysis methods could be employed. The procedures used were designed to be as consistent as possible with U.S. Army procedures for performing ballistic computations. The major difference between current practices and those adopted in this study was the referencing of meteorological zone data to a geographical location representative of the radiosonde's actual location, rather than the customary practice of assigning the launching station's geographical coordinates to a piece of meteorological information regardless of how far away from that station the balloon had subsequently drifted. Also taken into account in this study was the referencing of the balloon's height to the terrain over which it was passing, rather than to the elevation of the launch station.

3.1 Computation of Ballistic Quantities

3.1.1 Conventional Methods

Ballistic wind, temperature, and density are computed in order to apply artillery corrections using known unit effects from firing tables. To arrive at these ballistic quantities for a particular station, measurements of upper-air parameters are made by means of a radiosonde which is tracked by a rawin set (AN/GMD-1). The location of the balloon at each artillery zone limit (see Table 3-1), as projected to the earth's surface, is plotted on a plotting board. From these plots, the average wind speed and direction for each of the atmospheric zones is determined. The computation of these zone winds is a preliminary step in the determination of ballistic winds. The mean virtual temperature and mean density for each zone are also determined and presented in terms of percent of standard as referenced to mean standard zone density and temperature based on the ICAO (International Civil Aviation Organization) atmosphere. The zone values of wind, density, and temperature are then weighted according to specified zone weighting factors, with the resulting weighted quantities being the ballistic values. The weighting factors, developed by ballisticians, are used to establish the proportional effect of the meteorological conditions in each zone upon the total effect exerted by the atmosphere through which a projectile passes. Table 3-1 shows the weighting factors for the artillery problem in the Ft. Huachuca experiment where the maximum ordinate of the trajectory was in Zone 10 (these are known

TABLE 3-1
ZONE STRUCTURE AND WEIGHTING FACTORS FOR BALLISTIC
COMPUTATIONS (maximum ordinate: 8,000 m)

Zone	Height (m)		Weighting factors*		
	Base	Top	Wind	Temperature	Density
1	Surface	200	0.01	0.00	0.03
2	200	500	0.02	0.01	0.04
3	500	1000	0.02	0.02	0.07
4	1000	1500	0.04	0.02	0.07
5	1500	2000	0.03	0.03	0.07
6	2000	3000	0.07	0.07	0.13
7	3000	4000	0.08	0.13	0.12
8	4000	5000	0.09	0.22	0.11
9	5000	6000	0.09	0.23	0.11
10	6000	8000	0.55	0.27	0.25

*From FM 6-16, Tables for Artillery Meteorology.

as "Line 10" weighting factors). The zone values for Zones 1, 2, 3, ..., 10 are weighted and summed to arrive at the ballistic values for Line 10. When there is a difference in altitude between the artillery piece and the meteorological station, the temperature and density values are corrected using calculations based on the ICAO standard atmosphere. No effort is made to adjust the ballistic winds for such a height difference because there is no known specific relation between the speed and direction of the wind and this height difference.

3.1.2 Modified Methods

Objective analyses of individual atmospheric zones are required to construct analyzed fields of ballistic wind, temperature, and density. In preparing the data for analysis, it was decided to account for balloon drift such that data values for individual zones would be assigned horizontal coordinates based on the location of the balloon for the midpoint of the zone. When dealing with conventional synoptic-scale data it is customary to ignore balloon drift with altitude. However, for a mesoscale problem,

as pointed out by Fujita (1960), a significant error could result in the analyses of higher zones if it were assumed that the observations were representative of points directly above the launch sites. Figure 3-1 shows the displaced locations of the several radiosondes from their launch sites for the Ft. Huachuca network at 1400 MST on January 25, 1965 upon reaching the mid-level of Zone 10. Of particular importance is the fact that Zone 10 receives the largest weight in computing Line 10 ballistic winds. Note that all the balloons have moved to the east or southeast of Ft. Huachuca. The radiosonde launched at Ft. Huachuca is actually located nearly 10 km southeast of Hereford at Zone 10.

Another consideration in analyzing data from a multi-sounding network has to do with the manner in which height-above-terrain is handled. As stated above, zone winds are computed using the height above terrain rather than referencing observations to the height of the artillery piece. In this study, the terrain height at the location of the balloon, and not the terrain height at the launch site, was used in determining zone heights. This distinction can be significant in mountainous terrain, particularly for the lower zones.

3.2 Preprocessing the Data

The meteorological data contained on magnetic tapes represent approximately 900 radiosonde flights consisting of roughly 20 significant data levels each and 50 or so detailed wind data levels each, or about 240,000 relevant numbers on tape. With this quantity of data involved, certain gross error checking procedures are recommended. With the aid of the computer, the data were checked for such things as proper headings, station elevations, dates and times, etc. Routines which checked to assure that times and heights increased and pressures decreased monotonically were useful in uncovering bad data or data out of sequence. An additional test was made of times and heights based on the expected rate of balloon ascent. When this phase was completed, a relatively error-free meteorological data sample was available for additional processing.

The next phase consisted of the computation of zone winds, temperatures, and density from the raw data for each radiosonde flight. The zone winds were computed using the time and horizontal location at which the balloon entered the base of a

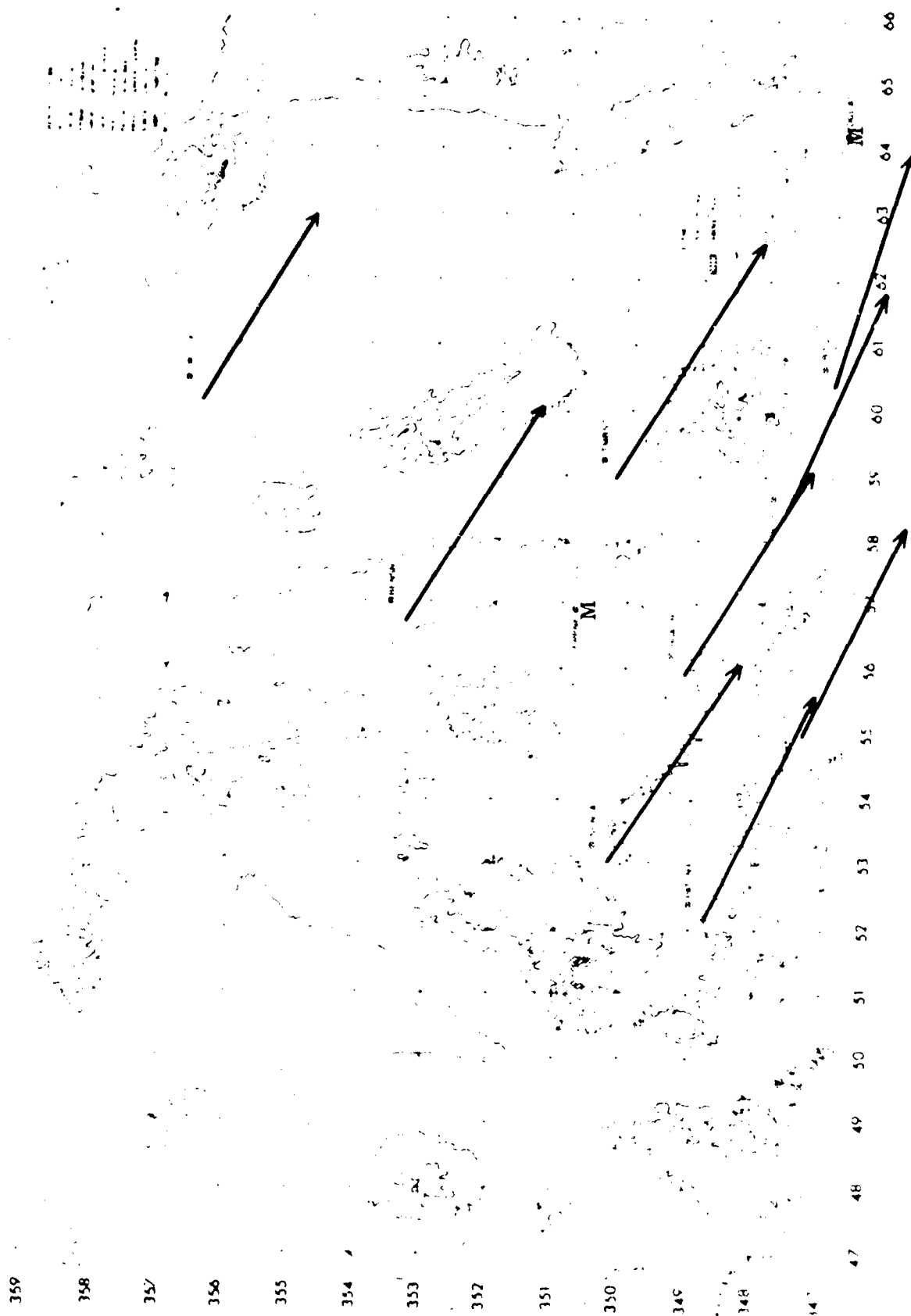


Fig. 3-1. Zone-10 balloon displacements, 1400 MST, 25 January 1965.

particular zone and similar information when the balloon reached the top of the zone. The mean virtual temperature for a zone was calculated from the significant level temperature and humidity data. Density was calculated from the equation of state using the mean virtual zone temperature and the pressure at the midpoint of the zone. Temperatures and densities were referenced to the ICAO standard atmosphere and expressed in terms of departure from standard in percent. The data were then ready for objective analysis.

3.3 The CRAM Objective Analysis Procedure

One objective of this study is to develop an automated objective analysis technique to produce map wind fields from which ballistic quantities may be estimated.

Objective analysis is concerned with defining the spatial distribution of a variable at a set of regularly spaced grid points given an irregularly spaced set of observations. The technique chosen for this study is one based on a generalized version of Carstensen's relaxation method (1962), which was developed and applied by Thomasell and Welsh (1963), called CRAM (the Conditional Relaxation Analysis Method). It is ideally suited to a three-dimensional analysis problem such as this one and is relatively fast from a computer time consideration.

In CRAM, the procedure for interpolating between observations requires that the analyzed grid-point values satisfy Poisson's equation, subject to the constraints imposed by the observations and an arbitrarily defined set of boundary values. The observations determine the analysis through their role as internal boundary points in the solution of Poisson's equation. Poisson's equation in finite-difference form is solved numerically by a relaxation procedure.

3.3.1 The Analysis Grid

The analysis grid is based on the Universal Transverse Mercator Grid system and is shown in Fig. 2-1. The horizontal grid spacing is 10 km. The I and J directions of the analysis grid are essentially east-west and north-south respectively. The analysis area consists of 17 grid units in the I-direction (from I = 50 to I = 66) and 15 grid units in the J-direction (from J = 345 to J = 359) or about 170 km x 150 km. The vertical coordinate (K) consists of the 10 atmospheric zones and is of variable spacing, being 250 m between Zones 1 and 2 and 1500 m between Zones 9 and 10.

Two additional zones—Zone "0" and Zone 11—are added to supply boundary values at the edges of the analysis volume.

Subsequent sections describe the various major components of CRAM: the initial guess technique, correction procedures, relaxation method, smoothing, and ballistic computation. Detailed program descriptions are contained in the supplement to this report.

3.3.2 The Initial Guess

CRAM requires the use of an initial-guess field, which undergoes subsequent corrections. In principle, the initial-guess field can be generated in a variety of ways. An accurate forecast of the field being analyzed makes the most ideal initial guess. Two rather reasonable approaches are to apply a surface-fitting technique to the data or to use a recent analysis (e.g., two hours earlier), if one is available, or some combination or "blend" of the two approaches. Our version of the program uses these surface fitting and persistence approaches.

In the surface fitting procedure, the three-dimensional surface is sought which best fits the observed field of data. The equation is of the form

$$\phi = a_0 + a_1x_1 + a_2x_2 + a_3x_3 + \dots + a_px_p \quad (3-1)$$

where the dependent variable ϕ is the variable to be analyzed over an evenly-spaced field of grid points, the a 's are the coefficients, and the x 's are the independent variables which are functions of the locations of the observations of ϕ , i.e., x , y , and z . Because there are a large number of terms that can be generated from the possible combinations of x , y , and z , many of which may not be significant in explaining the variability of ϕ , it seems reasonable to attempt to reduce the number of possible "predictors" through the use of a systematic, stepwise screening procedure. The method chosen is that of screening regression. From an array of possible predictors (x , y , z , xy , xz , etc.), the screening procedure first selects the one that has the highest linear correlation with the predictand in question. This predictor is then held constant, and partial-correlation coefficients between the predictand and each of the remaining predictors are examined; the predictor now associated with the highest coefficient is the second one selected. Additional predictors are chosen similarly until a selected predictor fails to explain a significant additional percentage of the

remaining variance of the predictand. The coefficients a_0, a_1 , etc., are then derived by the method of least squares. The initial-guess field is then generated by solving the derived equation at each of the grid points in the analysis volume.

The program is written so that it is possible to compute an initial guess from a blend of persistence and surface fitting. This is done to incorporate time continuity, as the observations are taken at two-hour intervals on alternate days between 0600 and 1400 MST. For the first observation time of the day (0600 MST), however, no weight is given to persistence because the previous available observation is usually forty hours old. The formula used in the program to calculate the initial-guess value of ϕ at a grid point is

$$\phi_{I.G.} = \frac{1}{1+W_p} \phi(\text{surface fit}) + \frac{W_p}{1+W_p} \phi(\text{persistence}) \quad (3-2)$$

where W_p = weight of persistence. By assigning a value of zero to W_p , persistence is given no weight and the initial guess is based solely on the surface fit. A value of one for W_p assigns half the weight to each while a very large value of W_p essentially gives all the weight to persistence.

The initial-guess portion of the computer program is a subroutine called IGUESS.

3.3.3 Correction Procedures (subroutines PCORR and TCORR)

Because the analysis during solution may only be defined at grid points, the information from observation points, which in general are at random locations within grid blocks, must be translated to grid points to permit the definition of internal boundary points. For each observation, the difference between the observed value and the value computed for that location by interpolating among the initial-guess values at the surrounding grid points is computed. This difference is then translated to the nearest grid point and added to that grid point as a correction to the initial guess. When a grid point is subject to multiple corrections (from several different observations), an overall correction is computed as the arithmetic average of the several individual corrections. Corrected grid points are designated as internal boundary points and are identified as such in the computer.

3.3.4 Relaxation Methods

After the internal boundary points have been defined, the next step in CRAM is to

compute interpolated values from these points at all uncorrected grid points. The interpolation is accomplished by requiring that the values at the uncorrected grid points satisfy Poisson's equation:

$$\nabla^2 \phi(i,j,k) = F(i,j,k) \quad (3-3)$$

where ϕ is the value of the analysis parameter at grid point (i,j,k) , F is a forcing function defining the shape of the field of ϕ , and ∇^2 is the finite-difference Laplacian operator in three dimensions. The Laplacian of a good initial-guess field provides a good forcing function. In the program (subroutine FORCE), the formula is written as follows:

$$\begin{aligned} \nabla^2 \phi(i,j,k) = & \phi(i+1,j,k) + \phi(i-1,j,k) + \phi(i,j+1,k) + \phi(i,j-1,k) \\ & - 4\phi(i,j,k) + K_A[\phi(i,j,k+1) - \phi(i,j,k)] \\ & - K_B[\phi(i,j,k) - \phi(i,j,k-1)] \end{aligned} \quad (3-4)$$

where K_A and K_B are coefficients pertaining to the vertical gradient computed above and below the analysis grid point, respectively.

The horizontal and vertical space gradients have been expressed separately in this equation. There are several practical reasons for doing this, all having to do with the scaling of the vertical coordinate used in the analysis technique. The basic horizontal grid length is 10 km, while in the vertical the grid length is about an order of magnitude smaller. Measuring gradients over this smaller distance is generally compensated for by the fact that, for most atmospheric variables, the vertical gradients are much larger than the horizontal gradients so that one may be justified in using $K_A = K_B = 1$ in Eq. (3-4). The relative inequalities between the grid distances above and below the grid point which arise from the uneven spacing of the artillery zones may be accounted for by assigning different values to K_A and K_B . Also, it is possible in the program to consider the objective analysis problem in a two-dimensional framework by simply setting $K_A = K_B = 0$.

The solution of Eq. (3-3) is accomplished by relaxation. Let the values at all the boundary points (internal and perimeter) remain unchanged throughout the relaxation computations. For each non-boundary point in the grid array, the residual, R , is computed by

$$R(i,j,k) = \nabla^2 \phi(i,j,k) - F(i,j,k). \quad (3-5)$$

New estimates of ϕ are then computed by

$$\hat{\phi}(i,j,k) = \alpha R(i,j,k) + \phi(i,j,k) \quad (3-6)$$

where α , a relaxation coefficient, is an input parameter. New residuals are then computed. The iterative procedure continues until all residuals are less than a specified value (ϵ). This procedure is accomplished in subroutine RELAX.

3.3.5 Smoothing (Subroutine SMOOTH)

A smoothing operator has been developed which is designed to eliminate from the analysis undesirable small-scale features. The expression used is

$$\begin{aligned} S[\phi(i,j,k)] = & W_1 \phi(i,j,k) + W_2 [\phi(i+1,j,k) + \phi(i-1,j,k) \\ & + \phi(i,j+1,k) + \phi(i,j-1,k)] \\ & + W_3 [\phi(i,j,k+1) + \phi(i,j,k-1)], \end{aligned} \quad (3-7)$$

$$\left(W_1 = \frac{6}{6 + 4B_h + 2B_v} ; W_2 = \frac{B_h}{6 + 4B_h + 2B_v} ; W_3 = \frac{B_v}{6 + 4B_h + 2B_v} \right)$$

The parameters B_h and B_v control the degree of smoothing to be performed. A value of zero assigned to each results in the entire weight being given to $\phi(i,j,k)$, i.e., no smoothing. Large values of B_h and B_v result in heavy smoothing. Also, the smoothing can be restricted to two dimensions by setting $B_v = 0$.

3.3.6 Ballistic Computation

The CRAM program produces analyses of u- and v-wind components, temperature, and density for each of ten artillery zones. These zones are listed in Table 2-1 for an analysis area 17 grid units in the I-direction (from I=50 to I=66) and 15 grid units in the J-direction (from J=345 to J=359) or about 170 km \times 150 km. A portion of this grid is shown in Fig. 2-1. The analysis area is purposely made large so that analysis problems associated with the boundaries are far enough removed to not contaminate the analysis in the region of interest, i.e., near the firing area. The ballistic fields are produced within the program by applying the zone weighting factors that are given in Table 3-1. A minor modification in the program will permit ballistic computations of "lines" other than merely Line 10.

An additional feature of the program is that the final printed output for the analysis field can be analyzed with contours printed for any desired isopleth interval.

If desired, portions of the analysis cycle may be repeated several times. The generated analyses may be used as an improved initial-guess field, with subsequent forcing, correcting, relaxing, and smoothing to make the analysis fit the observations more closely. This cycling feature can be employed for error checking purposes by discarding observations which differ from the analysis by a specified value. This value may be large for the first cycle with successively smaller values used for subsequent cycles.

3.4 Production of Analyses by Application of CRAM

The various options and parameters discussed above were given a limited amount of testing on a portion of the data sample. A much more extensive testing would be required in order to achieve the optimum results. Nevertheless, within the constraints of the present study, it was possible to produce meaningful analyses. In all, there were 80 observation times to be analyzed (16 days, 5 observation times per day) for 10 zones for four variables (u- and v-wind components, temperature, and density), making a grand total of 3,200 maps that were analyzed using the computer.

The initial-guess procedure of blending a surface fit with persistence was employed, using $W_p = 1/2$ in Eq.(3-2). The forcing function (F) was set equal to the Laplacian of the initial guess.

The values of K_A and K_B were chosen to be nearly equal to one (actually varying between 0.81 to 1.3 to account for the uneven zone spacing), causing the analysis to be made in three dimensions rather than two. The number of iterations required was near a minimum using a relaxation coefficient of $\alpha = 0.25$. (For two dimensions, $\alpha = 0.22$ should be used.) The smoothing operator was employed using $B_h = 2.0$ and $B_v = 2.0$, which gives one-third of the weight to the grid point being smoothed and two-thirds to the surrounding six grid points.

Analyses were produced for each of the ten artillery zones using the procedures outlined above. These zone analyses were then combined into ballistic analyses by computing the weighted sums using the weights given in Table 3-1. It should be emphasized that these analyses are the result of initial investigations and that further

work in this area, such as performing the force-relax-smooth cycle more than once, would likely lead to improved analyses. Figures 3-2 through 3-6 show the five analyzed fields of ballistic u- and v-wind components (in knots) for 0600, 0800, 1000, 1200, and 1400 MST. The temperature and density analyses (departure from Standard, in percent) are given in Figures 3-7 through 3-11.

The u-component ballistic wind analyses show a gradual increasing trend over the southern half of the analysis area, with only slight changes with time in the northern portion. This causes the contours that are originally oriented north-south to become nearly west-east by 1400 MST. There is also a gradual increase in the v-component value.

The temperature and density analyses (Figs. 3-7 through 3-11) show relatively small gradients, with the range of values over an entire map being generally less than 1% of Standard. The temperature values show a cooling trend through the series, reflecting a cooling trend in the upper zones. The surface heating affecting the lower zones does not contribute much to the overall ballistic temperature because of the way the individual zones are weighted (see Table 3-1). There is practically no spatial variability in density until the final map.

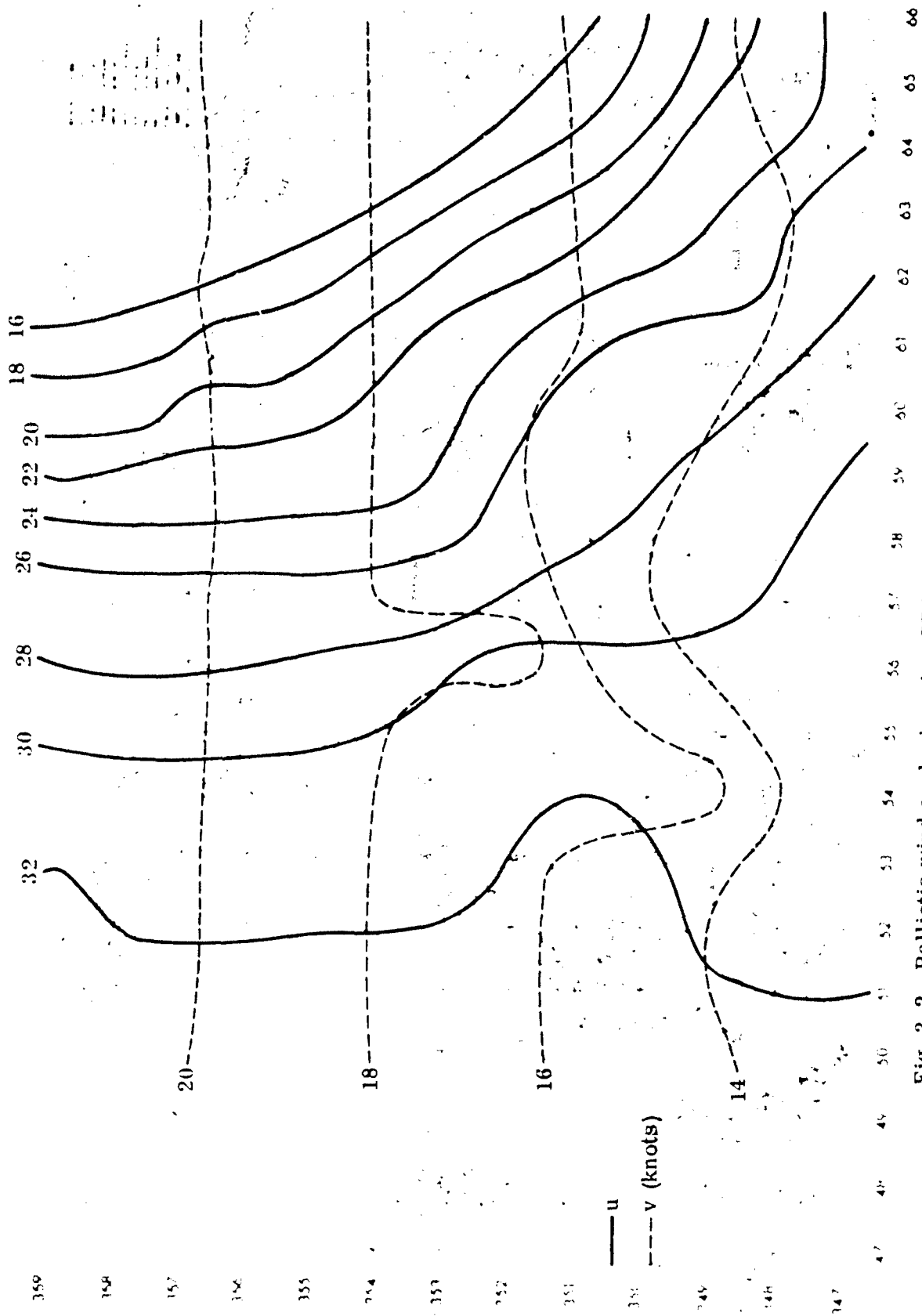


Fig. 3-2. Ballistic wind analysis using CRAM: 0600 MST, 20 January 1965.

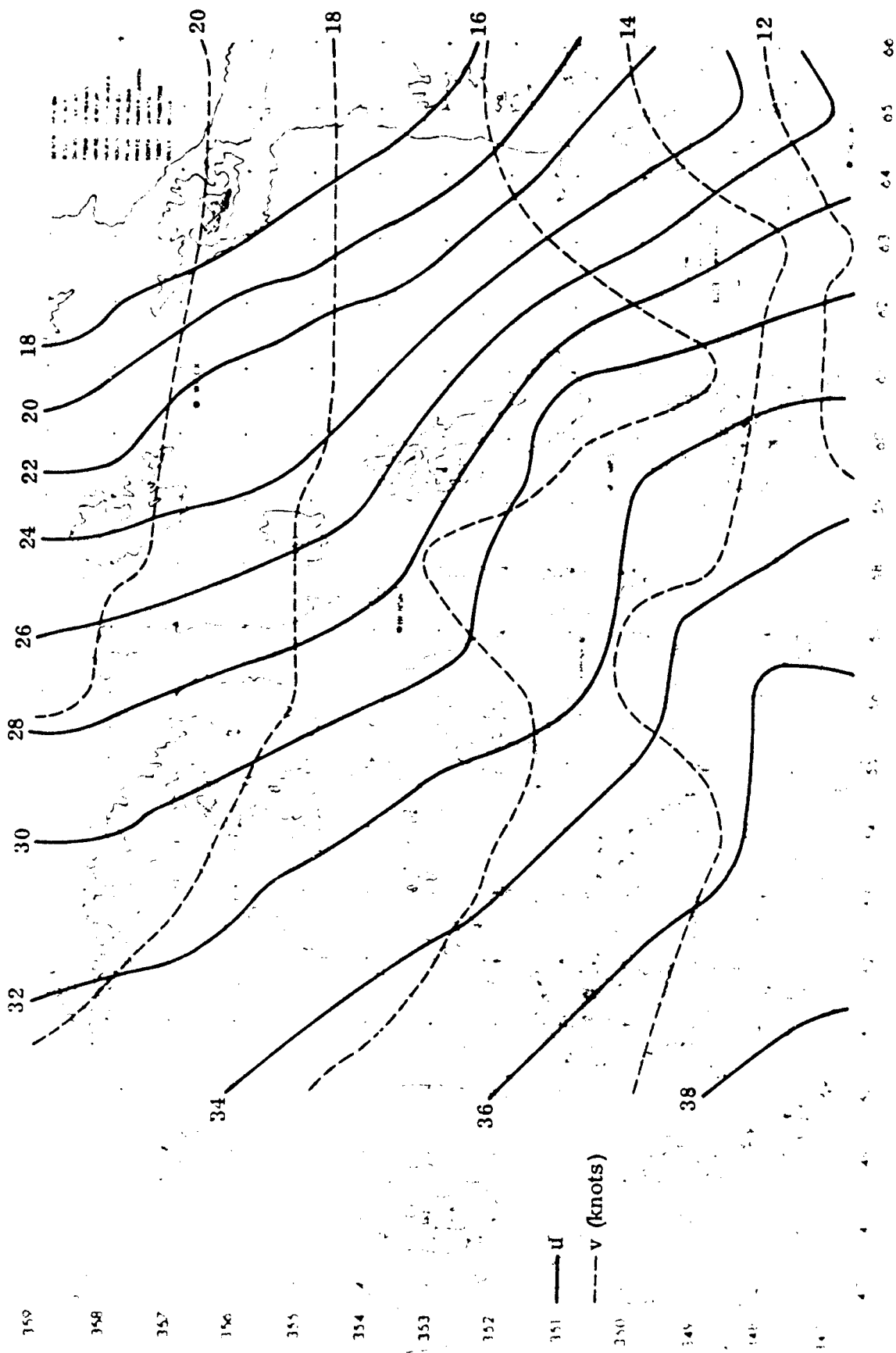


Fig. 3-3. Ballistic wind analysis using CRAM: 0800 MST, 20 January 1965.

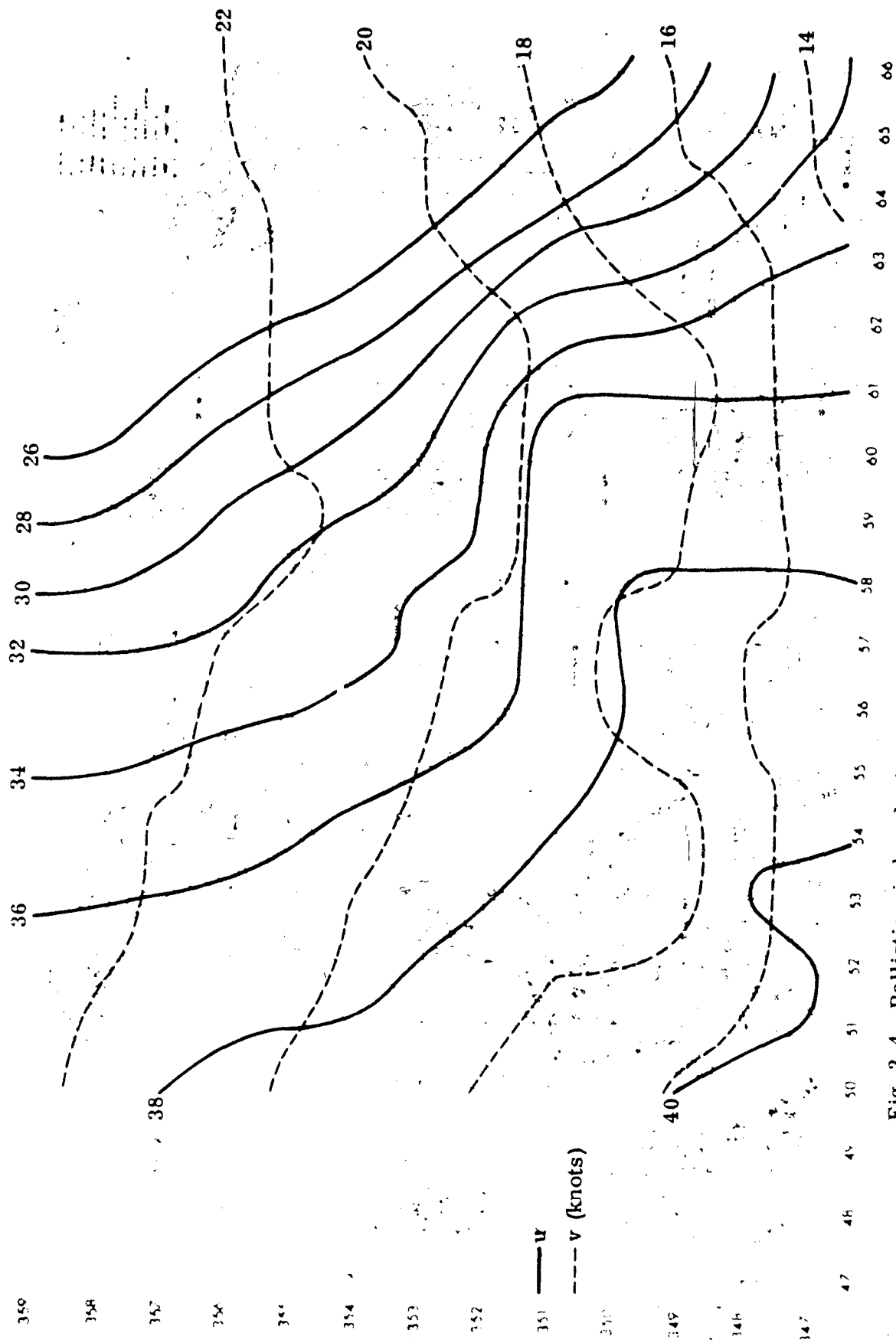


Fig. 3-4. Ballistic wind analysis using Cram: 1000 MST, 20 January 1965.

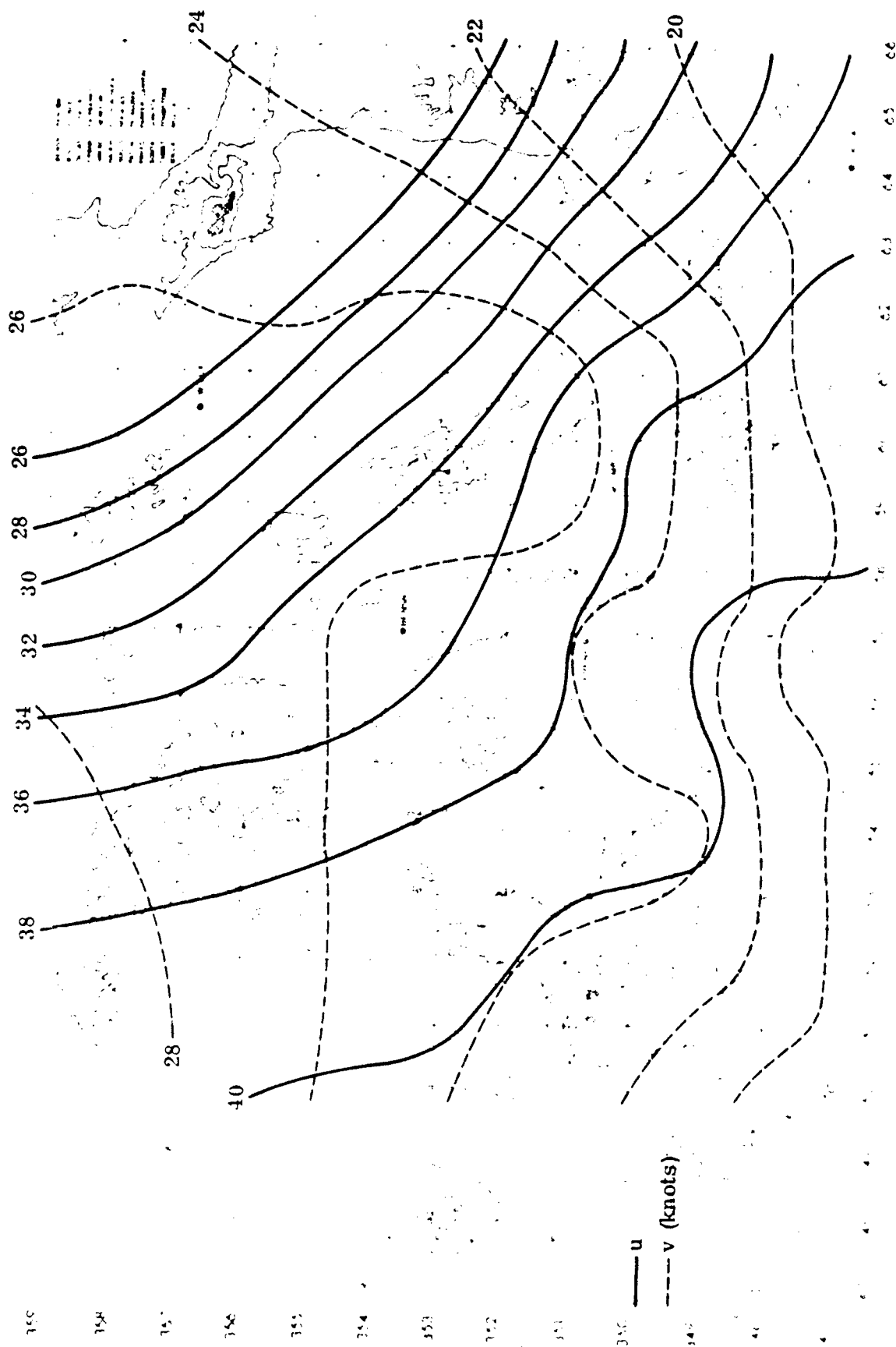


Fig. 3-5. Ballistic wind analysis using CRAM: 1200 MST, 20 January 1965.

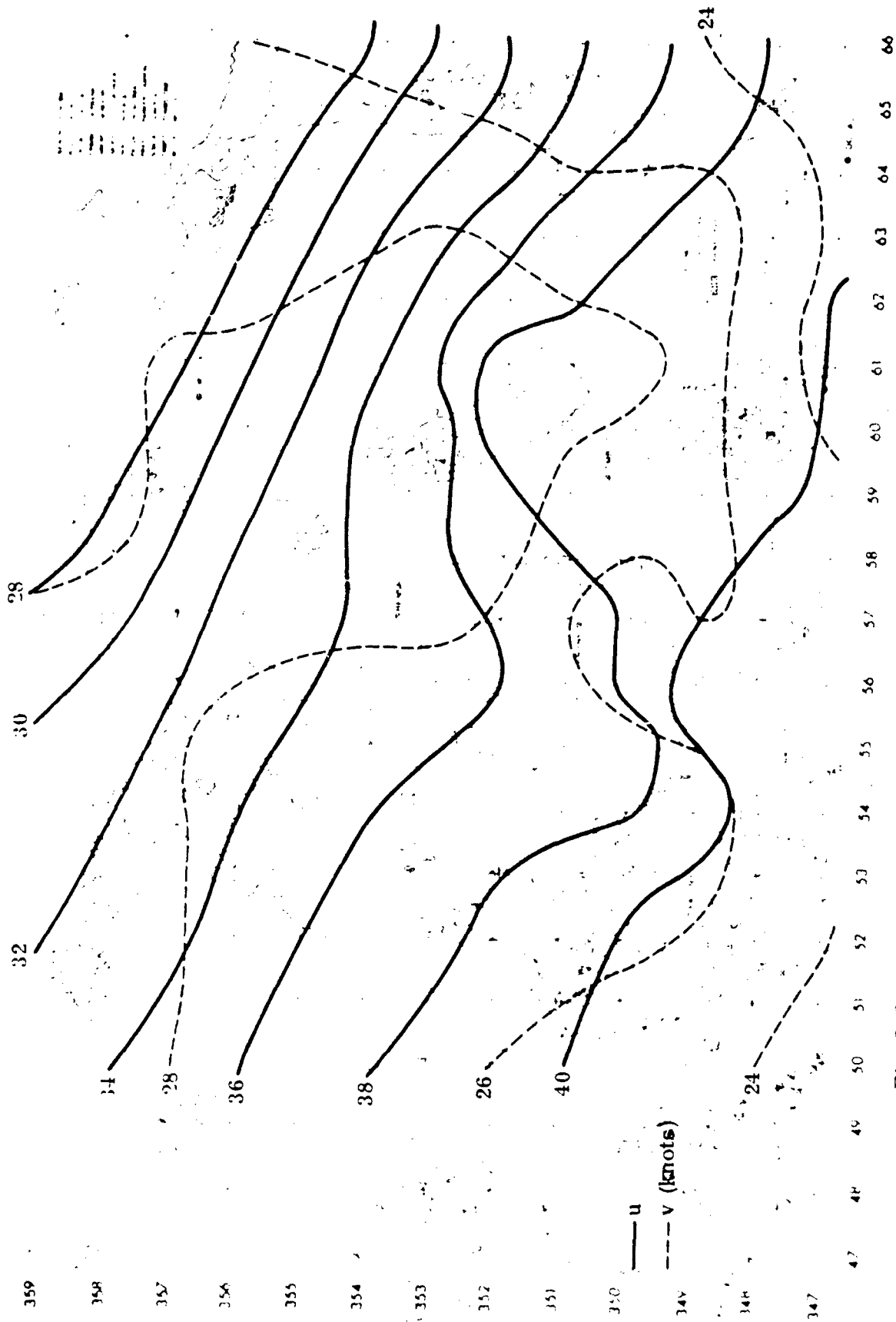


Fig. 3-6. Ballistic wind analysis using CRAM: 1400 MST, 20 January 1965.



Fig. 3-7. Ballistic temperature and density analysis using Cram: 0600 MST, 20 January 1965 (percent departure from Standard).

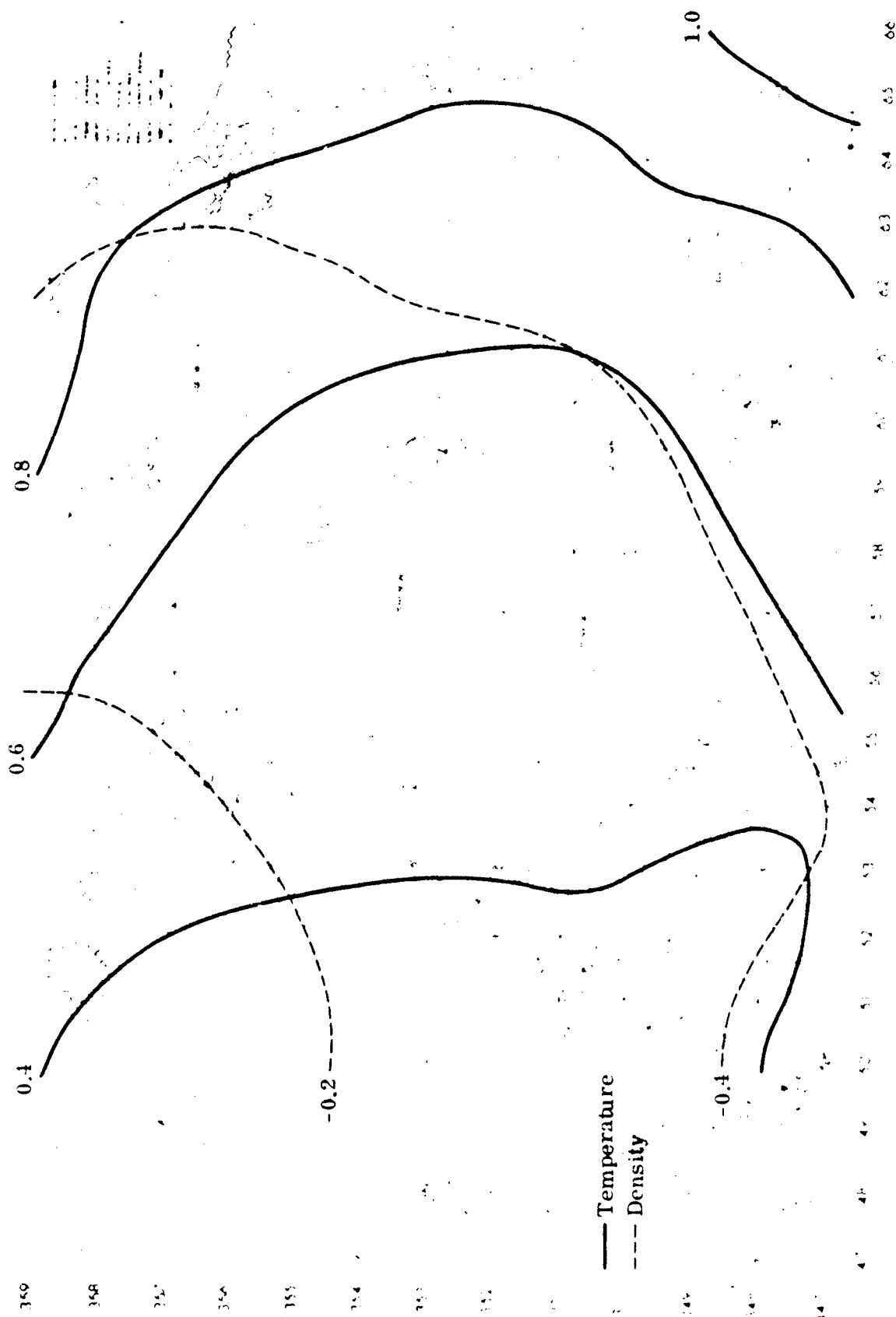


Fig. 3-8. Ballistic temperature and density analysis using Cram: 0800 MST, 20 January 1965 (percent departure from Standard).

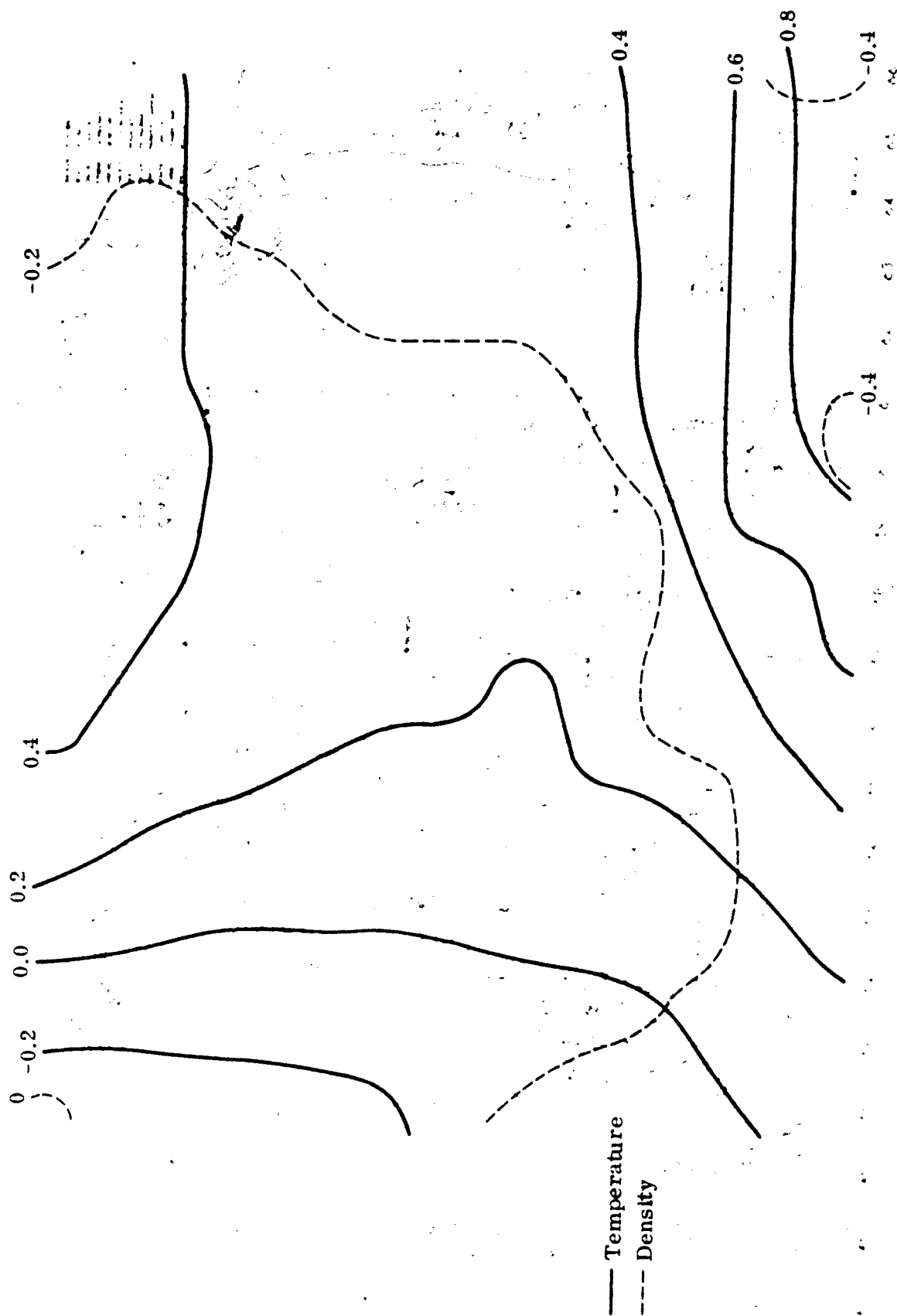


Fig. 3-9. Ballistic temperature and density analysis using CRAM: 1000 MST, 20 January 1965 (percent departure from Star^{1,rd}).

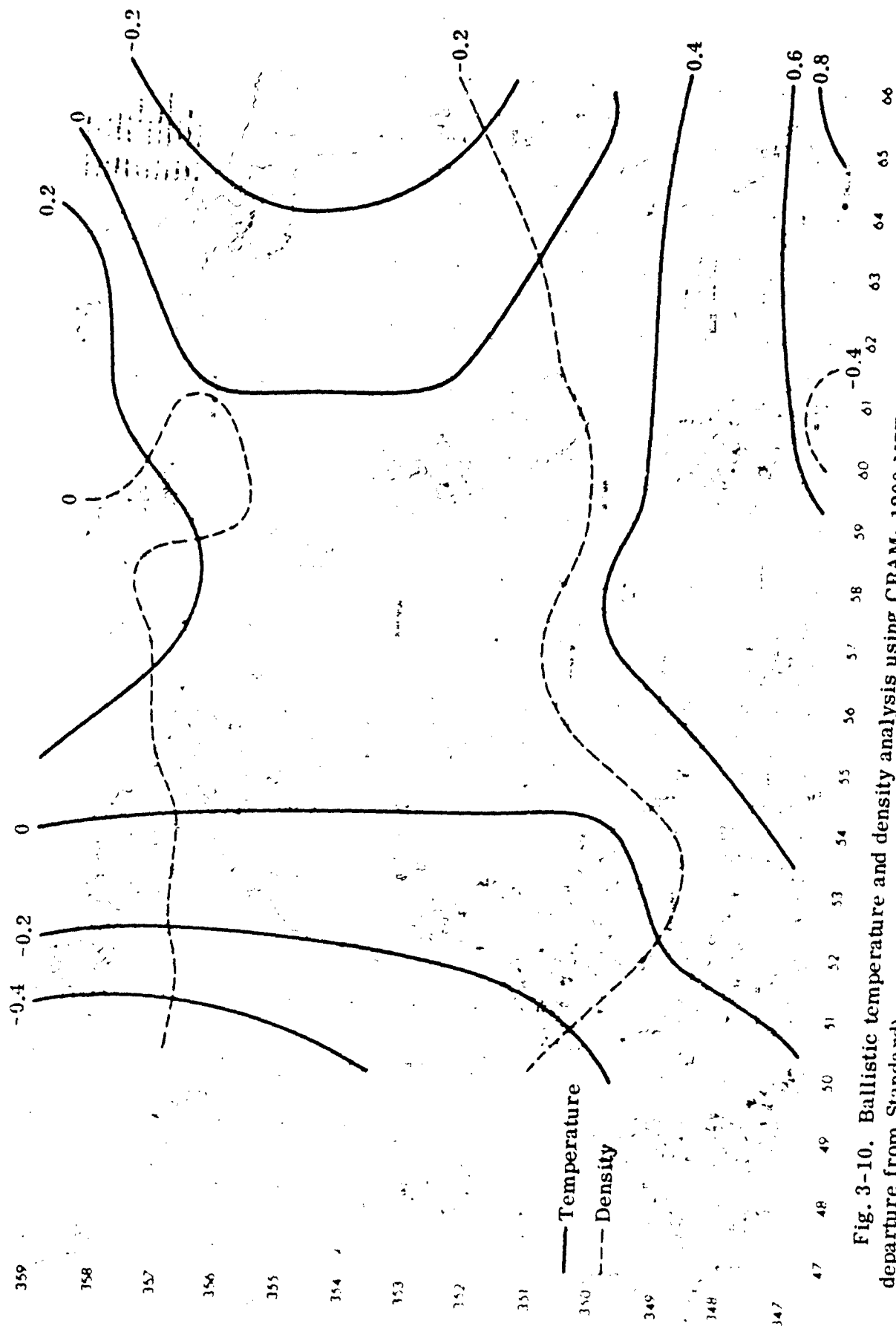


Fig. 3-10. Ballistic temperature and density analysis using CRAM; 1200 MST, 20 January 1965 (percent departure from Standard).

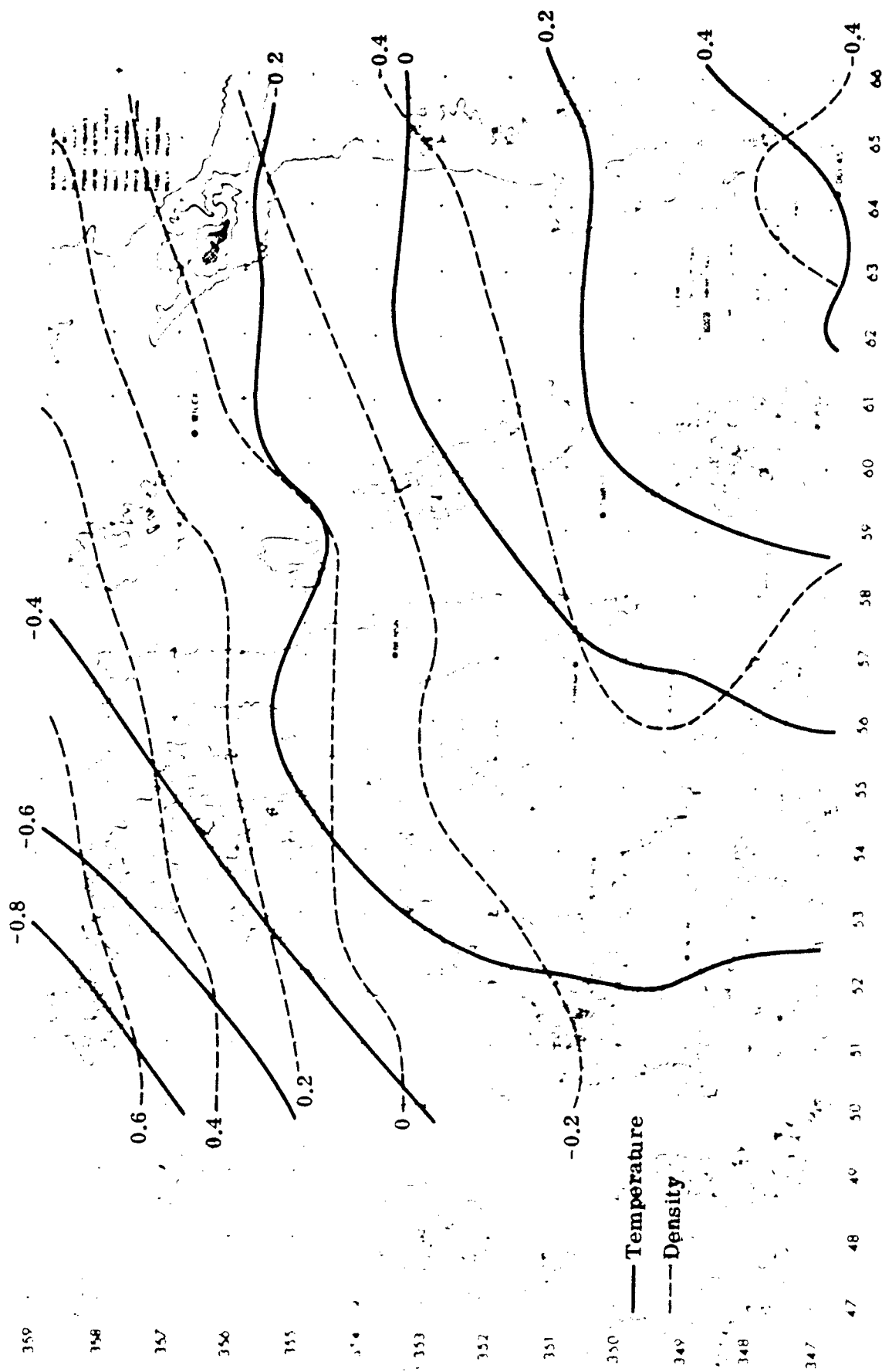


Fig. 3-11. Ballistic temperature and density analysis using CRAM: 1400 MST, 20 January 1965 (percent departure from Standard).

4.0 CALCULATION OF RESIDUAL ERRORS

The main purpose of developing an objective analysis technique for this study is to produce a representative estimate of the meteorological environment through which an artillery projectile travels. It is hoped that the analysis technique, which incorporates the map-wind concept, will be better than the ballistic winds derived from a single sounding. One meaningful way to evaluate the relative merits of two or more methods of computing ballistic winds is to make a comparison of residual errors using actual artillery firings.

Applying corrections to the firing data supplied for this study required the use of unit effect data supplied by BRL (Ballistic Research Laboratory, Aberdeen Proving Ground) based on firing table information. Ballisticians have derived these unit effects theoretically by first computing a trajectory from equations of motion using standard conditions. They then vary each of the variables from standard, one at a time, by a unit amount (1% for density or temperature, one knot for range wind or cross wind) and note the resulting difference in range or deflection. These differences are the unit effects.

For this study it was assumed that corrections for muzzle velocity, projectile weight, powder temperature, etc., were already accounted for in the computation of the range. Because the firings were conducted at fixed azimuths and quadrant elevations, the only corrections necessary to "move" the observed impact points in to the target were temperature, density, and range wind for the range correction, and drift, coriolis force, and cross wind for the deflection correction. The drift and coriolis force are independent of the meteorological values used, so that only ballistic wind, temperature, and density are pertinent in drawing comparisons among various analysis techniques.

4.1 Residual Errors Using CRAM and Ft. Huachuca Sounding

The provided gun data and unit effects were used in computing artillery corrections. (Only results using Gun No. 1 are presented here because the characteristics of Gun No. 2 were very similar.) Using CRAM analyses concurrent with the 24 firing times, values of ballistic temperature, density, and wind (resolved into range and cross wind components) valid at the midpoint of the firing trajectory were extracted. The results are shown in Table 4-1, where the odd-numbered cases refer to Gun No. 1.

TABLE 4-1
ARTILLERY CORRECTIONS BASED ON
GRAM ANALYSIS

DATE GUN CASE
16JAN65 A 1 1

GRAM ANALYSIS TRAJ MID POINT

TARGET										
COORDINATES										
3497838.8N 160300.2E										
	-NO CORRECTIONS-		-----WITH CORRECTIONS-----							
	VECT.	RANGE	DEFLT	VECT.	RANGE	DEFLT	X	Y		
	ERROR	ERROR	ERROR	ERROR	ERROR	ERROR	COMP.	COMP.		
	812.2	403.6	704.9	282.3	281.4	22.0	277.1	53.8		
METEOR. PARAMETER	METEOR. VALUE		UNIT EFFECT		CORRECTION					
TEMPERATURE	3.39		-12.25		-41.53					
DENSITY	-.27		67.45		-18.21					
RANGE WIND	3.1		-20.07		-62.39					
CROSS WIND	-6.0		-14.40		86.23					

CORIOLOIS CORRECTION= 30.09

DRIFT CORRECTION= 739.01

XX

DATE GUN CASE
16JAN65 P 1 3

GRAM ANALYSIS TRAJ MID POINT

TARGET										
COORDINATES										
3497872.5N 169520.9E										
	-NO CORRECTIONS-		-----WITH CORRECTIONS-----							
	VECT.	RANGE	DEFLT	VECT.	RANGE	DEFLT	X	Y		
	ERROR	ERROR	ERROR	ERROR	ERROR	ERROR	COMP.	COMP.		
	790.1	364.4	701.0	244.3	236.6	-60.8	211.9	121.7		
METEOR. PARAMETER	METEOR. VALUE		UNIT EFFECT		CORRECTION					
TEMPERATURE	3.57		-11.90		-42.48					
DENSITY	-.54		68.67		-37.08					
RANGE WIND	2.4		-20.25		-48.21					
CROSS WIND	-1.1		-14.58		16.12					

CORIOLOIS CORRECTION= 30.48

DRIFT CORRECTION= 747.44

XX

DATE GUN CASE
18 JAN 65 A 1 5

CHÂN ANALYSIS TRAJ WID POINT

TARGET COORDINATES	-NO CORRECTIONS-			-WITH CORRECTIONS-		
	VECT. EPOCH	RANGE EPOCH	DULIN EPOCH	VECT. EPOCH	RANGE EPOCH	DELTA EPOCH
3497865.0N 160404.0E	1032.7	500.2	071.4	208.6	205.1	-45.3
						COMP. CORR.
						272.4 122.3

METEOR. PARAMETER	METEOR. VALUE	UNIT EFFECT	CORRECTION
TEMPERATURE	4.21	-11.94	-50.44
DENSITY	-0.64	68.40	-43.78
RANGE WIND	5.5	-20.21	-110.84
CROSS WIND	16.6	-14.54	-240.79

CORIOLIS CORRECTION= 30.40 DRIFT CC RECTION= 745.57

29

[illegible]

DATE GUN CASE
18 JAN 65 P 1 7

CRAM ANALYSIS TRAJ MID POINT

TARGET COORDINATES	-NO CORRECTIONS-			-----WITH CORRECTIONS-----			Y
	VECT. ERROR	RANGE ERROR	DEFLTN ERROR	VECT. ERROR	RANGE ERROR	DEFLTN ERROR	
3497874.0N 569526.7E	1106.2	620.8	915.6	293.5	292.6	-21.9	276.2
COMD. 79.1							

METEOR. PARAMETER	METEOR. VALUE	UNIT	FFFFECT	CORRECTION
TEMPERATURE	4.22		-11.86	-50.00
DENSITY	-.93		68.77	-63.96
RANGE WIND	10.6		-20.25	-214.12
CROSS WIND	10.9		-14.58	-159.11

CORIOLIS CORRECTION= 30.48
DRIFT CORRECTION= 747.92[illegible]

TABLE 4-1 (continued)

DATE GUN CASE
20 JAN 65 A 1 9

GRAM ANALYSIS TRAJ MID POINT

TARGET		COORDINATES		3497867.6N 560503.3E		-NO CORRECTIONS-		-----WITH CORRECTIONS-----	
VECT.	RANGE	DEFLT	VECT.	RANGE	DEFLT	VECT.	RANGE	DEFLT	VECT.
ERROR	ERROR	ERROR	ERROR	ERROR	ERROR	ERROR	ERROR	ERROR	ERROR
1204.2	549.6	686.2	130.6	130.6	1.8	126.3	33.0		
METEOR. PARAMETER		METEOR. VALUE		UNIT EFFECT		CORRECTION			
TEMPERATURE		30		-11.96		-3.59			
DENSITY		-.21		68.49		-14.38			
RANGE WIND		41.6		-20.22		-841.06			
CROSS WIND		-6.3		-14.55		92.30			
CORIOLIS CORRECTION=		30.43		DRIFT CORRECTION=		746.22			

XX

DATE GUN CASE
20 JAN 65 P 1 11

GRAM ANALYSIS TRAJ MID POINT

TARGET		COORDINATES		3497868.1N 560505.3E		-NO CORRECTIONS-		-----WITH CORRECTIONS-----	
VECT.	RANGE	DEFLT	VECT.	RANGE	DEFLT	VECT.	RANGE	DEFLT	VECT.
ERROR	ERROR	ERROR	ERROR	ERROR	ERROR	ERROR	ERROR	ERROR	ERROR
1173.7	1029.9	563.0	101.1	100.5	-11.4	93.8	37.8		
METEOR. PARAMETER		METEOR. VALUE		UNIT EFFECT		CORRECTION			
TEMPERATURE		-.02		-8.75		.18			
DENSITY		-.40		68.52		-27.41			
RANGE WIND		44.6		-20.22		-902.25			
CROSS WIND		-13.9		-14.55		202.40			
CORIOLIS CORRECTION=		30.43		DRIFT CORRECTION=		746.36			

XX

TABLE 4-1 (continued)

DATE GUN CASE
22JAN65 A 1 13

TARGET
COORDINATES
3407860.6N 560442.0E

METEOR. PARAMETER METEOR. VALUE UNIT EFFECT CORRECTION

TEMPERATURE	1.32						
DENSITY	-0.16						
RANGE WIND	18.6						
CROSS WIND	64.1						

CORIOUS CORRECTION= 30.23 DRIFT CORRECTION= 741.90

-----NO CORRECTIONS----- WITH CORRECTIONS-----

VECT.	RANGE	DEFLTN	VECT.	RANGE	DEFLTN	X	Y
ERROR	ERROR	ERROR	ERROR	ERROR	ERROR	COMP.	COMP.
1617.2	826.3	1300.1	525.3	425.1	-308.6	327.5	410.8

DATE GUN CASE
22JAN65 P 1 15

TARGET
COORDINATES
3497867.3N 569502.2E

METEOR. PARAMETER METEOR. VALUE UNIT EFFECT CORRECTION

TEMPERATURE	1.38						
DENSITY	-0.28						
RANGE WIND	25.7						
CROSS WIND	61.0						

CORIOUS CORRECTION= 30.43 DRIFT CORRECTION= 746.13

-----NO CORRECTIONS----- WITH CORRECTIONS-----

VECT.	RANGE	DEFLTN	VECT.	RANGE	DEFLTN	X	Y
ERROR	ERROR	ERROR	ERROR	ERROR	ERROR	COMP.	COMP.
1673.1	948.8	1378.0	487.6	394.4	-286.8	303.7	381.5

TABLE 4-1 (continued)

DATE GUN CASE
25JAN65 A 1 17

TARGET
COORDINATES
3497847.5N 560430.8E

GRAM ANALYSIS TRAJ MID POINT

		-NO CORRECTIONS-		-----WITH CORRECTIONS-----			
		VECT.	RANGE DEFLT	VECT.	RANGE DEFLT	X	Y
ERROR		1827.5	842.5	1621.7	702.3	-538.6	450.7
COMP.						-399.0	-577.9

METEOR. PARAMETER		METEOR. VALUE	UNIT EFFECT	CORRECTION
TEMPERATURE		.36	-12.17	-4.38
DENSITY		.65	60.40	39.26
RANGE WIND		70.4	-20.12	-1415.93
CROSS WIND		27.7	-14.45	-399.64

CORIOLIS CORRECTION= 30.19 DRIFT CORRECTION= 741.19

DATE GUN CASE
25JAN65 P 1 19

TARGET
COORDINATES
3497847.5N 560442.2E

GRAM

		-NO CORRECTIONS-		-----WITH CORRECTIONS-----			
		VECT.	RANGE DEFLT	VECT.	RANGE DEFLT	X	Y
ERROR		1698.8	930.7	1421.2	246.6	-152.8	193.6
COMP.						-95.6	-227.3

METEOR. PARAMETER		METEOR. VALUE	UNIT EFFECT	CORRECTION
TEMPERATURE		-.02	-8.98	.18
DENSITY		.25	60.51	15.13
RANGE WIND		54.6	-20.13	-1098.75
CROSS WIND		31.5	-14.46	-455.29

CORIOLIS CORRECTION= 30.23 DRIFT CORRECTION= 742.00

DATE GUN CASE
27 JAN 65 A 1 21

CRA: ANALYSIS TRAJ MID POINT

TARGET I COORDINATES	-NO CORRECTIONS-			-WITH CORRECTIONS-		
	VECT.	RANGE	DEFLIN	VECT.	RANGE	DEFLIN
3407841.0N 160408.0E	1121.1	373.0	1067.1	183.4	183.4	1.5
				ERROR	ERROR	ERROR
						177.1
						47.5

METEOR. PARAMETER	WETTOR. VALUE	UNIT EFFECT	CORRECTION
TEMPERATURE	0.24	-12.22	-2.93
DENSITY	1.67	60.22	100.57
RANGE WIND	14.3	-20.08	-287.77
CROSS WIND	19.9	-14.41	-285.85

CORIOLIS CORRECTION= 30.12
DRIFT CORRECTION= 739.65[illegible]

DATE GUN CASE
27 JAN 65 P 1 22

CRAM ANALYSIS TRAJ MID POINT

TARGET COORDINATES	-NO CORRECTIONS-			-----WITH CORRECTIONS-----				
	VECT. ERROR	RANGE ERROR	DEFLTN ERROR	VECT. ERROR	RANGE ERROR	DEFLTN ERROR	X COMP.	Y COMP.
3497870.0N 160512.1E	1115.3	508.8	992.5	223.8	216.0	-58.4	192.7	113.8

METEOR. PARAMETER	METEOR. VALUE	UNIT EFFECT	CORRECTION
TEMPERATURE	.24	-11.93	-2.86
DENSITY	1.23	61.10	75.15
RANGE WIND	18.0	-20.23	-365.05
CROSS WIND	18.8	-14.56	-273.57

CORRECTION = 30.45
DRIFT CORRECTION = 746.84

XX

TABLE 4-1 (continued)

DATE GUN CASE
29 JAN 65 A 1 25

TARGET
COORDINATES
3497843.5N 160416.3E

METEOR. PARAMETER METEOR. VALUE UNIT EFFECT CORRECTION
TEMPERATURE 1.96 -12.20 -23.91
DENSITY -.13 67.63 -8.76
RANGE WIND -13.6 -20.84 282.69
CROSS WIND 4.0 -14.42 -58.12

CORIOUS CORRECTION= 30.14 DRIFT CORRECTION= 740.21

XX

DATE GUN CASE
29 JAN 65 P 1 27

TARGET
COORDINATES
3497881.0N 160551.6E

METEOR. PARAMETER METEOR. VALUE UNIT EFFECT CORRECTION
TEMPERATURE 2.08 -11.81 -24.56
DENSITY -.42 68.98 -28.97
RANGE WIND -7.5 -21.04 156.96
CROSS WIND 0.3 -14.62 -92.71

CORIOUS CORRECTION= 30.58 DRIFT CORRECTION= 749.58

XX

TABLE 4-1 (continued)

DATE GUN CASE
02FEB65 A 1 20

GRAM ANALYSIS TRAJ MID POINT

TARGET
COORDINATES
3497868.0N 160504.0E

-NO CORRECTIONS-		-WITH CORRECTIONS-	
VECT.	RANGE DEFLT	VECT.	RANGE DEFLT
ERROR	ERROR	ERROR	ERROR
754.0	442.0	711.0	229.2
METEOR. PARAMETER		METEOR. PARAMETER	
TEMPERATURE		TEMPERATURE	
DENSITY		DENSITY	
RANGE WIND		RANGE WIND	
CROSS WIND		CROSS WIND	
CORIOLIS CORRECTION= 30.43		CORIOLIS CORRECTION= 30.43	
DRIFT CORRECTION= 746.34		DRIFT CORRECTION= 746.34	

XX

DATE GUN CASE
02FEB65 P 1 31

GRAM ANALYSIS TRAJ MID POINT

TARGET
COORDINATES
3497870.2N 160545.3E

-NO CORRECTIONS-		-WITH CORRECTIONS-	
VECT.	RANGE DEFLT	VECT.	RANGE DEFLT
ERROR	ERROR	ERROR	ERROR
804.2	375.7	711.1	150.2
METEOR. PARAMETER		METEOR. PARAMETER	
TEMPERATURE		TEMPERATURE	
DENSITY		DENSITY	
RANGE WIND		RANGE WIND	
CROSS WIND		CROSS WIND	
CORIOLIS CORRECTION= 30.56		CORIOLIS CORRECTION= 30.56	
DRIFT CORRECTION= 740.15		DRIFT CORRECTION= 740.15	

XX

TABLE 4-1 (continued)

DATE GUN CASE
06FEB65 A 1 27

GRAM ANALYSIS TRAJ MID POINT

TARGET		-----WITH CORRECTIONS-----	
COORDINATES		VECT. RANGE DEFLTIN	VECT. RANGE DEFLTIN
3497893.0N 160443.0E		ERROR ERROR	ERROR ERROR
		1202.4 1117.6	640.2 43.2
			-27.9 33.0
			COMP. COMP.
			-18.1 -39.2

METEOR. PARAMETER	METEOR. VALUE	UNIT EFFECT	CORRECTION
TEMPERATURE	1.76	-12.09	-21.28
DENSITY	-1.01	68.00	-68.68
RANGE WIND	52.4	-20.15	-1055.49
CROSS WIND	-10.8	-14.48	156.83

CORIOUS CORRECTION= 30.26 DRIFT CORRECTION= 742.81

XX

DATE GUN CASE
06FEB65 P 1 30

GRAM ANALYSIS TRAJ MID POINT

TARGET		-----WITH CORRECTIONS-----	
COORDINATES		VECT. RANGE DEFLTIN	VECT. RANGE DEFLTIN
3497840.0N 160436.0E		ERROR ERROR	ERROR ERROR
		1523.1 1361.1	683.5 119.2
			78.1 90.1
			COMP. COMP.
			99.3 -66.0

METEOR. PARAMETER	METEOR. VALUE	UNIT EFFECT	CORRECTION
TEMPERATURE	1.33	-12.15	-16.16
DENSITY	-1.20	67.82	-81.38
RANGE WIND	58.9	-20.12	-1185.49
CROSS WIND	-12.3	-14.45	178.35

CORIOUS CORRECTION= 30.21 DRIFT CORRECTION= 741.57

XX

TABLE 4-1 (continued)

DATE GUN CASE
10FER65 A 1 41

GRAM ANALYSIS TRAJ MID POINT

TARGET COORDINATES	-NO CORRECTIONS-			-WITH CORRECTIONS-		
	VECT. ERROR	RANGF DEFULTN	VECT. ERROR	RANGF DEFULTN	X	Y
3497850.4N 560441.3E	1401.0	1133.0	824.2	333.3	-252.6	217.4
						-185.5
						-276.9

METEOR. PARAMETER	METEOR. VALUE	UNIT EFFECT	CORRECTION
TEMPERATURE	-1.94	-8.98	17.42
DENSITY	.75	60.50	45.38
RANGF WIND	72.0	-20.13	-1448.37
CROSS WIND	-11.4	-14.46	165.38

CORIOLIS CORRECTION= 30.22 DRIFT CORRECTION= 741.94

XX

DATE GUN CASE
10FER65 P 1 43

GRAM ANALYSIS TRAJ MID POINT

TARGET COORDINATES	-NO CORRECTIONS-			-WITH CORRECTIONS-		
	VECT. ERROR	RANGF DEFULTN	VECT. ERROR	RANGF DEFULTN	X	Y
3497851.4N 569444.9E	1217.8	888.1	833.3	213.5	-149.2	152.7
						-103.1
						-186.9

METEOR. PARAMETER	METEOR. VALUE	UNIT EFFECT	CORRECTION
TEMPERATURE	-2.30	-8.97	20.63
DENSITY	.84	60.53	50.85
RANGF WIND	55.1	-20.13	-1108.85
CROSS WIND	-6.3	-14.47	91.86

CORIOLIS CORRECTION= 30.24 DRIFT CORRECTION= 742.19

XX

The target (hypothetical) coordinates are given in meters in the Universal Transverse Mercator grid system. The range, deflection, and vector errors designated "NO CORRECTIONS" are based on the distance between the target and the given center of impact (CI). The correction due to any one meteorological parameter is obtained by multiplying its value by the unit effect for that parameter. The range, deflection, and vector errors "WITH CORRECTIONS" are residual errors based on the corrected impact point after the drift, coriolis, and meteorological effects have been accounted for. (Negative range errors refer to impact short of the target and negative deflection errors refer to impact to the left of the target when viewed from the gun location.) Also given are the x and y components of the vector error which, when added to the target coordinates, give the coordinates of the corrected impact point. The corrections due to temperature, density, and range wind affect only the range (negative corrections decrease the range), while corrections due to cross wind affect only the deflection (negative corrections displace the impact point to the left). The variations in target coordinates and unit effects are due to adjustments made for non-meteorological factors by BRL.

Ballistic quantities determined using the Ft. Huachuca sounding alone were also applied to the firing data. Of the 24 firing times, there were 5 in which the data were not available to construct a Line-10 ballistic message. The results of the 19 cases are shown in Table 4-2.

4.2 Comparison of Residual Errors

A tabulation of average range and deflection errors for the CRAM and Ft. Huachuca data showed rather conclusively a systematic error in range of about 190 m, the mean CI being about 190 m beyond the target. Discussions with ballistics experts at BRL were held to see if the reason for the error could be detected and corrected. It was brought out that the ballistic coefficient used in the solution of the equations of motion was not accurately known for high angle firing situations, i.e., quadrant elevation above 45 degrees. One reason for this is that when the projectile is oriented at a high angle as it leaves the gun barrel, it is subjected to a "summital yaw" in the vicinity of the top of the trajectory. This results in an erratic descent to the ground and, thus, an unreliable trajectory. The ballistic coefficient when determined by a relatively small

number of high angle firings is therefore subject to error. Because the quadrant elevation for the Ft. Huachuca firings was of the order of 63°, a suggestion was made to have the ballistic coefficient computed by BRL using the Ft. Huachuca firing and meteorological data. The detailed results were not available in time for publication, but it was learned that, based on about one half of the data sample, there were discrepancies in the ballistic coefficient of about 5 to 10%. This was not enough to change the unit effects significantly, but it did cause changes in range (target location) of as much as 600 m.

Rather than complete elimination of any comparison of range residual errors, it was decided as an interim measure to remove some of the systematic error empirically. A linear regression equation relating range error to range wind was derived by the method of least squares on the combined sample of 24 CRAM cases and the 19 Ft. Huachuca cases. The data are plotted in Fig. 4-1. The correlation coefficient was -0.82. The equation for the regression line is

$$C = 322.87 - 7.33 (RW) \quad (4-1)$$

where C is the correction factor, in meters, to be subtracted from the conventionally determined range error and RW is the range wind in knots. Corrections made by this method are in good qualitative agreement with those made to date by recomputing the ballistic coefficient.

Table 4-3 shows a summary of residual errors for CRAM and the single sounding from Ft. Huachuca where the range residual error has been empirically corrected. The average absolute errors are based on the 19 cases where comparison is possible. The average range and deflection errors are 9.6 m and 9.9 m smaller for CRAM than for Ft. Huachuca. The residual vector difference is 12.1 m lower for CRAM. The average residual range errors before the empirical corrections were 231.1 m for CRAM and 243.6 m for Ft. Huachuca. The differences in deflection errors are significant at the 15% level when a Student's T-test for paired comparisons (Wadsworth and Bryan, 1963) is employed.

The residual errors are shown graphically in Fig. 4-2.

Differences in residual errors between the two methods should be the largest when winds are strong and/or considerable horizontal gradient in the meteorological parameters exists.

TABLE 4-2
ARTILLERY CORRECTIONS BASED ON FT. HUACHUCA
METEOROLOGICAL SOUNDINGS*

DATE GUN CASE
16 JAN 65 A 1 1

HUACH 10 ZONES FIXED STATION

TARGET	-NO CORRECTIONS-				-WITH CORRECTIONS-			
COORDINATES	VECT.	RANGE	DEFLT	VECT.	RANGE	DEFLT	X	Y
3497838.8N 569399.2E	812.2	403.6	704.9	307.7	304.4	45.4	305.5	37.4

METEOR. PARAMETER	METEOR. VALUE	UNIT	EFFECT	CORRECTION
TEMPERATURE	3.38		-12.25	-41.41
DENSITY	-0.23		67.45	-15.51
RANGE WIND	2.1		-20.07	-42.26
CROSS WIND	-7.6		-14.40	109.65

CORIOLIS CORRECTION= 30.09 DRIFT CORRECTION= 739.01

XX

DATE GUN CASE
16 JAN 65 A 2 2

HUACH 10 ZONES FIXED STATION

TARGET	-NO CORRECTIONS-				-WITH CORRECTIONS-			
COORDINATES	VECT.	RANGE	DEFLT	VECT.	RANGE	DEFLT	X	Y
3497867.7N 569320.2E	798.9	410.7	685.3	312.4	311.4	24.4	306.5	60.2

METEOR. PARAMETER	METEOR. VALUE	UNIT	EFFECT	CORRECTION
TEMPERATURE	3.38		-12.21	-41.27
DENSITY	-0.23		67.16	-15.45
RANGE WIND	2.1		-20.03	-42.53
CROSS WIND	-7.6		-14.41	109.55

CORIOLIS CORRECTION= 29.80 DRIFT CORRECTION= 740.77

*Ft. Huachuca soundings were not available for Cases 11, 12, 13, 14, 17, 18, 31, 32, 41, and 42.

TABLE 4-2 (continued)

DATE GUN CASE
16 JAN 65 P 1 3

HUACH 10 ZONES FIXED STATION

TARGET COORDINATES	-NO CORRECTIONS-			-----WITH CORRECTIONS-----				
	VECT. ERROR	RANGE ERROR	DEFLTN ERROR	VECT. ERROR	RANGE ERROR	DEFLTN ERROR	X	Y
3497872.5N 569520.9E	790.1	364.4	701.0	263.2	243.0	-101.2	207.2	162.3

METEOR. PARAMETER	METEOR. VALUE	UNIT EFFECT	CORRECTION
TEMPERATURE	3.65	-11.90	-43.44
DENSITY	-0.69	68.67	-47.38
RANGE WIND	1.5	-20.25	-30.61
CROSS WIND	1.7	-14.58	-24.25

CORIOLIS CORRECTION= 30.48 DRIFT CORRECTION= 747.44

XX

DATE GUN CASE
16 JAN 65 P 2 4

HUACH 10 ZONES FIXED STATION

TARGET COORDINATES	-NO CORRECTIONS-			-----WITH CORRECTIONS-----				
	VECT. ERROR	RANGE ERROR	DEFLTN ERROR	VECT. ERROR	RANGE ERROR	DEFLTN ERROR	X	Y
3497883.8N 569378.0E	797.0	409.2	684.0	310.3	288.2	-115.0	246.6	188.2

METEOR. PARAMETER	METEOR. VALUE	UNIT EFFECT	CORRECTION
TEMPERATURE	3.65	-12.04	-43.95
DENSITY	-0.69	67.74	-46.74
RANGE WIND	1.5	-20.12	-30.33
CROSS WIND	1.7	-14.50	-24.16

CORIOLIS CORRECTION= 29.99 DRIFT CORRECTION= 744.81

TABLE 4-2 (continued)

DATE GUN CASE
18JAN65 A 1 5

HUACH 10 ZONES FIXED STATION

TARGET	-NO CORRECTIONS-		-WITH CORRECTIONS-	
COORDINATES	VECT.	RANGE DFLTN	VECT.	RANGE DFLTN
3497865.0N 160404.0E	ERROR	ERROR	ERROR	ERROR
	1092.7	500.2	971.4	305.3
METEOR. PARAMETER	METLOR. VALUE	UNIT EFFECT	CORRECTION	
TEMPERATURE	4.16	-11.98	-49.04	
DENSITY	-0.68	68.40	-46.51	
RANGE WIND	5.3	-20.21	-107.86	
CROSS WIND	13.0	-14.54	-270.37	
CORIOLIS CORRECTION=	30.40			
DRIFT CORRECTION= 745.57				

XX

DATE GUN CASE
18JAN65 A 2 6

HUACH 10 ZONES FIXED STATION

TARGET	-NO CORRECTIONS-		-WITH CORRECTIONS-	
COORDINATES	VECT.	RANGE DFLTN	VECT.	RANGE DFLTN
3497882.1N 160371.7E	ERROR	ERROR	ERROR	ERROR
	1073.8	540.8	927.6	357.6
METEOR. PARAMETER	METLOR. VALUE	UNIT EFFECT	CORRECTION	
TEMPERATURE	4.16	-12.07	-50.41	
DENSITY	-0.68	67.68	-46.02	
RANGE WIND	5.3	-20.11	-106.45	
CROSS WIND	18.6	-14.49	-269.62	
CORIOLIS CORRECTION=	29.97			
DRIFT CORRECTION= 744.37				

TABLE 4-2 (continued)

DATE GUN CASE
18JAN65 P 1 7

HUACH 10 ZONES FIXED STATION

TARGET COORDINATES	-NO CORRECTIONS-			-WITH CORRECTIONS-		
	VECT. ERROR	RANGE DEFLECTN ERROR	VECT. RANGE DEFLECTN ERROR	VECT. RANGE DEFLECTN ERROR	VECT. RANGE DEFLECTN ERROR	VECT. RANGE DEFLECTN ERROR
3497874.0N 569526.7E	1106.2	620.8	915.6	240.9	240.3	-16.1
METEOR. PARAMETER	METEOR. VALUE	UNIT EFFECT	CORRECTION			
TEMPERATURE	4.14	-11.86	-49.10			
DENSITY	-1.03	68.77	-70.83			
RANGE WIND	12.9	-20.25	-260.51			
CROSS WIND	10.5	-14.58	-153.22			
CORIOLIS CORRECTION=	30.45					
						DRIFT CORRECTION= 747.92

XX

DATE GUN CASE
18JAN65 P 2 8

HUACH 10 ZONES FIXED STATION

TARGET COORDINATES	-NO CORRECTIONS-			-WITH CORRECTIONS-		
	VECT. ERROR	RANGE DEFLECTN ERROR	VECT. RANGE DEFLECTN ERROR	VECT. RANGE DEFLECTN ERROR	VECT. RANGE DEFLECTN ERROR	VECT. RANGE DEFLECTN ERROR
3497890.3N 569433.6E	1050.3	605.8	235.2	226.8	-62.3	201.7
METEOR. PARAMETER	METEOR. VALUE	UNIT EFFECT	CORRECTION			
TEMPERATURE	4.14	-11.90	-49.27			
DENSITY	-1.03	68.28	-70.33			
RANGE WIND	12.8	-20.20	-259.36			
CROSS WIND	10.5	-14.58	-153.66			
CORIOLIS CORRECTION=	30.15					
						DRIFT CORRECTION= 748.65

TABLE 4-2 (continued)

DATE GUN CASE		HUACH 10 ZONES FIXED STATION									
20JAN65 A 1 0											
TARGET		-NO CORRECTIONS-		-----WITH CORRECTIONS-----							
COORDINATES		VECT.	RANGE	DEFLT	VECT.	RANGE	DEFLT	X	Y		
		ERROR	ERROR	ERROR	ERROR	ERROR	ERROR	COMP.	COMP.		
3497867.6N	560503.3E	1204.2	989.6	686.2	140.4	133.0	45.2	140.2	-8.1		
METEOR. PARAMETER		METEOR. VALUE		UNIT EFFECT		CORRECTION					
TEMPERATURE		.22		-11.96		-2.63					
DENSITY		-.16		68.49		-10.96					
RANGE WIND		41.7		-20.22		-843.04					
CROSS WIND		-9.3		-14.55		135.68					
CORIOLIS CORRECTION=		30.43		DRIFT CORRECTION=		746.22					
XX											
DATE GUN CASE		HUACH 10 ZONES FIXED STATION									
20JAN65 A 2 10											
TARGET		-NO CORRECTIONS-		-----WITH CORRECTIONS-----							
COORDINATES		VECT.	RANGE	DEFLT	VECT.	RANGE	DEFLT	X	Y		
		ERROR	ERROR	ERROR	ERROR	ERROR	ERROR	COMP.	COMP.		
3497893.4N	560412.2E	1155.1	959.0	643.9	104.1	104.1	.8	100.5	27.2		
METEOR. PARAMETER		METEOR. VALUE		UNIT EFFECT		CORRECTION					
TEMPERATURE		.22		-11.95		-2.63					
DENSITY		-.16		68.08		-10.89					
RANGE WIND		41.7		-20.17		-841.40					
CROSS WIND		-9.2		-14.55		134.25					
CORIOLIS CORRECTION=		30.10		DRIFT CORRECTION=		747.19					

TABLE 4-2 (continued)

DATE GUN CASE
22 JAN 65 P 1 15

HUACH 10 ZONE 5 FIXED STATION

TARGET COORDINATES	-NO CORRECTIONS-			-WITH CORRECTIONS-		
	VECT. ERROR	RANGE DEFLT	VECT. ERROR	RANGE DEFLT	VECT. ERROR	COMP. Y
3497867.3N 569502.2E	1673.1	945.8	1374.0	645.9	556.3	-325.2
METEOR. PARAMETER	UNIT EFFECT			CORRECTION		
TEMPERATURE	-0.15		-8.77			1.32
DENSITY	.24		61.01			14.64
RANGE WIND	20.2		-20.22			-408.47
CROSS WIND	63.9		-14.55			-929.68
CORIOLIS CORRECTION=	30.43			DRIFT CORRECTION= 746.13		

XX

DATE GUN CASE
22 JAN 65 P 2 16

HUACH 10 ZONE 5 FIXED STATION

TARGET COORDINATES	-NO CORRECTIONS-			-WITH CORRECTIONS-		
	VECT. ERROR	RANGE DEFLT	VECT. ERROR	RANGE DEFLT	VECT. ERROR	COMP. Y
3497877.0N 569493.4E	1663.1	981.9	1342.3	693.1	595.1	-355.3
METEOR. PARAMETER	UNIT EFFECT			CORRECTION		
TEMPERATURE	-0.15		-8.98			1.35
DENSITY	.24		60.15			14.44
RANGE WIND	20.1		-20.08			-402.61
CROSS WIND	63.9		-14.46			-924.61
CORIOLIS CORRECTION=	29.91			DRIFT CORRECTION= 743.08		

XX

TABLE 4-2 (continued)

DATE GUN CASE
25JAN65 P 1 10

HUACH 10 ZONES FIXED STATION

TARGET	-NO CORRECTIONS-		-----WITH CORRECTIONS-----	
COORDINATES	VECT.	RANGE DEFLT	VECT.	RANGE DEFLT
3497850.7N 569442.2E	ERROR	ERROR	ERROR	ERROR
	1698.3	930.7	238.8	-192.5
				141.2
				-147.9
				-187.4
METEOR. PARAMETER	METEOR. VALUE	UNIT EFFECT	CORRECTION	
TEMPERATURE	-0.08	-8.98	.72	
DENSITY	.70	60.51	42.36	
RANGE WIND	57.9	-20.13	-1166.28	
CROSS WIND	35.1	-14.46	-507.72	
CORIOLIS CORRECTION=	30.23		DRIFT CORRECTION= 742.00	

XX

DATE GUN CASE
25JAN65 P 2 20

HUACH 10 ZONES FIXED STATION

TARGET	-NO CORRECTIONS-		-----WITH CORRECTIONS-----	
COORDINATES	VECT.	RANGE DEFLT	VECT.	RANGE DEFLT
3497849.9N 569256.5E	ERROR	ERROR	ERROR	ERROR
	1651.3	957.0	1345.7	171.1
				-153.8
				75.0
				-128.0
				-113.5
METEOR. PARAMETER	METEOR. VALUE	UNIT EFFECT	CORRECTION	
TEMPERATURE	-0.08	-9.33	.75	
DENSITY	.70	59.34	41.54	
RANGE WIND	57.9	-19.93	-1153.04	
CROSS WIND	35.2	-14.32	-504.75	
CORIOLIS CORRECTION=	29.60		DRIFT CORRECTION= 736.35	

TABLE 4-2 (continued)

DATE GUN CASE
27JAN65 A 1 21

HUACH 10 ZONES FIXED STATION

TARGET	-NO CORRECTIONS-		-----WITH CORRECTIONS-----					
COORDINATES	VECT.	RANGE	DEFLTN	VECT.	RANGE	DEFLTN	X	Y
3497841.3N 569408.3E	112.1	373.5	1057.1	197.9	197.8	7.3	192.6	45.7
METEOR. PARAMETER	METEOR. VALUE	UNIT EFFECT		CORRECTION				
TEMPERATURE	.19	-12.22		-2.32				
DENSITY	1.66	60.22		99.97				
RANGE WIND	13.6	-20.08		-273.36				
CROSS WIND	19.4	-14.41		-280.00				

CORIOLIS CORRECTION= 30.12

DRIFT CORRECTION= 739.65

XX

DATE GUN CASE
27JAN65 A 2 22

HUACH 10 ZONES FIXED STATION

TARGET	-NO CORRECTIONS-		-----WITH CORRECTIONS-----					
COORDINATES	VECT.	RANGE	DEFLTN	VECT.	RANGE	DEFLTN	X	Y
3497864.0N 569307.1E	1061.0	397.1	983.9	232.0	222.5	-65.8	196.6	123.1
METEOR. PARAMETER	METEOR. VALUE	UNIT EFFECT		CORRECTION				
TEMPERATURE	.19	-12.25		-2.33				
DENSITY	1.66	59.77		99.22				
RANGE WIND	13.6	-20.01		-271.49				
CROSS WIND	19.5	-14.39		-280.08				

CORIOLIS CORRECTION= 29.76

DRIFT CORRECTION= 739.87

TABLE 4-2 (continued)

DATE GUN CASE
27JAN65 P 1 23

HUACH 10 ZONES FIXED STATION

TARGET COORDINATES	-NO CORRECTIONS-			-----WITH CORRECTIONS-----		
	VECT. ERROR	RANGE DEFULTN	VECT. ERROR	VECT. ERROR	RANGE DEFULTN	VECT. ERROR
3497870.0N 569512.1E	1115.3	508.8	992.5	247.2	234.8	-77.2
METEOR. PARAMETER	METEOR. VALUE			CORRECTION		
TEMPERATURE	.33			-11.93		
DENSITY	.99			61.10		
RANGE WIND	16.3			-20.23		
CROSS WIND	20.1			-14.56		

CORIOLIS CORRECTION= 30.45

DRIFT CORRECTION= 746.84

XX

DATE GUN CASE
27JAN65 P 2 24

HUACH 10 ZONES FIXED STATION

TARGET COORDINATES	-NO CORRECTIONS-			-----WITH CORRECTIONS-----		
	VECT. ERROR	RANGE DEFULTN	VECT. ERROR	VECT. ERROR	RANGE DEFULTN	VECT. ERROR
3497886.6N 569388.0E	1088.7	541.0	944.8	295.6	268.9	-122.7
METEOR. PARAMETER	METEOR. VALUE			CORRECTION		
TEMPERATURE	.33			-12.01		
DENSITY	.99			60.46		
RANGE WIND	16.3			-20.13		
CROSS WIND	20.1			-14.51		

CORIOLIS CORRECTION= 30.02

DRIFT CORRECTION= 745.51

TABLE 4-2 (continued)

DATE GUN CASE
29JAN65 A 1 25

HUACH 10 ZONES FIXED STATION

TARGET		-NO CORRECTIONS-		-WITH CORRECTIONS-			
COORDINATES		VECT.	RANGE DEFLT	VECT.	RANGE DEFLT	X	Y
3497843.5N	569416.3E	882.5	195.4	860.7	462.1	460.6	37.9
						454.0	86.2
METEOR. PARAMETER		METEOR. VALUE		UNIT EFFECT		CORRECTION	
TEMPERATURE		1.79		-12.20		-21.84	
DENSITY		-0.03		67.63		-2.03	
RANGE WIND		-13.9		-20.84		289.06	
CROSS WIND		3.6		-14.42		-52.41	
CORIOLIS CORRECTION=	30.14			DRIFT CORRECTION=		740.21	

XX

DATE GUN CASE
29JAN65 A 2 26

HUACH 10 ZONES FIXED STATION

TARGET		-NO CORRECTIONS-		-WITH CORRECTIONS-			
COORDINATES		VECT.	RANGE DEFLT	VECT.	RANGE DEFLT	X	Y
3497860.1N	569292.9E	850.3	200.4	826.4	464.3	464.3	6.0
						448.8	119.0
METEOR. PARAMETER		METEOR. VALUE		UNIT EFFECT		CORRECTION	
TEMPERATURE		1.79		-12.28		-21.98	
DENSITY		-0.03		66.90		-2.01	
RANGE WIND		-13.9		-20.74		287.85	
CROSS WIND		3.6		-14.37		-51.76	
CORIOLIS CORRECTION=	29.71			DRIFT CORRECTION=		738.88	

TABLE 4-2 (continued)

DATE GUN CASE
29JAN65 P 1 27

HUACH 10 ZONES FIXED STATION

TARGET	-NO CORRECTIONS-				-WITH CORRECTIONS-			
COORDINATES	VECT.	RANGE	DEFLT	VECT.	RANGE	DEFLT	X	Y
3497881.0N 569551.6E	963.2	333.6	903.6	401.2	401.2	4.5	387.9	102.6

METEOR. PARAMETER	METEOR. VALUE	UNIT EFFECT	CORRECTION
TEMPERATURE	2.19	-11.81	-25.86
DENSITY	-0.66	68.98	-45.53
RANGE WIND	-6.6	-21.04	139.01
CROSS WIND	8.1	-14.62	-118.91

CORIOLIS CORRECTION= 30.58 DRIFT CORRECTION= 749.58

XX

DATE GUN CASE
29JAN65 P 2 28

HUACH 10 ZONES FIXED STATION

TARGET	-NO CORRECTIONS-				-WITH CORRECTIONS-			
COORDINATES	VECT.	RANGE	DEFLT	VECT.	RANGE	DEFLT	X	Y
3497896.3N 569422.8E	919.6	338.9	854.9	408.6	406.5	-41.4	380.4	149.1

METEOR. PARAMETER	METEOR. VALUE	UNIT EFFECT	CORRECTION
TEMPERATURE	2.19	-11.91	-26.08
DENSITY	-0.66	68.19	-45.01
RANGE WIND	-6.6	-20.93	138.68
CROSS WIND	8.1	-14.56	-118.19

CORIOLIS CORRECTION= 30.13 DRIFT CORRECTION= 747.94

TABLE 4-2 (continued)

DATE GUN CASE
02FEB65 A 1 20

HUACH 10 ZONES FIXED STATION

TARGET	-NO CORRECTIONS-		-----WITH CORRECTIONS-----	
COORDINATES	VECT.	RANGE DEFLT	VECT.	RANGE DEFLT
3497868.0N 569504.9E	ERROR	ERROR	ERROR	ERROR
	754.4	442.0	611.9	257.9
METEOR. PARAMETER	METEOR. VALUE	UNIT EFFECT	CORRECTION	
TEMPERATURE	1.85	-11.95	-22.11	
DENSITY	-.27	68.51	-18.30	
RANGE WIND	23.0	-20.22	-465.51	
CROSS WIND	-28.5	-14.55	414.58	
CORIOLIS CORRECTION=	30.43		DRIFT CORRECTION=	746.34

XX

DATE GUN CASE
02FEB65 A 2 30

HUACH 10 ZONES FIXED STATION

TARGET	-NO CORRECTIONS-		-----WITH CORRECTIONS-----	
COORDINATES	VECT.	RANGE DEFLT	VECT.	RANGE DEFLT
3497882.4N 569372.9E	ERROR	ERROR	ERROR	ERROR
	733.4	447.5	581.1	226.2
METEOR. PARAMETER	METEOR. VALUE	UNIT EFFECT	CORRECTION	
TEMPERATURE	1.85	-12.05	-22.29	
DENSITY	-.27	67.69	-18.28	
RANGE WIND	23.1	-20.11	-464.42	
CROSS WIND	-28.4	-14.49	412.08	
CORIOLIS CORRECTION=	29.97		DRIFT CORRECTION=	744.45

TABLE 4-2 (continued)

DATE GUN CASE
04FEB65 A 1 33

HUACH 10 ZONES FIXED STATION

TARGET		-NO CORRECTIONS-		-----WITH CORRECTIONS-----			
COORDINATES		VECT.	RANGE DEFLT	VECT.	RANGE DEFLT	X	Y
3497880.5N	569549.8E	779.9	122.4	770.0	204.8	203.7	-21.0
						190.8	74.5

METEOR. PARAMETER		METEOR. VALUE	UNIT EFFECT	CORRECTION
TEMPERATURE		2.23	-11.82	-26.36
DENSITY		-0.01	68.97	-1.38
RANGE WIND		-5.2	-21.04	109.12
CROSS WIND		.7	-14.62	-10.89

CORIOLIS CORRECTION= 30.57 DRIFT CORRECTION= 749.46

XX

DATE GUN CASE
04FEB65 A 2 34

HUACH 10 ZONES FIXED STATION

TARGET		-NO CORRECTIONS-		-----WITH CORRECTIONS-----			
COORDINATES		VECT.	RANGE DEFLT	VECT.	RANGE DEFLT	X	Y
3497887.9N	569392.4E	765.5	184.7	742.9	268.5	264.9	-43.6
						243.5	113.2

METEOR. PARAMETER		METEOR. VALUE	UNIT EFFECT	CORRECTION
TEMPERATURE		2.23	-12.00	-26.76
DENSITY		-0.02	67.89	-1.36
RANGE WIND		-5.2	-20.89	108.37
CROSS WIND		.7	-14.52	-10.64

CORIOLIS CORRECTION= 30.03 DRIFT CORRECTION= 745.82

TABLE 4-2 (continued)

DATE GUN CASE
04FEB65 P 1 35

HUACH 10 ZONES FIXED STATION

TARGET COORDINATES	-NO CORRECTIONS-			-----WITH CORRECTIONS-----				
	VECT. ERROR	RANGE ERROR	DEFLT N	VECT. ERROR	RANGE ERROR	DEFLT N	X	Y
3497892.4N 569593.1E	790.5	225.1	757.8	225.2	223.6	27.0	222.7	33.5

METEOR. PARAMETER	METEOR. VALUE	UNIT EFFECT	CORRECTION
TEMPERATURE	2.12	-11.69	-24.78
DENSITY	-.28	69.40	-19.43
RANGE WIND	-2.0	-21.10	42.67
CROSS WIND	-3.6	-14.68	52.38

CORIOLIS CORRECTION= 30.71

DRIFT CORRECTION= 752.46

XX

DATE GUN CASE
04FEB65 P 2 36

HUACH 10 ZONES FIXED STATION

TARGET COORDINATES	-NO CORRECTIONS-			-----WITH CORRECTIONS-----				
	VECT. ERROR	RANGE ERROR	DEFLT N	VECT. ERROR	RANGE ERROR	DEFLT N	X	Y
3497885.4N 569383.5E	785.0	284.3	731.7	282.0	281.8	8.4	273.7	57.7

METEOR. PARAMETER	METEOR. VALUE	UNIT EFFECT	CORRECTION
TEMPERATURE	2.12	-12.02	-25.48
DENSITY	-.28	67.80	-18.98
RANGE WIND	-2.0	-20.88	42.05
CROSS WIND	-3.6	-14.51	51.84

CORIOLIS CORRECTION= 30.00

DRIFT CORRECTION= 745.20

TABLE 4-2 (continued)

DATE GUN CASE
06 FEB 65 A 1 37

HUAICH 10 ZONES, FIXED STATION

TARGET		-NO CORRECTIONS-			-----WITH-----			CORRECTIONS-----		
COORDINATES		VECT.	RANGE	DEFLTN	VECT.	RANGE	DEFLTN	X	Y	
		ERROR	ERROR	ERROR	ERROR	ERROR	ERROR	COMP.	COMP.	COMP.
3497853.0N	569453.9E	1292.4	1117.5	649.2	63.6	-30.8	55.7	-14.8	-61.9	

METEOR. PARAMETER	METEOR. VALUE	UNIT	LFFECT	CORRECTION
TEMPERATURE	1.39		-12.09	-16.81
DENSITY	-1.02		68.00	-69.36
RANGE WIND	52.7		-20.15	-1062.14
CROSS WIND	-12.4		-14.48	179.55

COROLIS CORRECTION= 30.26 DRIFT CORRECTION= 742.81

[illegible]

DATE GUN CASE
06FEB65 A 2 38

HUACH 10 ZONES FIXED STATION

TARGET		-NO CORRECTIONS-				-WITH-				CORRECTIONS-			
COORDINATES		VECT.	RANGE	DLFLTN		VECT.	RANGE	DLFLTN		X	Y	COMP.	
		ERRR	ERRR	ERRR		-ERRR	ERRR	ERRR		ERRR	ERRR	COMP.	
3497878.9N	569360.3E	1268.4	1098.8	633.6		59.8	-46.5	37.7		-34.6		-48.8	

METEOR. PARAMETER	METEOR. VALUE	UNIT EFFECT	CORRECTION
TEMPERATURE	1.39	-12.09	-16.81
DENSITY	-1.02	67.57	-68.92
RANGE WIND	52.7	-20.09	-1059.56
CROSS WIND	-12.3	-14.47	177.63

CORIOLIS CORRECTION= 20.93 DRIFT CORRECTION= 743.58

TABLE 4-2 (continued)

DATE GUN CASE
-6FEB65 P 1 39

HUACH 10 ZONES FIXED STATION

TARGET		-NO CORRECTIONS-	-WITH CORRECTIONS-	
COORDINATES		VECT.	RANGE DEFLTN	X Y
		ERROR	ERROR	COMP.
3497849.0N	-69436.0E	1523.1	1351.1	683.5
METEOR. PARAMETER		METEOR. VALUE	EFFECT	CORRECTION
TEMPERATURE		- .01	- .00	.09
DENSITY		- .76	- .82	-51.54
RANGE WIND		00.0	- 0.12	-1371.82
CROSS WIND		- 17.0	- -.45	174.33

CORIOLIS CORRECTION= 30.2.
DATE CORRECTION= 741.57[illegible]

DATE GUN CASE
06FEB65 P 2 40

" " 19 / 20 , FIXED STATION

[illegible]CORIOLIS CORRECTION= 30.02
DRIFT CORRECTION= 745.57

TABLE 4-2 (continued)

DATE GUN CASE
10FEB65 P 1 43

HUACH 10 ZONES FIXED STATION

TARGET COORDINATES	-NO CORRECTIONS-			-----WITH CORRECTIONS-----		
	VECT. ERROR	RANGE DEFULTN ERROR	VECT. ERROR	RANGE DEFULTN ERROR	VECT. ERROR	RANGE DEFULTN ERROR
3497851.4N 169444.0E	1217.8	488.1	833.3	233.2	-191.4	133.3
METEOR. PARAMETER	UNIT EFFECT			CORRECTION		
TEMPERATURE	-2.45			21.98		
DENSITY	.86			52.06		
RANGE WIND	57.3			-1153.60		
CROSS WIND	-5.0			72.46		
CORIOLIS CORRECTION=	30.24			DRIFT CORRECTION= 742.19		

XX

DATE GUN CASE
10FEB65 P 2 44

HUACH 10 ZONES FIXED STATION

TARGET COORDINATES	-NO CORRECTIONS-			-----WITH CORRECTIONS-----		
	VECT. ERROR	RANGE DEFULTN ERROR	VECT. ERROR	RANGE DEFULTN ERROR	VECT. ERROR	RANGE DEFULTN ERROR
3497871.2N 569332.9E	1184.8	861.2	813.6	242.0	-214.3	112.4
METEOR. PARAMETER	UNIT EFFECT			CORRECTION		
TEMPERATURE	-2.45			22.17		
DENSITY	.86			51.58		
RANGE WIND	57.3			-1149.25		
CROSS WIND	-4.9			70.31		
CORIOLIS CORRECTION=	29.84			DRIFT CORRECTION= 741.66		

TABLE 4-2 (continued)

DATE GUN CASE
12FEB65 P 1 47

HUACH 10 ZONES FIXED STATION

TARGET COORDINATES	-NO CORRECTIONS-			-----WITH CORRECTIONS-----		
	VECT. ERROR	RANGE ERROR	DEFLT N	VECT. ERROR	RANGE ERROR	DEFLT N
3497844.5N 569419.9E	1158.0	345.0	1105.4	350.3	332.5	-110.2
						291.1
						194.8

METEOR. PARAMETER	METEOR. VALUE	UNIT EFFECT	CORRECTION
TEMPERATURE	-1.57	-9.06	14.22
DENSITY	1.21	60.32	72.99
RANGE WIND	5.0	-20.10	-99.71
CROSS WIND	30.8	-14.43	-444.99

CORIOLIS CORRECTION= 30.16 DRIFT CORRECTION= 740.45

XX

DATE GUN CASE
12FEB65 P 2 48

HUACH 10 ZONES FIXED STATION

TARGET COORDINATES	-NO CORRECTIONS-			-----WITH CORRECTIONS-----		
	VECT. ERROR	RANGE ERROR	DEFLT N	VECT. ERROR	RANGE ERROR	DEFLT N
3497867.7N 569320.4E	1156.4	365.2	1097.2	373.1	354.0	-117.9
						309.3
						208.7

METEOR. PARAMETER	METEOR. VALUE	UNIT EFFECT	CORRECTION
TEMPERATURE	-1.57	-9.09	14.27
DENSITY	1.21	59.88	72.45
RANGE WIND	4.9	-20.03	-97.90
CROSS WIND	30.8	-14.41	-444.54

CORIOLIS CORRECTION= 29.80 DRIFT CORRECTION= 740.80

TABLE 4-3
COMPARISON OF RESIDUAL ERRORS USING CRAM
VS. SINGLE STATION (FT. HUACHUCA), IN METERS

Date/time	Case	CRAM analysis			Ft. Huachuca		
		Vector error	Range* error	Deflection error	Vector error	Range* error	Deflection error
1/16 AM	1	28.9	- 18.8	22.0	45.5	- 3.1	45.4
PM	3	91.7	- 68.7	- 60.8	122.4	- 68.9	-101.2
1/18 AM	5	47.0	12.5	- 45.3	75.8	11.9	- 74.9
PM	7	52.2	47.4	- 21.9	20.1	12.0	- 16.1
1/20 AM	9	112.6	112.6	1.8	124.3	115.8	45.2
PM	11	105.1	104.5	- 11.4	—	—	—
1/22 AM	13	390.0	238.5	-308.6	—	—	—
PM	15	387.0	259.9	-296.8	503.2	381.5	-328.2
1/25 AM	17	567.9	-345.5	450.7	—	—	—
PM	19	208.5	- 77.3	193.6	168.0	- 91.0	141.2
1/27 AM	21	34.7	- 34.7	1.5	26.4	- 25.4	7.3
PM	23	63.5	25.0	- 58.4	83.3	31.4	- 77.2
1/29 AM	25	39.5	22.8	32.2	52.1	35.8	37.9
PM	27	66.6	59.1	30.7	30.2	29.9	4.5
2/2 AM	29	251.4	-127.9	216.4	331.8	-218.5	249.7
PM	31	236.4	-181.1	151.9	—	—	—
2/4 AM	33	146.6	-139.2	- 45.9	158.7	-157.3	- 21.0
PM	35	89.8	- 89.6	5.5	117.2	-114.0	27.0
2/6 AM	37	46.9	33.3	33.0	64.5	32.6	55.7
PM	39	207.5	186.9	90.1	143.4	114.8	86.0
2/10 AM	41	224.2	- 54.7	217.4	—	—	—
PM	43	167.2	- 68.2	152.7	163.3	- 94.3	133.3
2/12 AM	45	43.1	- 9.8	- 42.0	65.9	35.4	- 55.6
PM	47	99.5	45.0	- 88.7	119.5	46.2	-110.2
Average absolute†		115.0	75.7	75.2	127.1	85.3	85.1

*With empirical correction.

†For the 19 comparative cases.

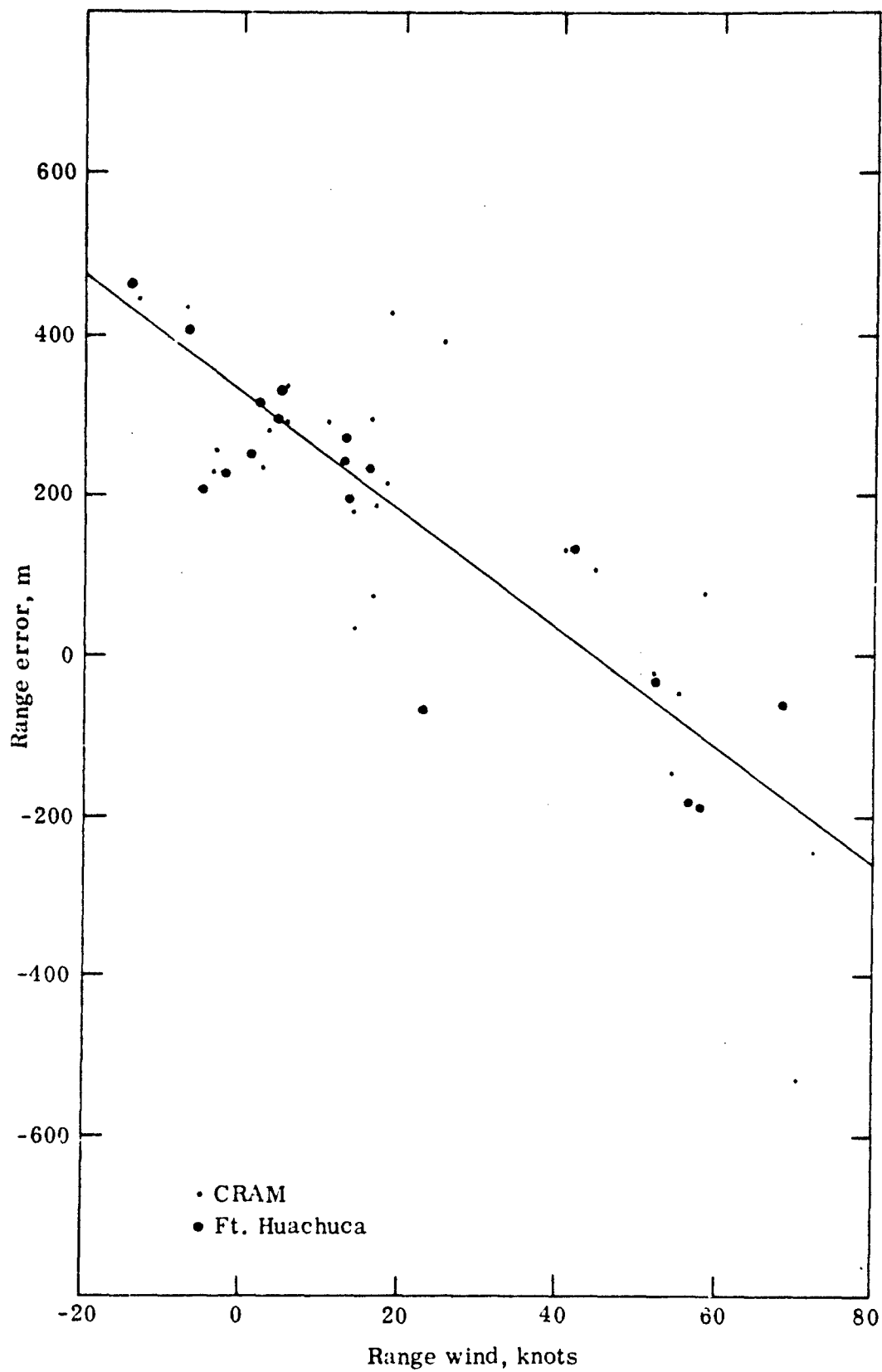


Fig. 4-1. Range wind versus range error.

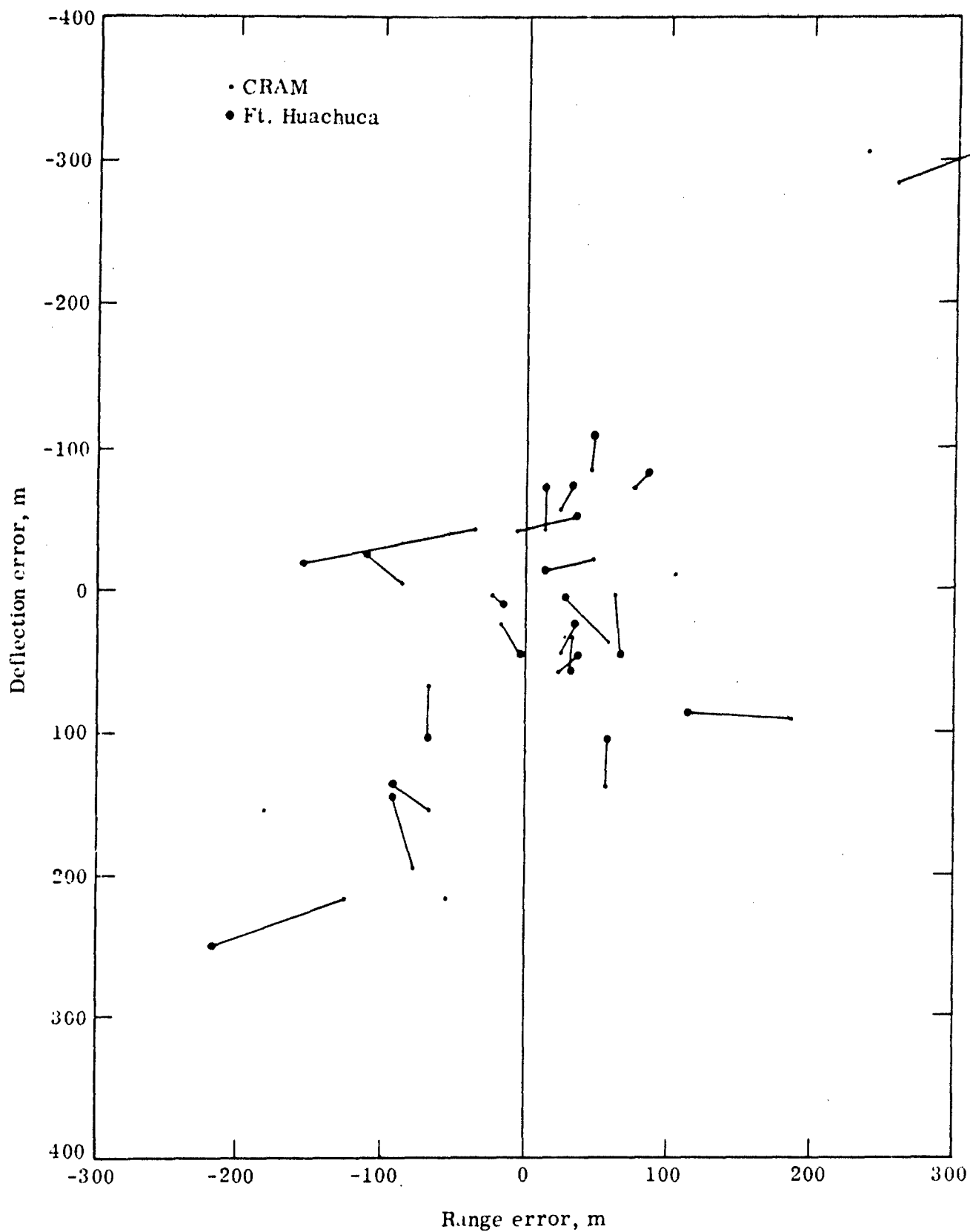


Fig. 4-2. Residual errors for artillery firings (Gun No. 1) based on CRAM and Ft. Huachuca (from Table 4-3).

5.0 TIME VARIATIONS IN THE BALLISTIC WIND

5.1 Computation Procedure

Variability measures appropriate to the ballistic wind data and to the way in which the basic rawinsonde observations were scheduled are the root-mean-square (rms) wind component differences and the rms difference vector magnitudes.

These quantities were computed at all grid points for the time lags of 2, 4, 6, and 8 hours, and for lines 2, 4, 6, 8, and 10. The sample size varied with time lag because of the procedure used in scheduling the observation runs. Table 5-1 shows the distribution of differences computed by lag and terminal hour, for any given line.

TABLE 5-1
DISTRIBUTION OF WIND DIFFERENCES COMPUTED BY LAG AND TERMINAL HOUR

Lag (hr)	Terminal hour (MST)				Row totals
	0800	1000	1200	1400	
2	16	16	16	16	64
4	X	16	16	16	48
6	X	X	16	16	32
8	X	X	X	16	16

The computer output consisted of a field of grid-point values of the variability measures for each terminal hour and lag, and pooled values for all terminal hours for each lag. Subsequently, field-averages were calculated from the computer output. These field-averages were obtained from that portion of the analysis field in which the data are densest, extending from grid-point 347 through 355 inclusive in the north-south direction, and from grid-point 52 through 64 inclusive in the east-west direction. Details of the computational procedure are given in the computer program specifications that follow.

5.1.1 Computations for Time Variability Studies

These specifications outline the computation of the rms vector difference between pairs of ballistic winds separated by given time intervals, for a set of time intervals. The statistics are computed for selected line ballistic winds and at each grid point in the analysis field. Also computed are various quantities to be used in predictability studies.

5.1.2 Input

The following quantity is input:

$\begin{bmatrix} u \\ v \end{bmatrix} (L, i, j, t)$ The two-component vector ballistic winds (knots) for the line L , at the time t , and the horizontal grid point with coordinate i, j , where

$L = 2, 4, 6, 8, 10$

$t = 1/12-0600 \text{ MST}, \dots, 2/12-1400 \text{ MST}$

$i = 1, \dots, I$

$j = 1, \dots, J.$

5.1.3 Output

The following quantities are to be output:

$\sigma_u(\tau, L, i, j, q)$ Root-mean-square ballistic wind component difference (knots) over the time interval τ , ending at the observation hour q , where,

$\tau = 2, 4, 6, 8 \text{ hours}$

$q = 1 + \tau/2 (\tau = 2, 4, 6, 8)$

$\sigma_v(\tau, L, i, j, q)$ Same as immediately preceding, but for v -component.

$\sigma(\tau, L, i, j, q)$ Same as immediately preceding, but for vector difference.

$\sigma_u(\tau, L, i, j)$ Same as σ_u above, but for all observation hours.

$\sigma_v(\tau, L, i, j)$ Same as σ_v above, but for all observation hours.

$\sigma(\tau, L, i, j)$ Same as σ above, but for all observation hours.

The following quantities are to be output with the predictability experiment output (see Section 8.0):

$\sigma_{u,p}(\tau, L, i, j, q)$ Root-mean-square u -component error of selected persistence forecasts over time period τ , and valid at the observation hour q .

$q = 2 + \tau/2 (\tau = 2, 4, 6)$

$\sigma_{v,p}(\tau, L, i, j, q)$ Same as immediately preceding, but for v -component error.

$\sigma_p(\tau, L, i, j, q)$ Same as immediately preceding, but for vector error.

$\sigma_{u,p}(\tau, L, i, j)$ Same as $\sigma_{u,p}$ above, but for all valid times.

$\sigma_{v,p}(\tau, L, i, j)$ Same as $\sigma_{v,p}$ above, but for all valid times.

$\sigma_p(\tau, L, i, j)$ Same as σ_p above, but for all valid times.

The following quantities are to be used in the predictability experiments:

$D_u(\tau, L, i, j, q)$ u-component differences

$D_v(\tau, L, i, j, q)$ v-component differences

$$q = 1 + \tau/2 \quad (\tau = 2, 4, 6, 8)$$

5.1.4 Computations

The sequence of map times is to be indexed (p, q) where the index p represents the observation day, $p = 1, \dots, 16$, and the index q represents the observation hour, $q = 1, 2, 3, 4, 5$.

Then, for fixed L, p, i, j , the difference components

$$D_u(L, p, i, j, \tau, q) = U_q - U_{q-\tau/2}$$

$$D_v(L, p, i, j, \tau, q) = V_q - V_{q-\tau/2}$$

$$[(1 + \tau/2) \leq q \leq 5]$$

are computed.

For each q , the mean square differences over all p are computed:

$$\sigma_u^2(\tau, L, i, j, q) = \frac{1}{16} \sum_{p=1}^{16} D_u^2(\tau, L, i, j, p, q)$$

$$\sigma_v^2(\tau, L, i, j, q) = \frac{1}{16} \sum_{p=1}^{16} D_v^2(\tau, L, i, j, p, q)$$

$$\sigma^2(\tau, L, i, j, q) = \sigma_u^2 + \sigma_v^2$$

$$[(1 + \frac{\tau}{2}) \leq q \leq 5]$$

and the mean square errors of the selected persistence forecasts,

$$\sigma_{u,p}^2(\tau, L, i, j, q)$$

$$\sigma_{v,p}^2(\tau, L, i, j, q)$$

$$\sigma_p^2(\tau, L, i, j, q),$$

are obtained by the same formulas, but with q restricted to

$$\left(2 + \frac{\tau}{2}\right) \leq q \leq 5 .$$

The corresponding root-mean-square output quantities are obtained by

$$\sigma = (\sigma^2)^{1/2} .$$

Now, for fixed τ , L , i , j , the mean square differences over all hours q are obtained from the above by

$$\sigma^2(\tau, L, i, j) = \frac{1}{\left(5 - \frac{\tau}{2}\right)} \sum_{q=1+\frac{\tau}{2}}^5 \sigma^2(\tau, L, i, j, q)$$

and similarly for σ_u^2 and σ_v^2 .

The mean square persistence forecast errors are obtained by

$$\sigma_p^2(\tau, L, i, j) = \frac{1}{\left(4 - \frac{\tau}{2}\right)} \sum_{q=1+\frac{\tau}{2}}^5 \sigma^2(\tau, L, i, j, q)$$

and similarly for $\sigma_{u,p}^2$ and $\sigma_{v,p}^2$.

5.2 Time-variability as a Function of Lag

5.2.1 Variability of Line-10 Ballistic Winds

Line-10 component variability parameters obtained from objective analyses at the midpoint of the test-firing trajectory are shown in Figs. 5-1 and 5-2. For these firings the u -component corresponds approximately to the range-wind component and the v -component to the cross-wind component. As may be seen from Table 5-1, there is a systematic reduction of sample size with time lag, which would tend to produce progressively more uncertainty in the variability estimate as time lag increases.

A qualitative estimate of the effect of the sampling inconsistency on the slope of the variability-lag curve was obtained by reducing the sample size for the 2-, 4-, and 6-hr lag variability estimates to that of the 8-hr lag estimates. This was done by including only differences between the 1400 ballistic wind and other ballistic winds in the sample. The reduced sample variability is also shown in Figs. 5-1 and 5-2. When compared to the full sample, a slight but systematic decrease in variability is evident which is more pronounced in the u -component variability.

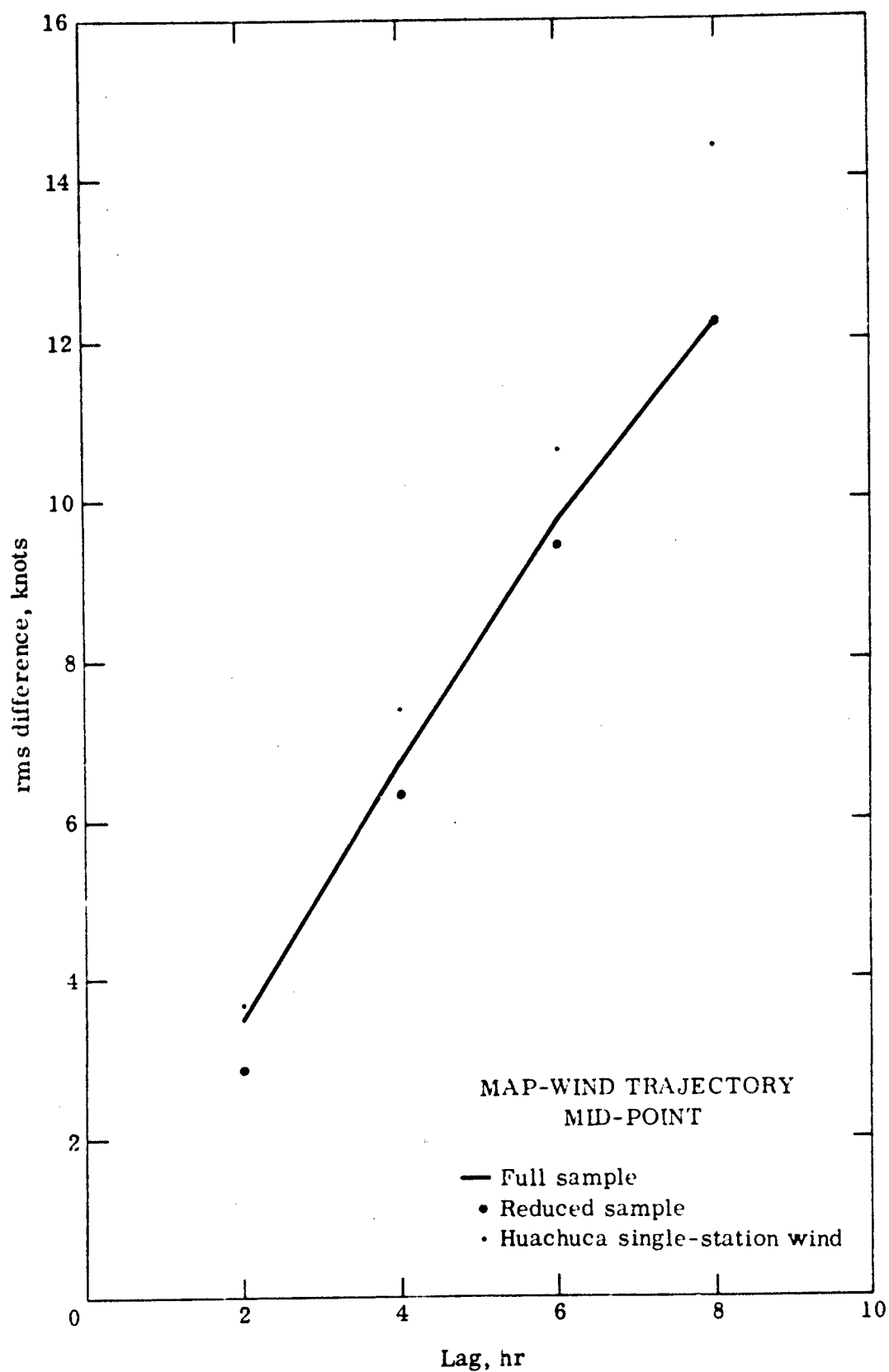


Fig. 5-1. Line-10 time variability, u-component.

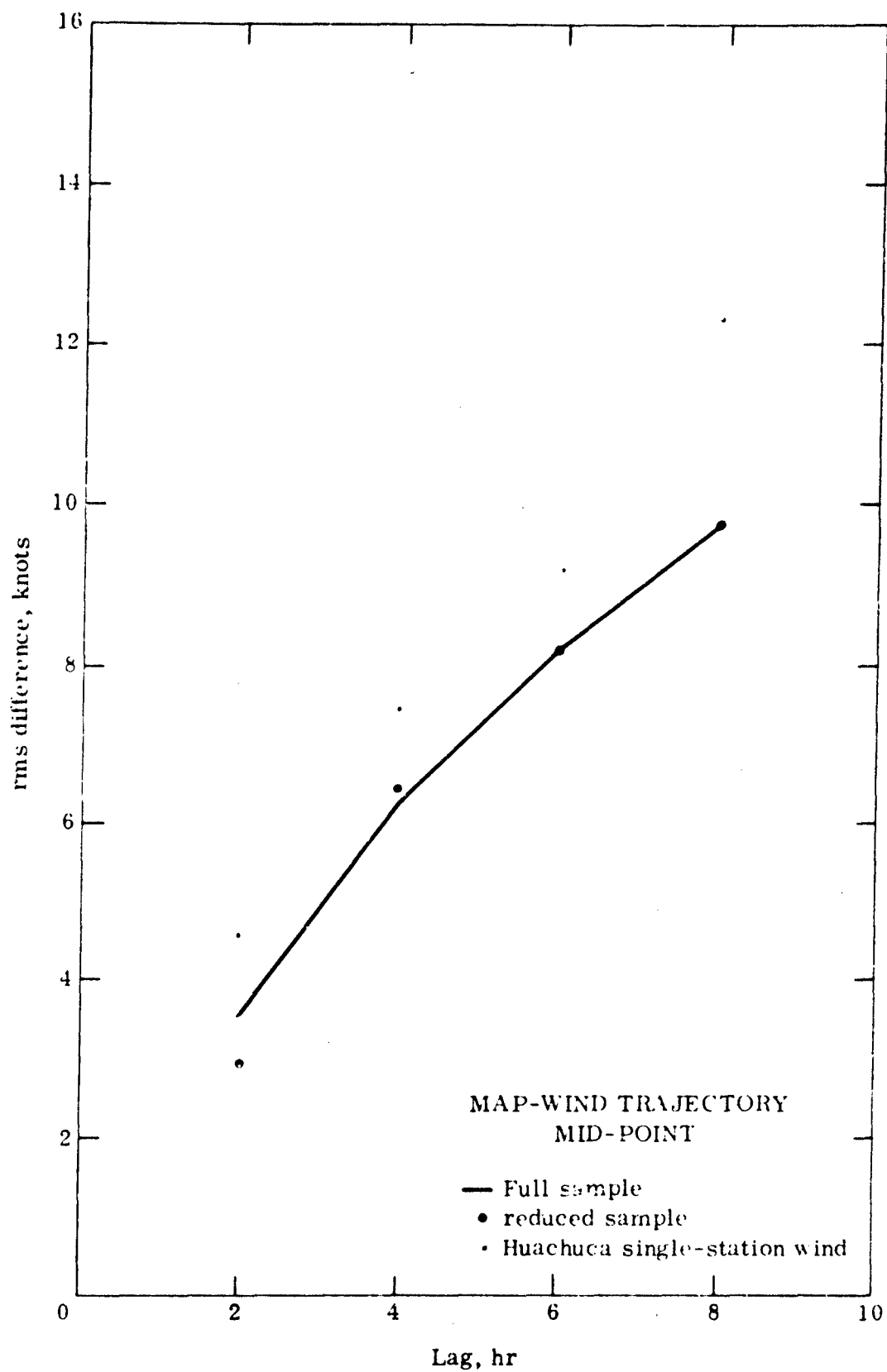


Fig. 5-2. Line-10 time variability, v-component.

The variability parameters obtained for the single sounding at Ft. Huachuca and the full sample are also shown. As would be expected, the map ballistic winds show smaller rms differences than do the single-sounding winds. This would imply a slower rate of decay of map wind with time, for artillery correction purposes. However, the variability parameter values exceed 5 knots in both components by the 4th hour, for the 16-day sample. Approximate unit effects applicable to the test firings would give rms displacement errors of 70 m and 100 m in deflection and range, respectively, for 5 knot rms wind differences.

5.2.2 Comparison with Ft. Sill Experiment Results

Figures 5-3 and 5-4 show the variability as a function of lag for the Line 4 ballistic wind components for an 8-day sample at Ft. Sill, as obtained from Bellucci (1961). Also shown are Line 4 rms component differences for the data obtained in the present study. In these figures the field-average variability (see Section 5.1) is shown for the analysis region, as well as the variability in selected single soundings. The lower variability characteristic of space-averaged map ballistic winds as compared to single sounding ballistic winds is evident in both figures. Terrain effects on the variability of low level ballistic winds, which will be discussed in more detail in Section 5.3 below, are seen in the generally higher u-component variability (Fig. 5-3) at Ft. Huachuca than at Ft. Sill. The v-component variability at Douglas is noticeably lower than at Ft. Sill in Fig. 5-4. The significance of these differences, of course, is questionable because of the limited sample size obtained in the two experiments. However, the irregularity in the Ft. Sill curve does suggest an underlying phenomenon characteristic of the western Great Plains which would be absent in mountainous terrain. This is the breakdown of the low-level nocturnal jet during the morning hours. The Ft. Sill variability at 4-hr lag is computed from differences between the 0600- and 1000-CST ballistic winds, as well as from differences between 0800- and 1200-CST ballistic winds. Where the nocturnal jet is present, these periods would be those of relatively large change in the morning hours (to which the observational sample was confined).

The curve for the relationship

$$\sigma_t = 2t^{1/2}$$

where σ is in knots and t in hours (Bellucci, 1961), is also shown in Figs. 5-3 and 5-4.

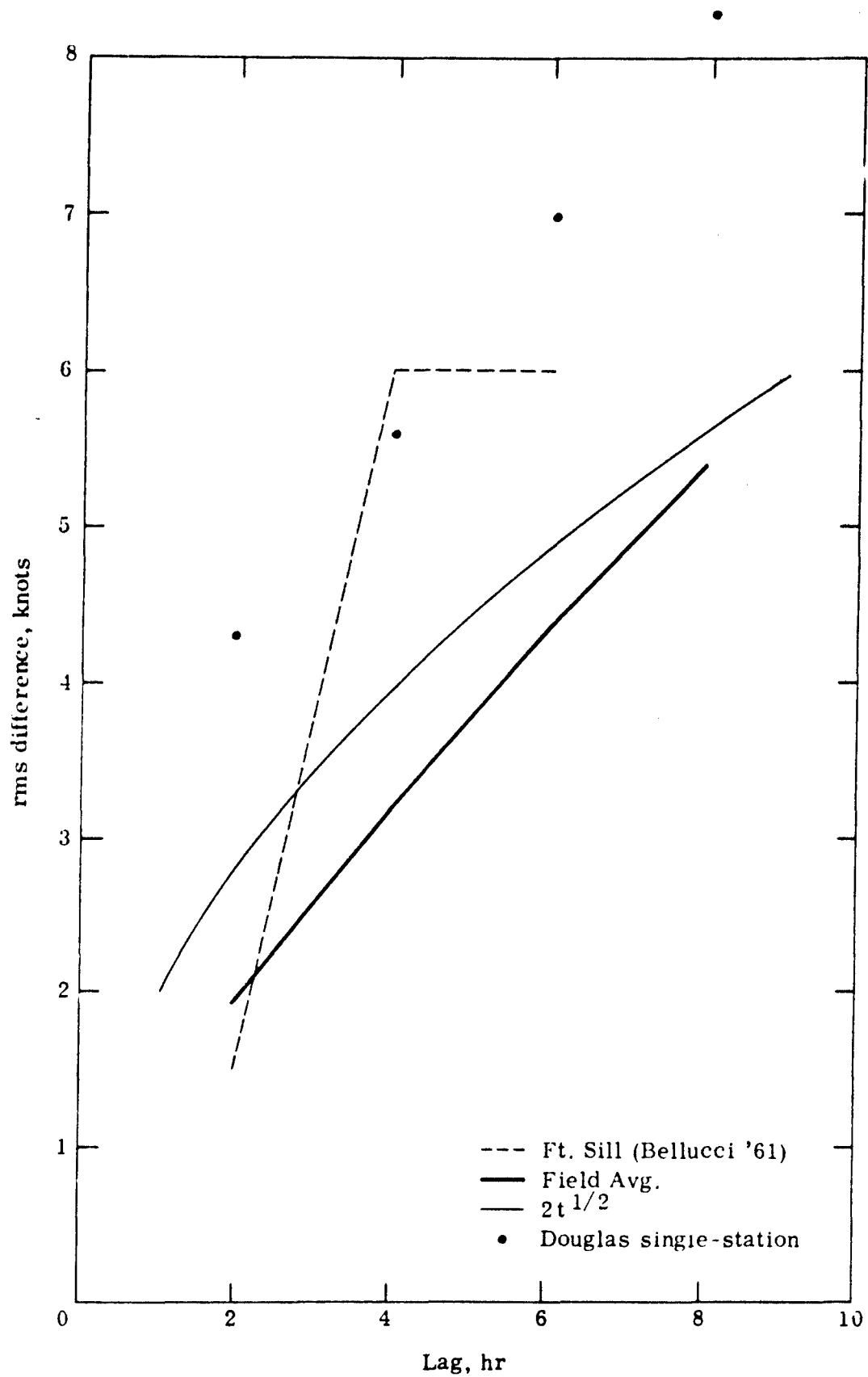


Fig. 5-3. Line-4 time variability, u-component.

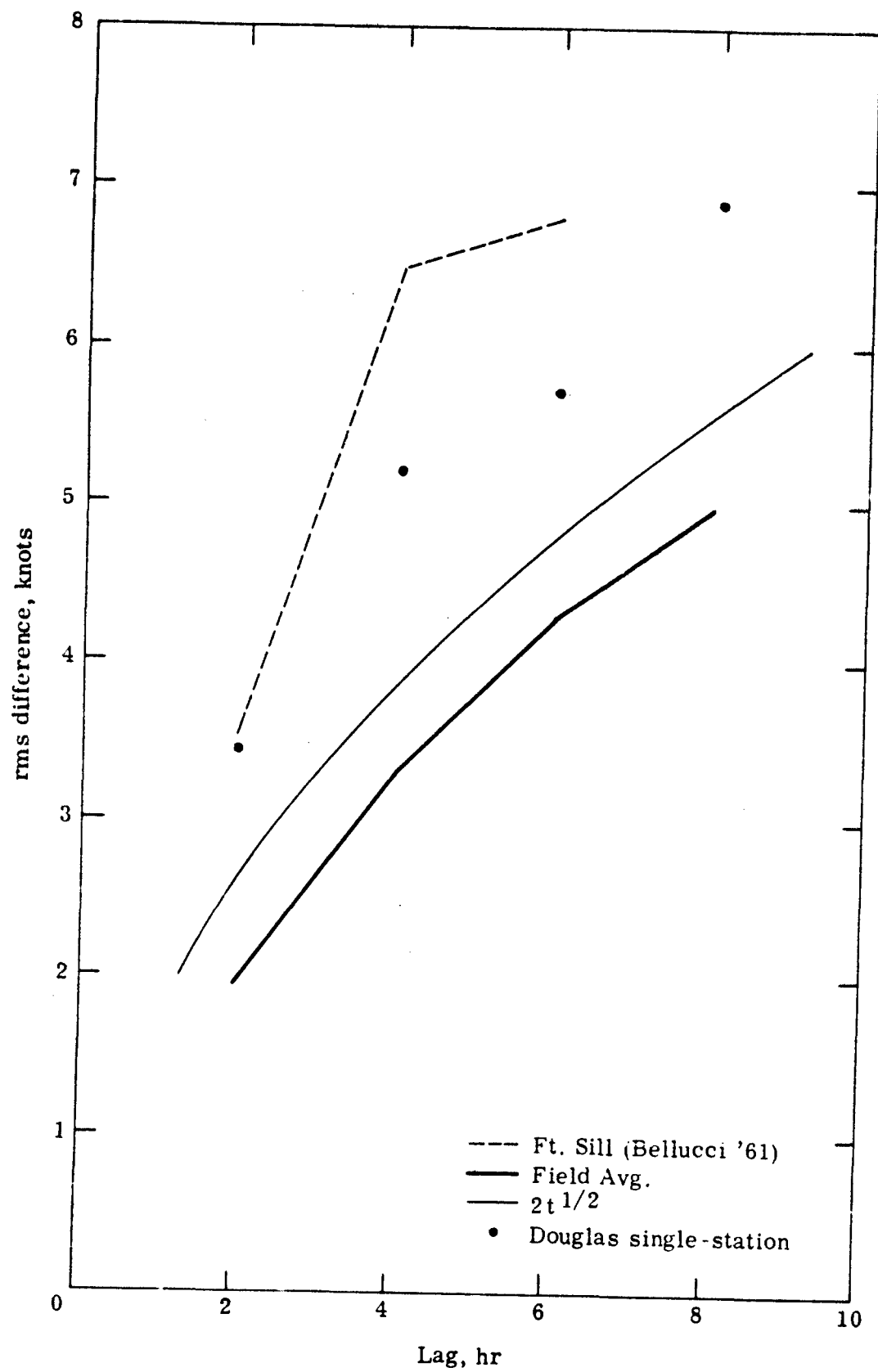


Fig. 5-4. Line-4 time variability, v-component.

This relationship appears more consistent with the mountainous terrain rms wind component differences than with Bellucci's variability for the Ft. Sill data, and agrees better with the field-average map-wind variability than with the single-sounding variability. Note, however, that this relationship does not fit the Line-10 data well (see Figs. 5-1 and 5-2).

5.3 Spatial Distribution of Time-variability Parameters

5.3.1 Effects of Analysis Procedure on Computed rms Differences

The method used for obtaining the initial-guess zone wind fields for the analysis procedure obviously has influence on the computed fields of time-variability parameters. Use of the preceding map for the initial-guess field would tend to produce maximum rms differences at the data points, while use of a second-order surface of best fit would tend to produce maximum variability at those boundary points furthest from data-dense regions.

Initial-guess fields were actually generated by combining the 2-hr previous map, where one was available, with the best fit surface, with equal weights. Thus, as would be expected, the two features described above are evident in the grid-point fields of rms differences.

These features are most pronounced for the lower level ballistic winds, where the data points are clustered about the fixed balloon release points. Figures 5-5 and 5-6 show typical fields of rms vector difference magnitude, in this case for time lag 2 hr, as obtained for Line 2 and Line 10. Note the contrast between the two fields caused by the more widespread distribution of data points used to obtain the Line-10 analyses.

The local maxima evident in the low-level fields tend to become more pronounced with increasing time lag. Figure 5-7 shows the field of vector variability for Line 2 based on an 8-hr time lag, which may be compared with Fig. 5-5.

5.3.2 Horizontal Distribution of Time Variability Parameters

Figure 5-6 is typical of the upper level rms ballistic wind difference fields by being remarkably uniform over most of the analysis area. In fact, the range in variability over the data-dense portion of the field specified in Section 5.1.1 is approximately one-half knot at Line 10, for 2-hr time lag, and increases to about one and a half

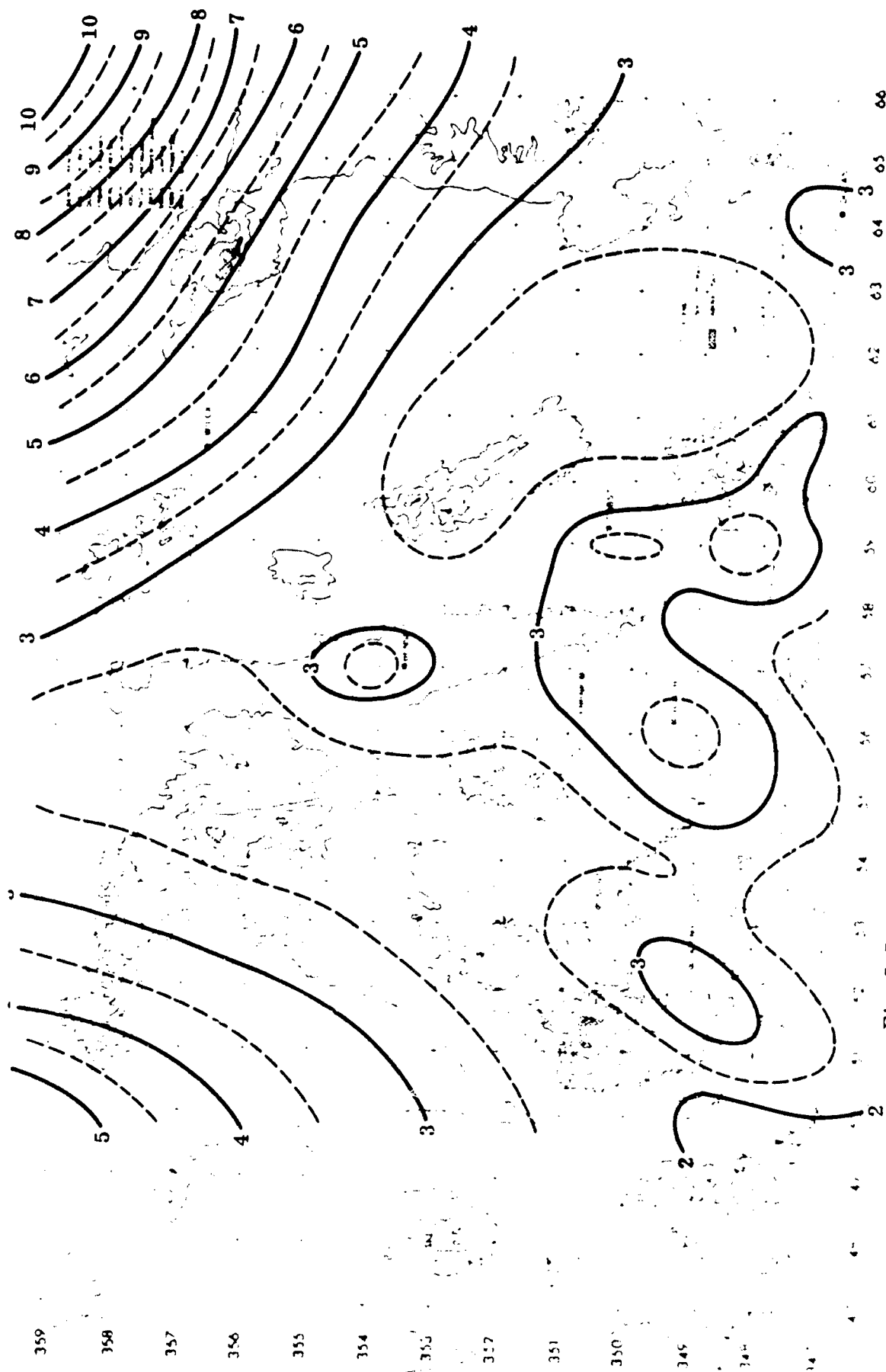


Fig. 5-5. Line-2 rms time differences, vector ($\tau = 2$).

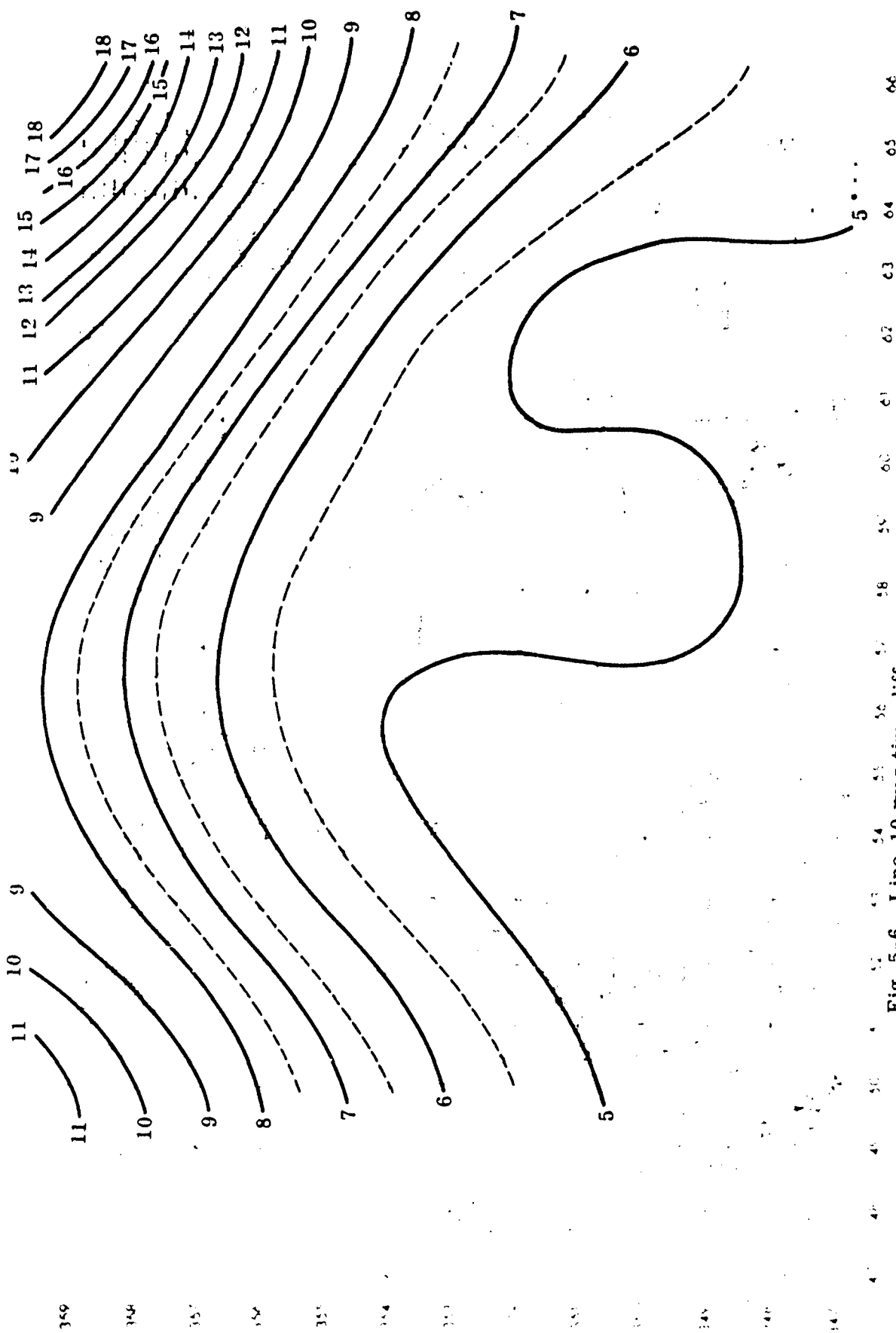


Fig. 5-6. Line-10 rms time differences, vector ($\tau = 2$).

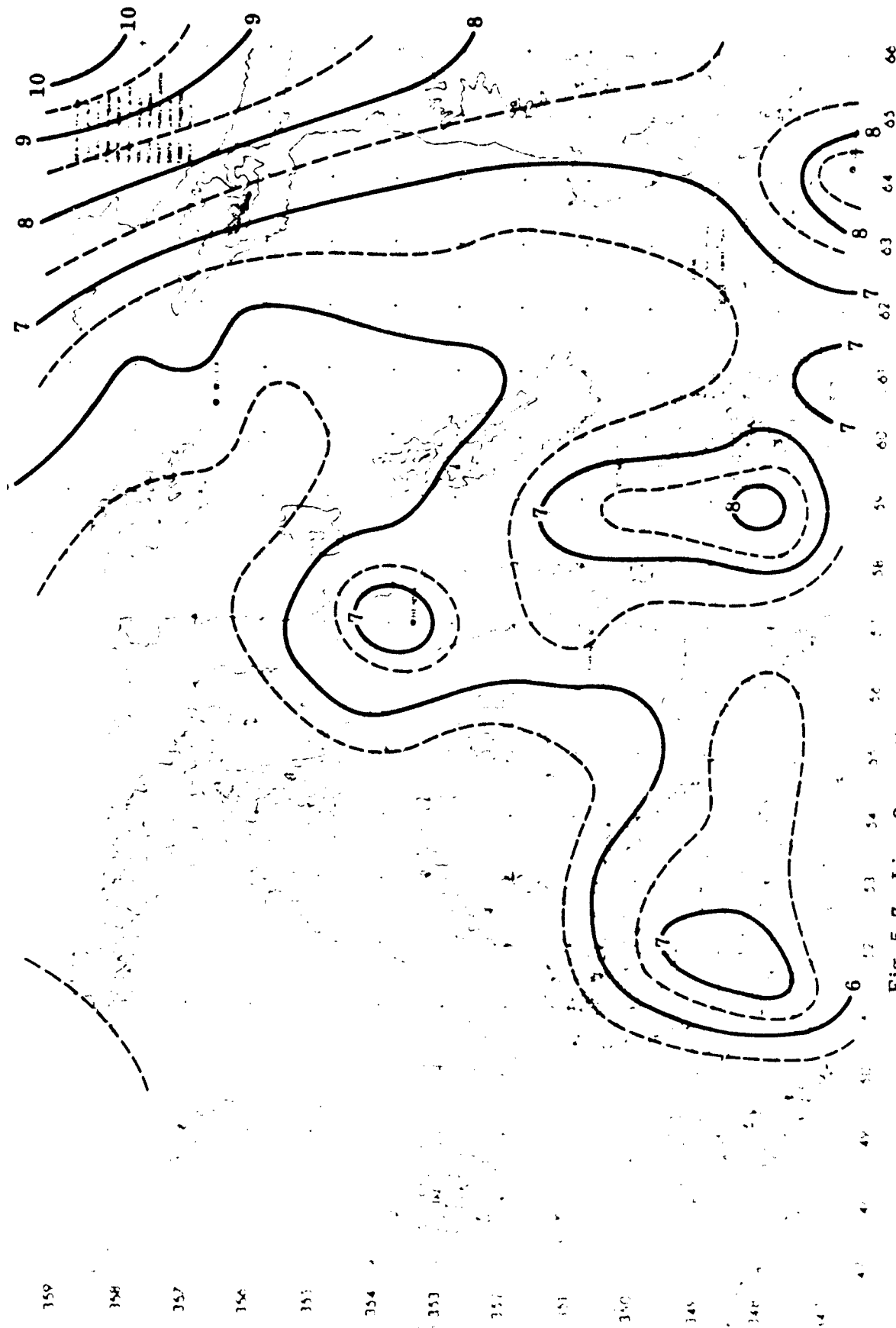


Fig. 5-7. Line-2 rms time differences, vector ($\tau = 8$).

knots for 8-hr time lag.

At the lower levels, however, some terrain effects on the time variability may be noted. If only those grid-point values nearest the balloon release points are plotted, and isopleths of equal rms wind (component or vector) differences are drawn with a topographic map as background, maps similar to those illustrated in Figs. 5-8, 5-9, and 5-10 may be obtained for all four values of time lag. The maps shown are for 8-hr time lag, and thus, show generally larger magnitude rms differences than maps for shorter time lags would exhibit. However, the patterns evident are characteristic of the shorter time lags also. A region of maximum variability on the v-component is seen in the triangle Hereford, Tombstone, Fairbanks, near the head of a large north-south valley (see Fig. 5-9), and lower values are seen in the Nogales-Patagonia-Sonoita region where topographic features have a more east-west orientation. The opposite arrangement of maxima and minima may be seen in the u-component variability, while both regions exhibit maxima in the vector wind variability.

The range in variability over the data-dense portion of the analysis field is generally larger at Line 2 than at Line 10. The spatial range in variability is about 1 knot at Line 2 for 2-hr time lag, and increases to almost 2 knots for an 8-hr time lag (see Fig. 5-10).

5.3.3 Vertical Distribution of Time Variability Parameters

Vertical profiles of the time variability show the expected general increase with height. Figure 5-11 shows such profiles for field-average rms vector difference magnitudes, for lags of 2, 4, 6, and 8 hr, as a function of height. Topographic effects are noticeable, particularly with regard to short period variability, in the irregularity of the rate of increase with height in the lower 5000 m in Fig. 5-11. Figure 5-12 shows similar profiles for rms u-component differences, in which the topographic effects on the low level profiles are less pronounced. Figure 5-14 shows the v-component differences in which the topographic effects are most evident.

Some evidence for the association of these low level effects with the topography is evident in Figs. 5-13 and 5-15, in which selected individual grid-point values, rather than field averages, are shown. Two pairs of grid points closest to stations with (a) large contrast in component variability as indicated by the Figs. 5-8 and 5-9,

349

358

357

356

355

354

353

352

351

350

349

348

347

47

46

45

44

43

42

41

40

39

38

37

36

35

34

33

32

31

30

29

28

27

26

25

Fig. 5-8. Line-2 rms time differences, u-component ($\tau = 8$).



349

348

347

346

345

344

343

342

341

340

339

338

337

336

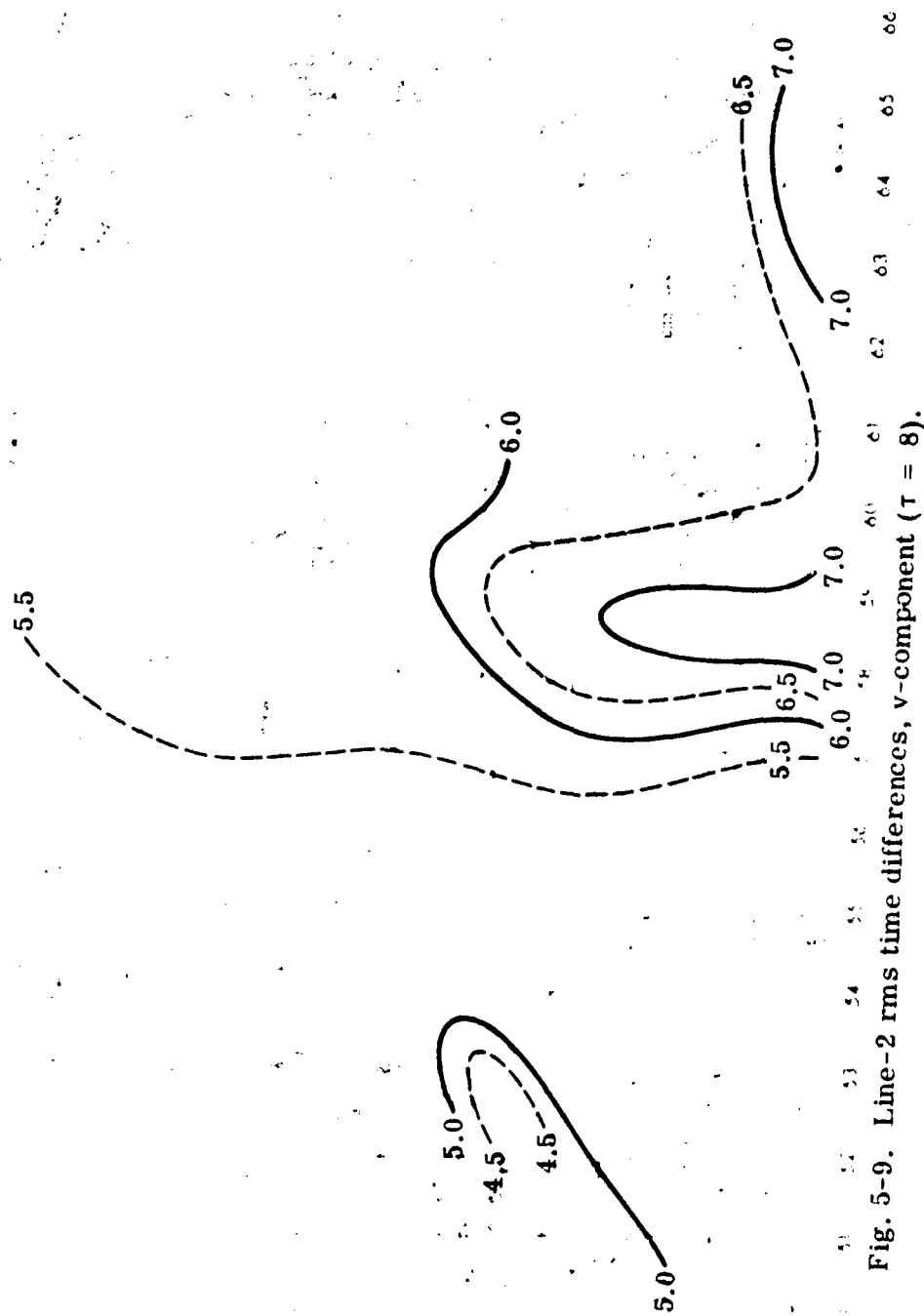


Fig. 5-9. Line-2 rms time differences, v-component ($\tau = 8$).

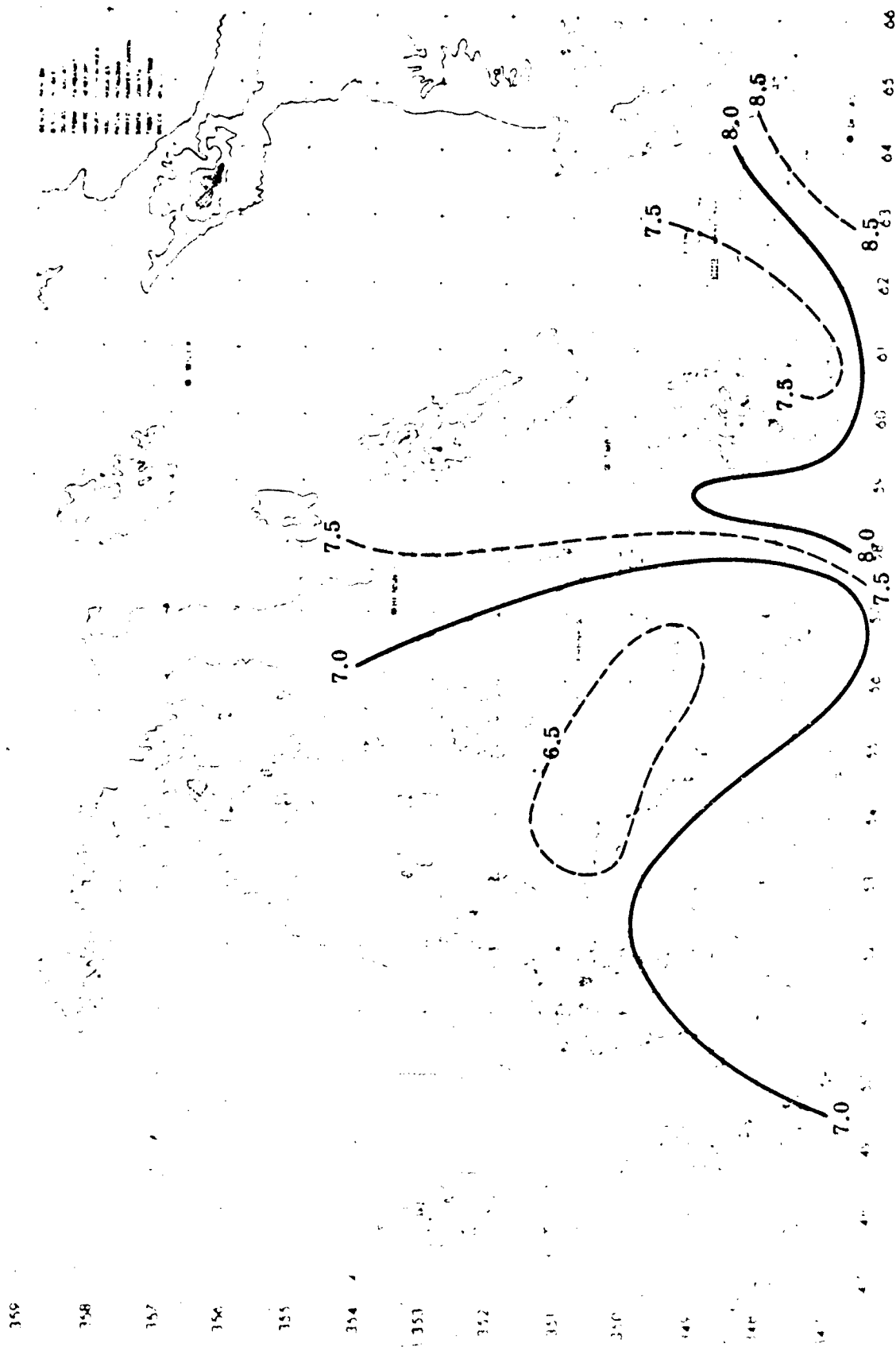


Fig. 5-10. Line-2 rms time differences, vector ($\tau = 2$)—based on selected grid points.

and (b) a similar number of total observations in each sample, were selected to illustrate the range in profiles within the sample.

Figure 5-13 shows that the lower portions of the profiles of u-component short-period variability represent larger variability in this component at Huachuca than at Fairbanks. Figure 5-15 shows a similar contrast in the v-component profiles for Hereford and Patagonia. Note the decrease with height in v-component variability at Hereford at all time lags in the height interval between Line 2 and Line 4.

5.4 Hour-to-hour Range of Time Variability Parameters

Figure 5-16 shows the range of variation of 2-hr and 4-hr lag variability at the grid point nearest Ft. Huachuca at Line 10 as a function of the hour of the day. The hour here is that of the later map ballistic wind used in computing the vector ballistic wind differences.

It is evident that the range in variability for a given lag is definitely smaller than the difference in variability between lags, being approximately one-half to one knot as compared to four knots. An interesting feature to be investigated in later studies is the peak in both 2-hr and 4-hr lag variability in the observations made at 1200 MST for Line 10.

This feature is also evident in the Line-2 variability for 2-hr lag at the same grid point.

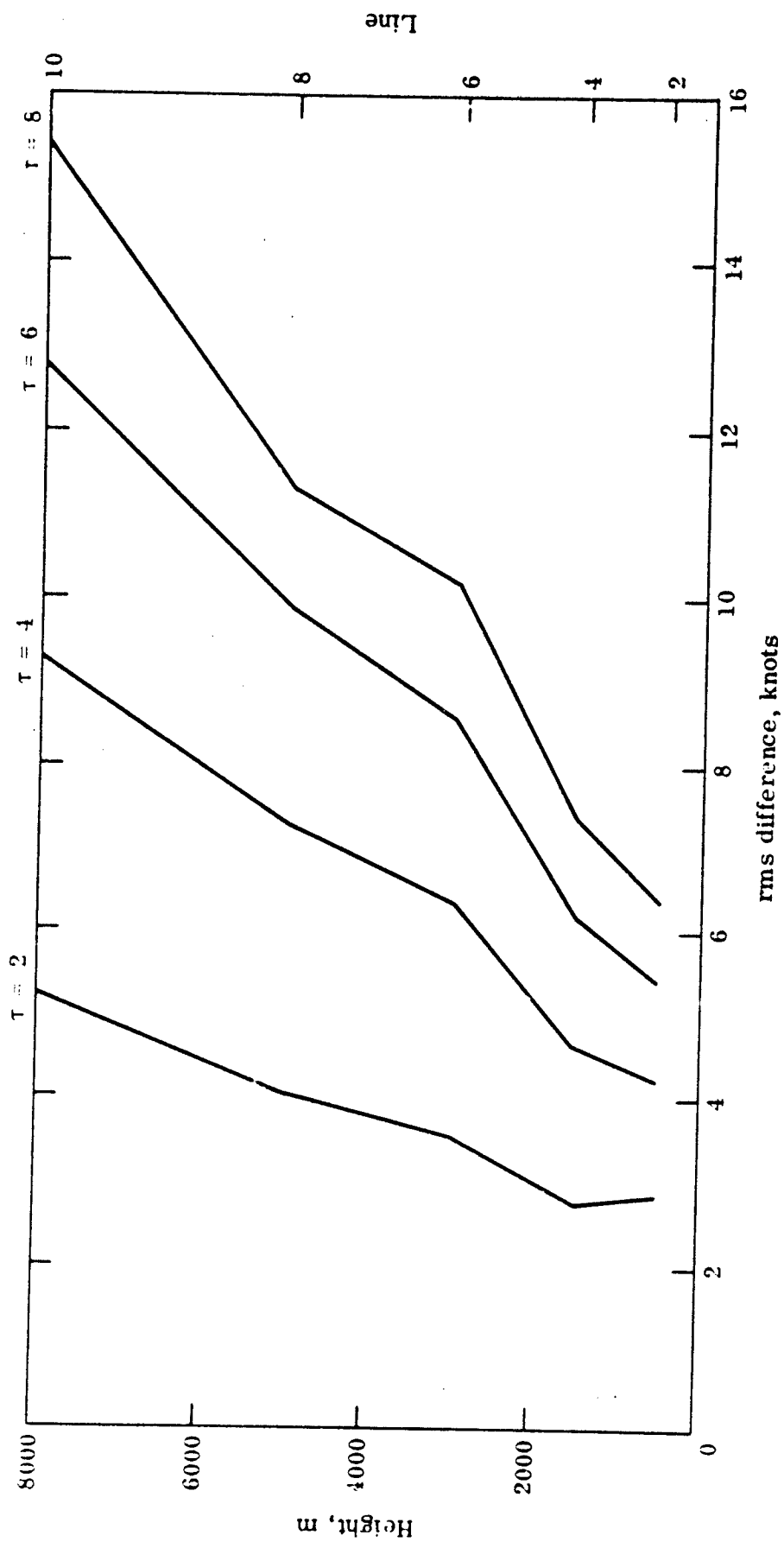


Fig. 5-11. Field-averaged time variability (vector), vertical profile.

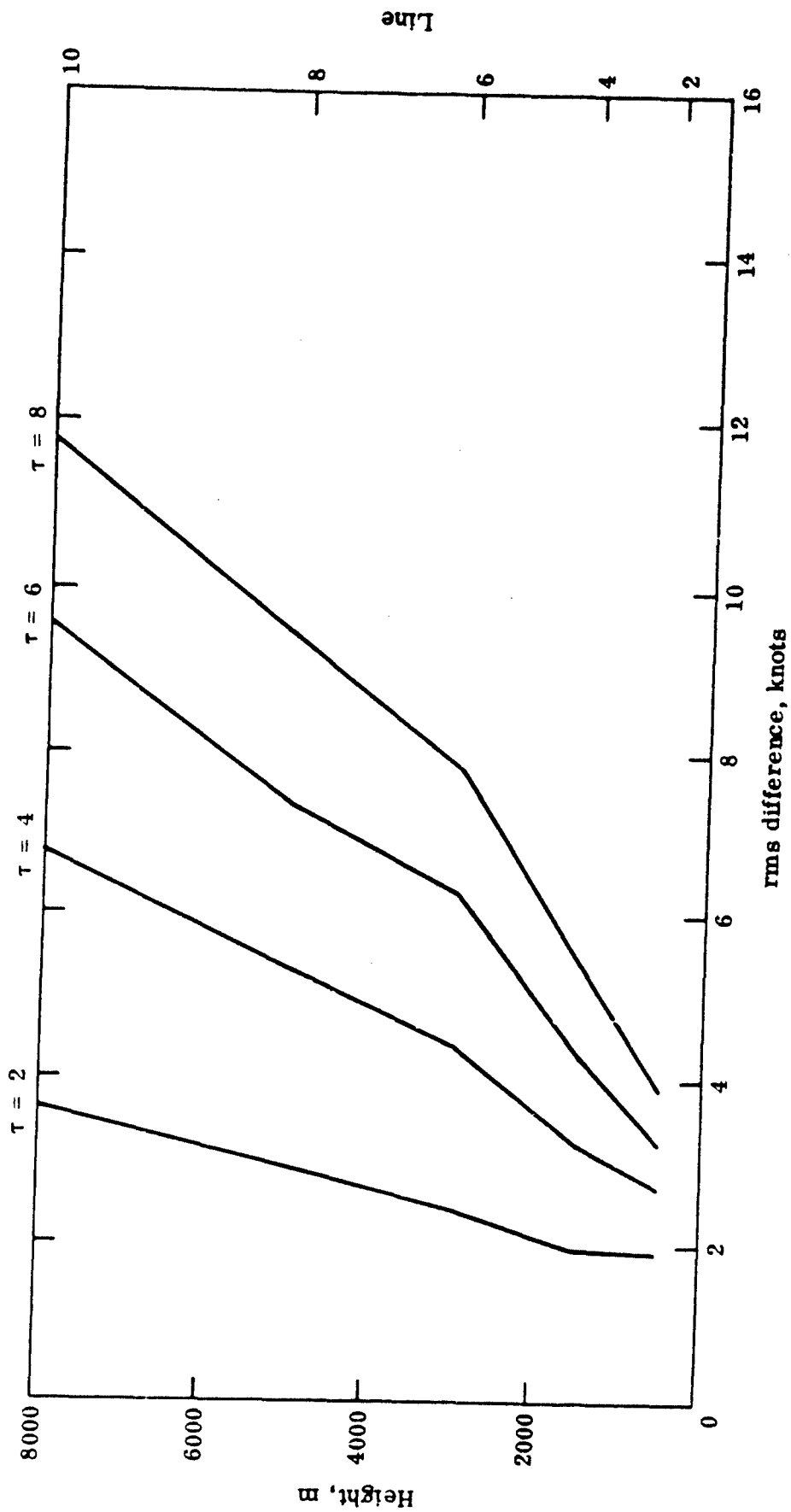


Fig. 5-12. Field-averaged time variability (u-component), vertical profile.

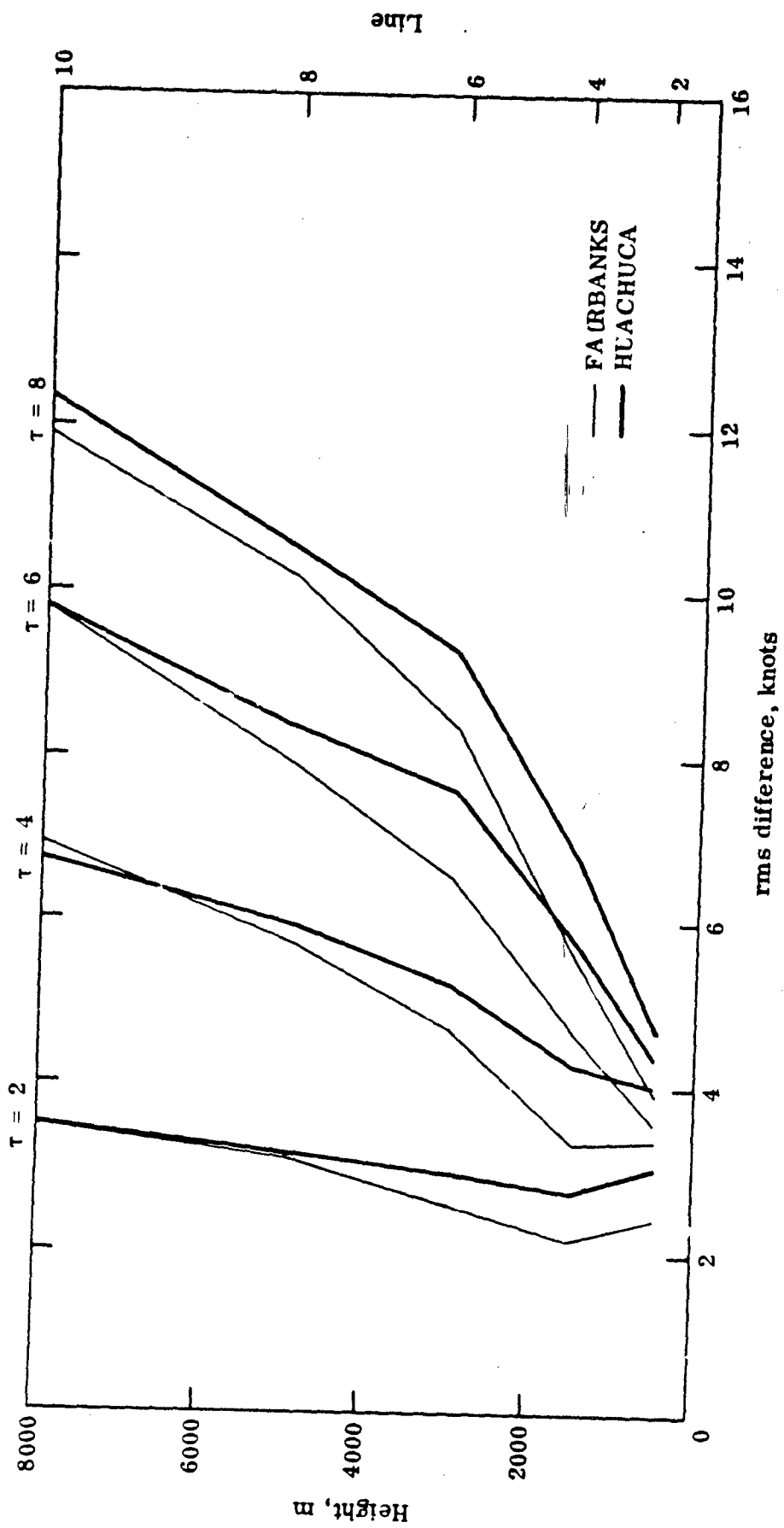


Fig. 5-13. Single-station time variability (u-component), vertical profile.

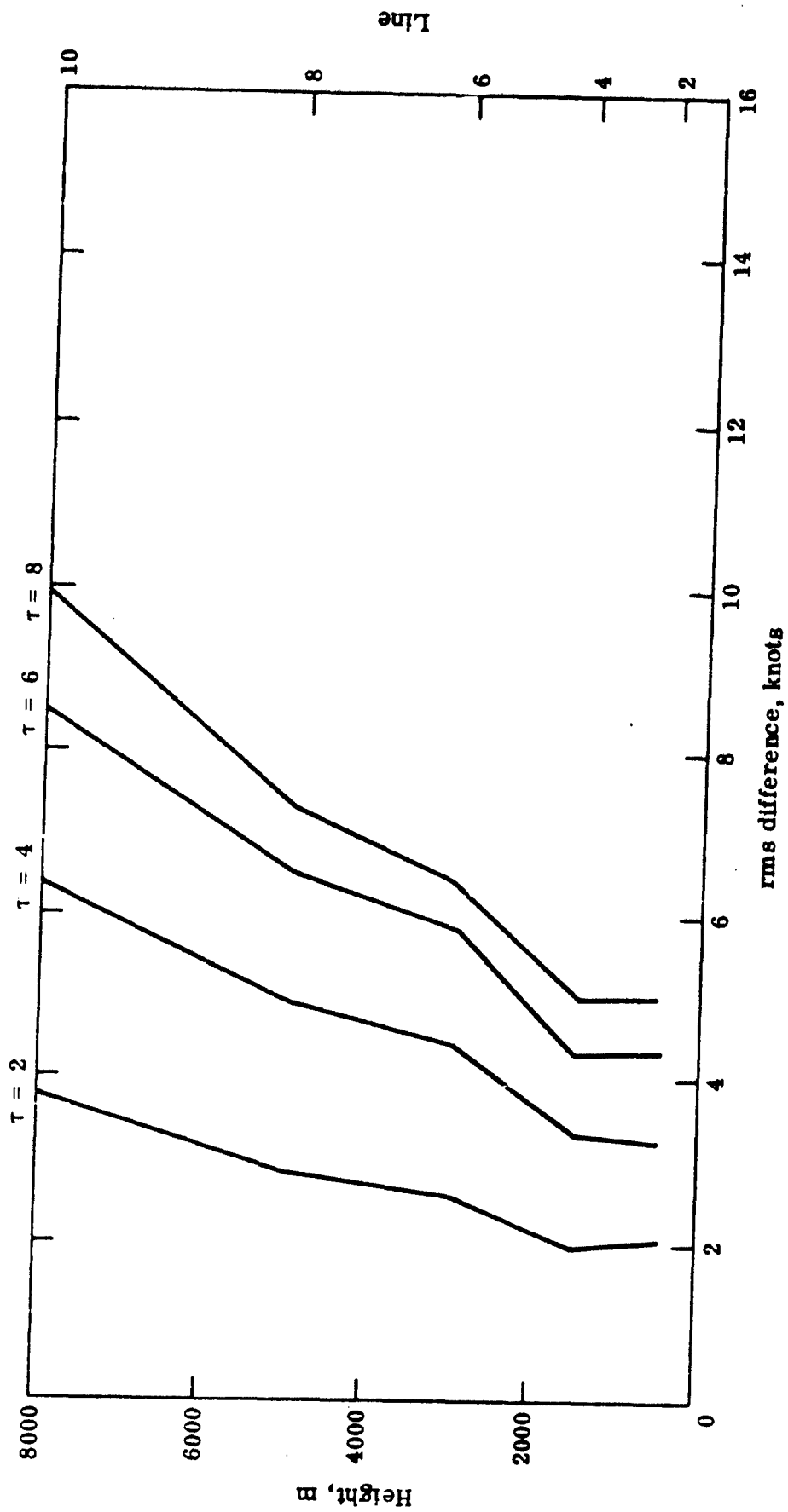


Fig. 5-14. Field-averaged time variability (v-component), vertical profile.

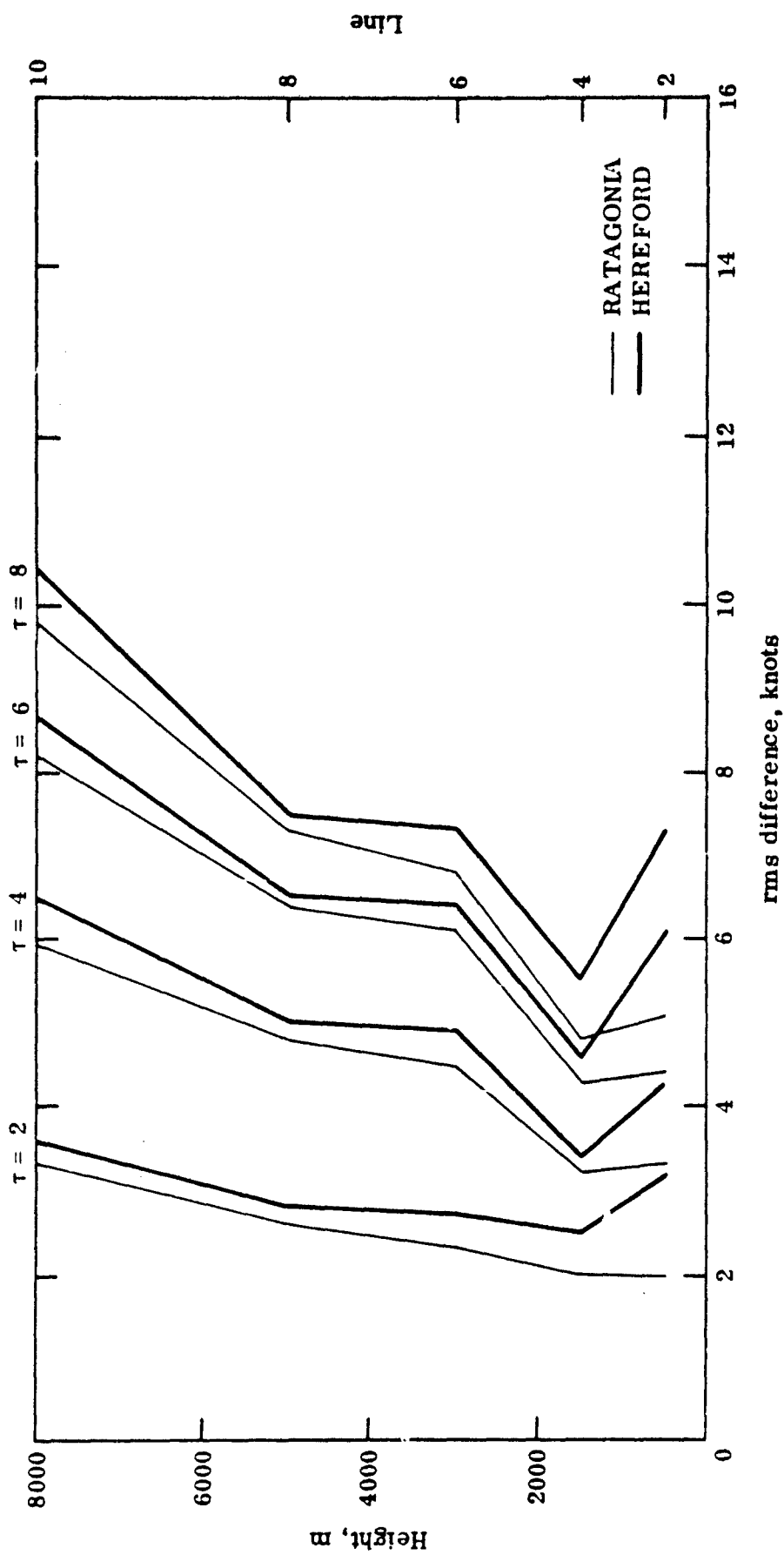


Fig. 5-15. Single-station time variability (v-component), vertical profile.

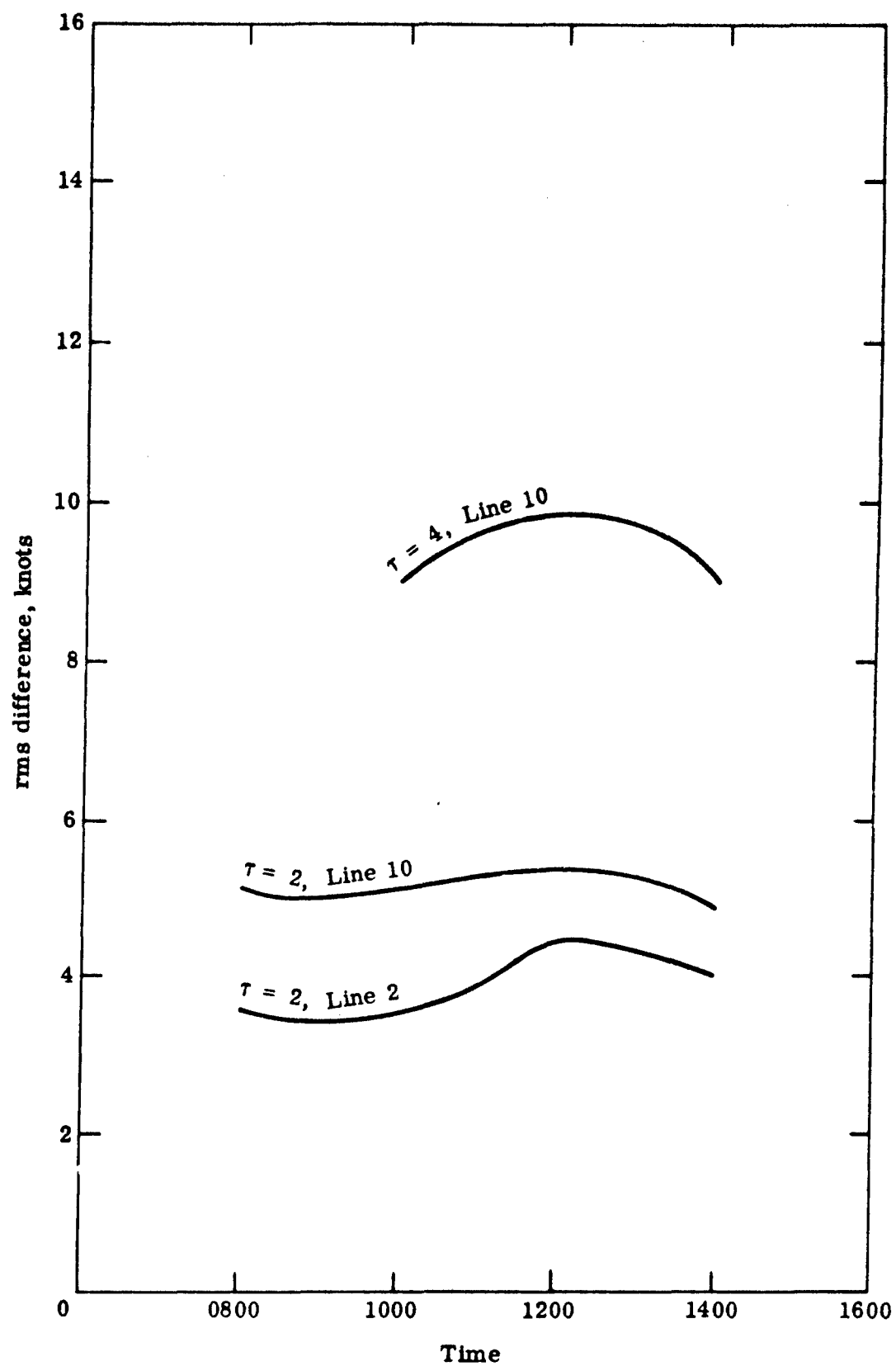


Fig. 5-16. Range of variability for selected lags and lines, vector.

6.0 SPATIAL VARIABILITY OF BALLISTIC WINDS

To examine the representativeness of ballistic winds estimated from observations somewhat removed from the environment the projectile actually passes through, differences between the ballistic wind components at the trajectory midpoint and all grid points in the analysis area were computed.

Summary maps were derived for all 80 sets of observations. The summary statistic employed is the rms difference of the ballistic wind components at the trajectory midpoint and all grid points in the analysis area. For example, at grid point i,j , the rms difference for the u -component of the ballistic wind is

$$D_u(i,j) = \left[\frac{1}{80} \sum (U_0 - U_{ij})^2 \right]^{1/2} \quad (6-1)$$

where U_0 is the u -component of the ballistic wind at the trajectory midpoint and U_{ij} is the u -component of the ballistic wind at grid point i,j .

Maps of the rms difference for the two components (as well as for the vector) of the ballistic winds were prepared for Lines 2, 4, 6, 8, and 10.

These maps were examined along with observational data to:

- (a) obtain estimates of the decrease in accuracy when observations are not available in the immediate vicinity of the gun emplacement,
- (b) compare the difference in spatial variability derived from the map winds with the measures of spatial variability derived directly from the individual soundings,
- (c) determine if topographic effects influence the areal distribution of measures of spatial variability, and
- (d) determine if systematic differences exist between individual single station ballistic winds, and, where such differences do exist, to consider the possibility of them being orographically induced.

6.1 Areal Distribution of the rms Differences of Analyzed Ballistic Winds

Examples of fields of the rms difference are shown for Line-4 ballistic winds in Fig. 6-1 through 6-3, for Line 6 in Fig. 6-4 through 6-6, and for Line 10 in Fig. 6-7 through 6-9.

As would be expected, the magnitude of the rms differences generally increases

with height. The rms difference for the v-component of the ballistic wind exceeds that for the u-component for all levels over most of the analysis area.

6.2 A Comparison of Ballistic Winds Computed from Single Station and Analyzed Winds

An important characteristic of the map winds is illustrated in Fig. 6-10. The rms differences of the two components of the ballistic wind based on the CRAM analyses for Line 10 are plotted as a function of distance from the trajectory midpoint along four headings as indicated. A similar statistic was computed for the differences between the Ft. Huachuca single-station ballistic wind and ballistic winds derived from five stations of the observing network. The five stations compared with Ft. Huachuca were Benson, Patagonia, Parker Canyon, Bisbee, and Tombstone. Their selection was based on all available 1000 and 1400 MST soundings. The rms differences computed from observations are, in general, systematically larger than those derived from the analysis. The implication here is that if several observations somewhat removed from the firing site represent the only ballistic information available, an objective analysis of these observations will lead, on the average, to an estimate of the ballistic wind that is superior to the ballistic wind derived from any of the individual soundings.

6.3 Systematic Differences Between Single-station Ballistic Winds

In deriving the rms differences for station pairs, it was noted that there were systematic differences between the ballistic winds derived from the Benson and Tombstone soundings. In particular, for Line-10 ballistic winds, for those cases where the wind had a westerly component and the magnitude of the wind vector exceeded 15 knots, the u-component of the Tombstone ballistic wind exceeded that of Benson in 13 out of 15 cases. The average difference was 7.7 knots. According to the Student's T-test for paired comparisons (Wadsworth and Bryan, 1960), these differences are significant at the 1% level.

These differences may be traced to instrumentation problems. However, an examination of the trajectories of the balloons of the two stations provides at least a clue that the observed differences may be a result of orographic effects. In Fig. 6-11, Area A encloses the locations of the Benson balloon at the time it was passing through

Zone 10 for the 15 cases studied. Similarly, Area B encloses the location of the Tombstone balloon at the time it was passing through Zone 10 for each of the 15 cases.

(There are two such areas for each since there were two prevailing wind directions—northwest and southwest.) In most instances, the Tombstone balloon at the important Zone-10 levels was over Sulpher Spring Valley, in contrast to the associated Benson balloons, which in most cases were well to the west over higher mountainous terrain.

There was also noted a systematic difference between the Line-10 single-station ballistic winds of Ft. Huachuca and Tombstone. For ballistic winds with a westerly component, the magnitude of Tombstones winds was greater than that of Ft. Huachuca in 10 out of 11 cases. The average difference was 4.5 knots. The Student's T-test for paired comparison indicates the differences to be significant at the 5% level.

6.4 Some Possible Orographic Effects for Low-level Ballistic Winds

Detection of low-level orographic effects was rather difficult due to certain characteristics of objective analysis techniques. In general, analysis errors are a minimum at grid points near the observations and a maximum between observations. To reduce the analysis error maxima, it is necessary to do a moderate amount of space smoothing (see Section 3.3.5). This apparently leads to a reduction in the estimates of the rms differences at grid points that are relatively far removed from observing sites. Note, for example, the secondary maximum in the rms-difference field near Nogales in Fig. 6-2. Thus, to examine the rms-difference fields for possible orographic effects in the lower-level ballistic wind fields, it is necessary to confine our attention to rms differences at grid points adjacent to observing sites. Figures 6-12 and 6-13 show the rms differences for Line-2 ballistic wind components in the vicinity of each of 12 observing stations. A minimum in the rms difference for the v-component of the ballistic wind extends up the San Pedro Valley, which includes Benson, while greater variability in the mountainous terrain can be noted to the west, south, and east of Ft. Huachuca. The rms differences for the u-component of the Line-2 ballistic winds yield a more symmetrical pattern, with only a slight indication of a minimum in the same region as noted above for the v-component differences.

6.5 Effect of Balloon Drift on Single-station Ballistic Wind Computations

The importance of accounting for the drift of the balloon in objective analysis procedures is readily apparent from an examination of Figs. 6-7 through 6-9. Superimposed over the analysis of the field of rms differences in this figure is the position of the Ft. Huachuca balloon as it passed through Zone 10 for those cases where the wind had a westerly component and the magnitude of the wind vector exceeded 15 knots. It can be seen that assuming that the balloon is over the station can lead to significant errors in the estimation of the ballistic wind.

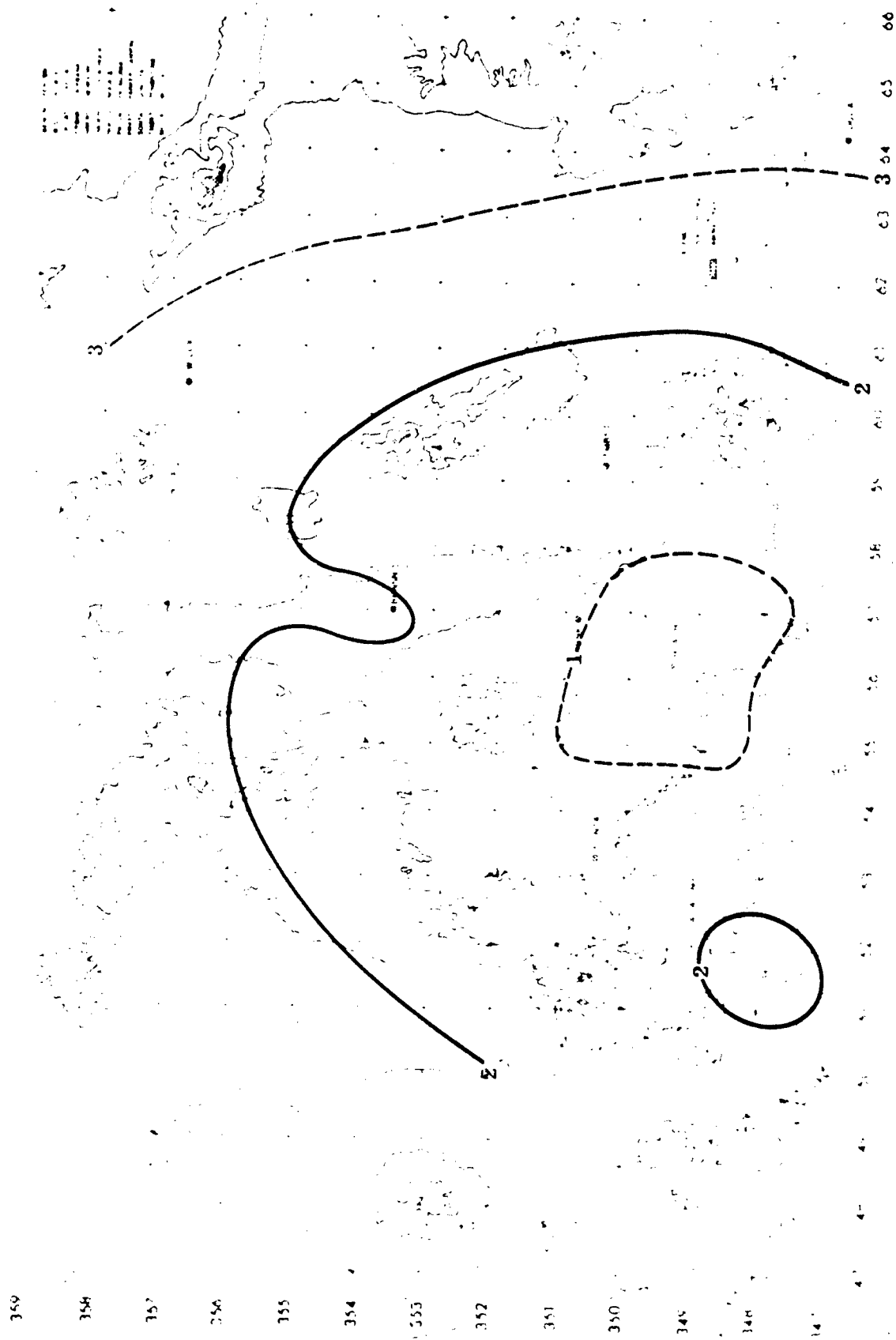


Fig. 6-1. Line-4 rms space differences, u-component (80 cases).

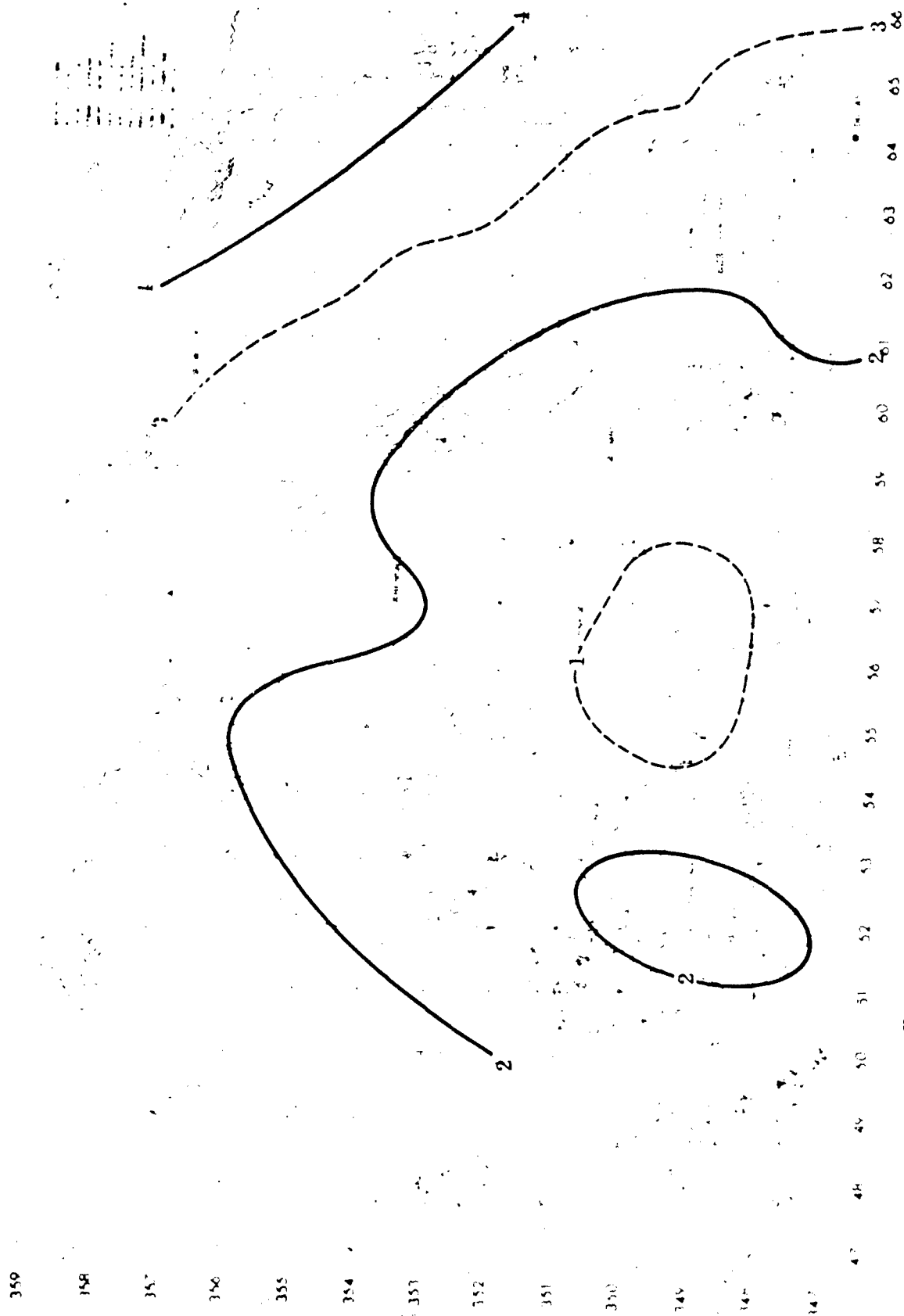


Fig. 6-2. Line-4 rms space differences, v-component (80 cases).

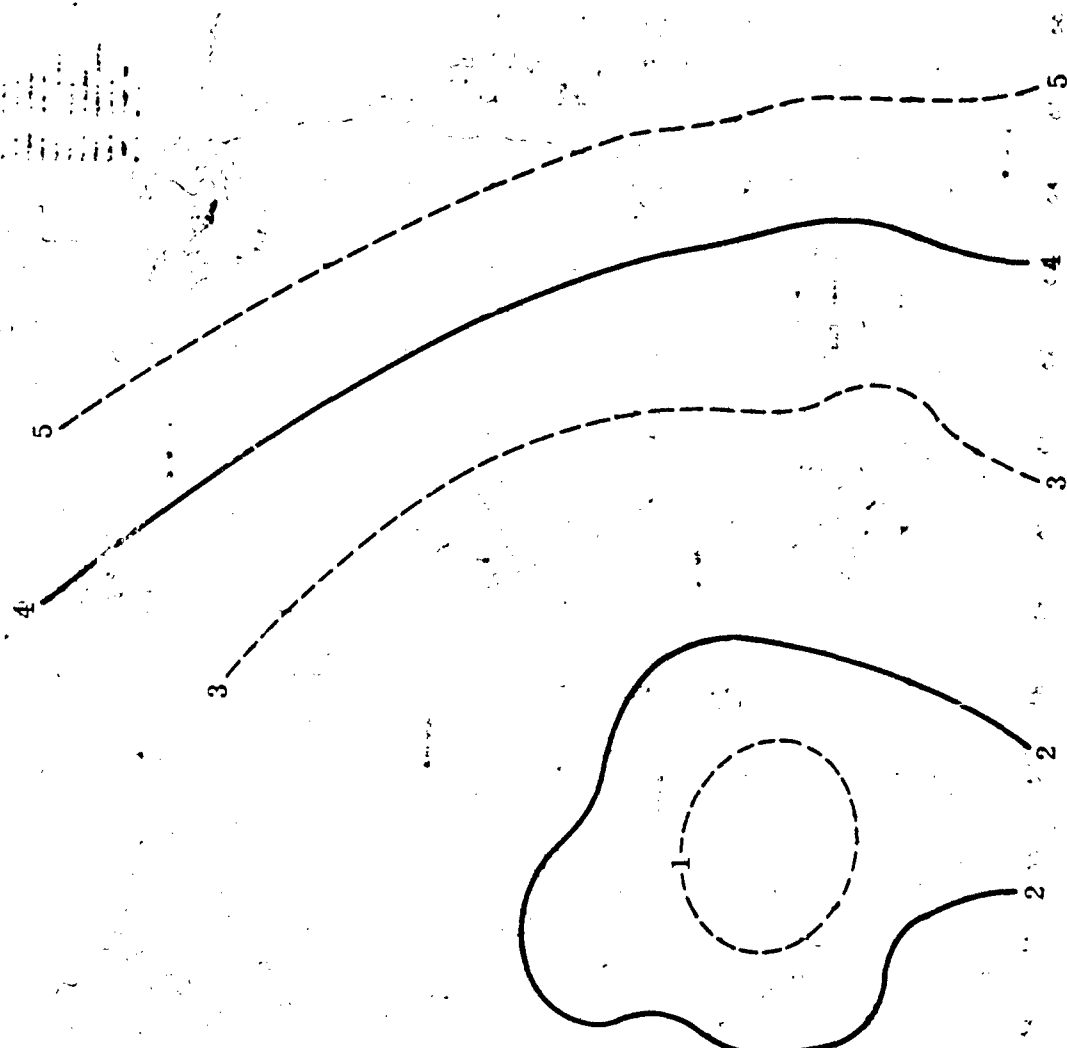


Fig. 6-3. Line-4 rms space differences, vector (80 cases).

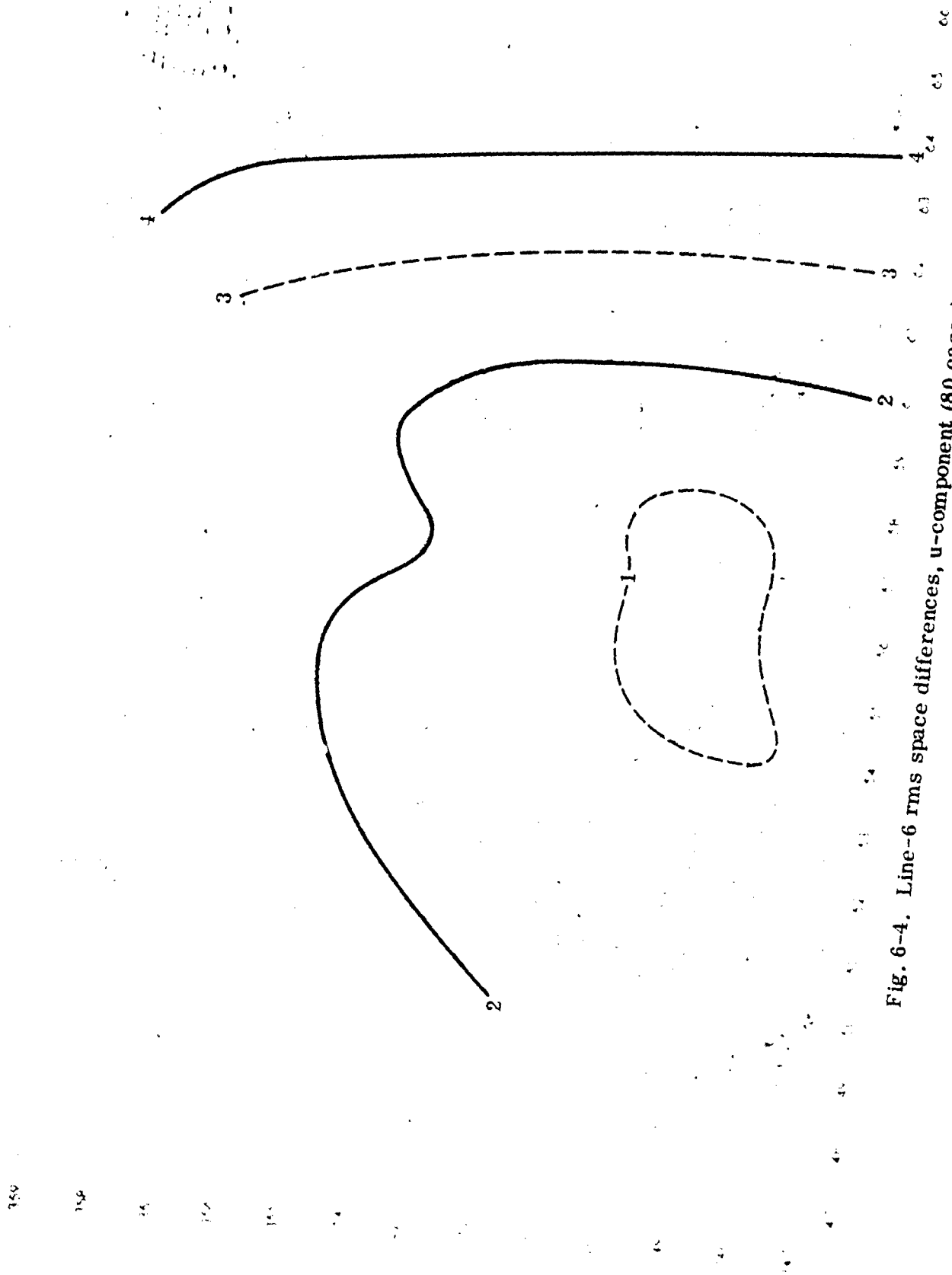


Fig. 6-4. Line-6 rms space differences, u-component (80 cases).

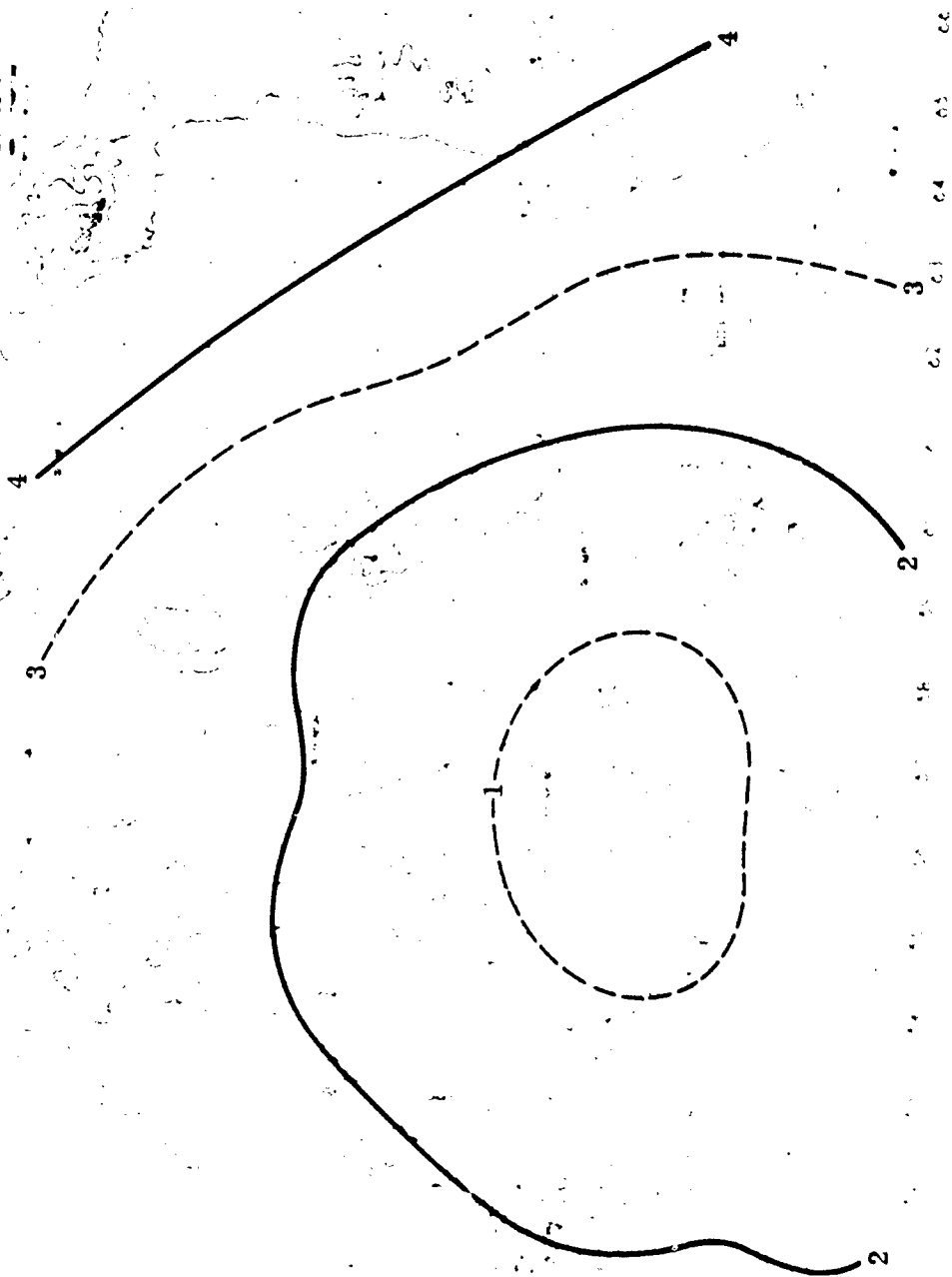


Fig. 6-5. Line-6 rms space differences, v-component (80 cuses).

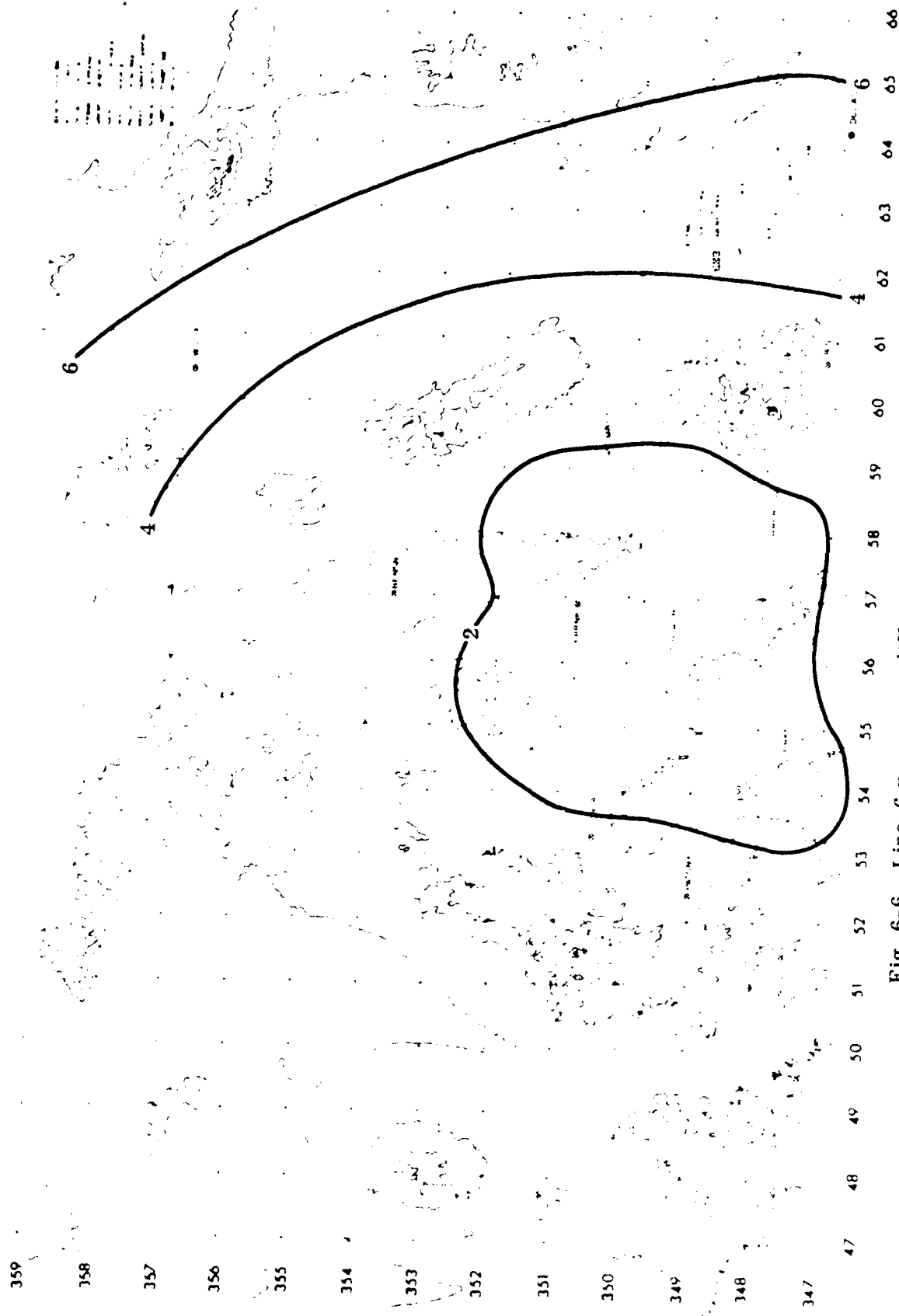


Fig. 6-6. Line-6 rms space differences, vector (80 cases).

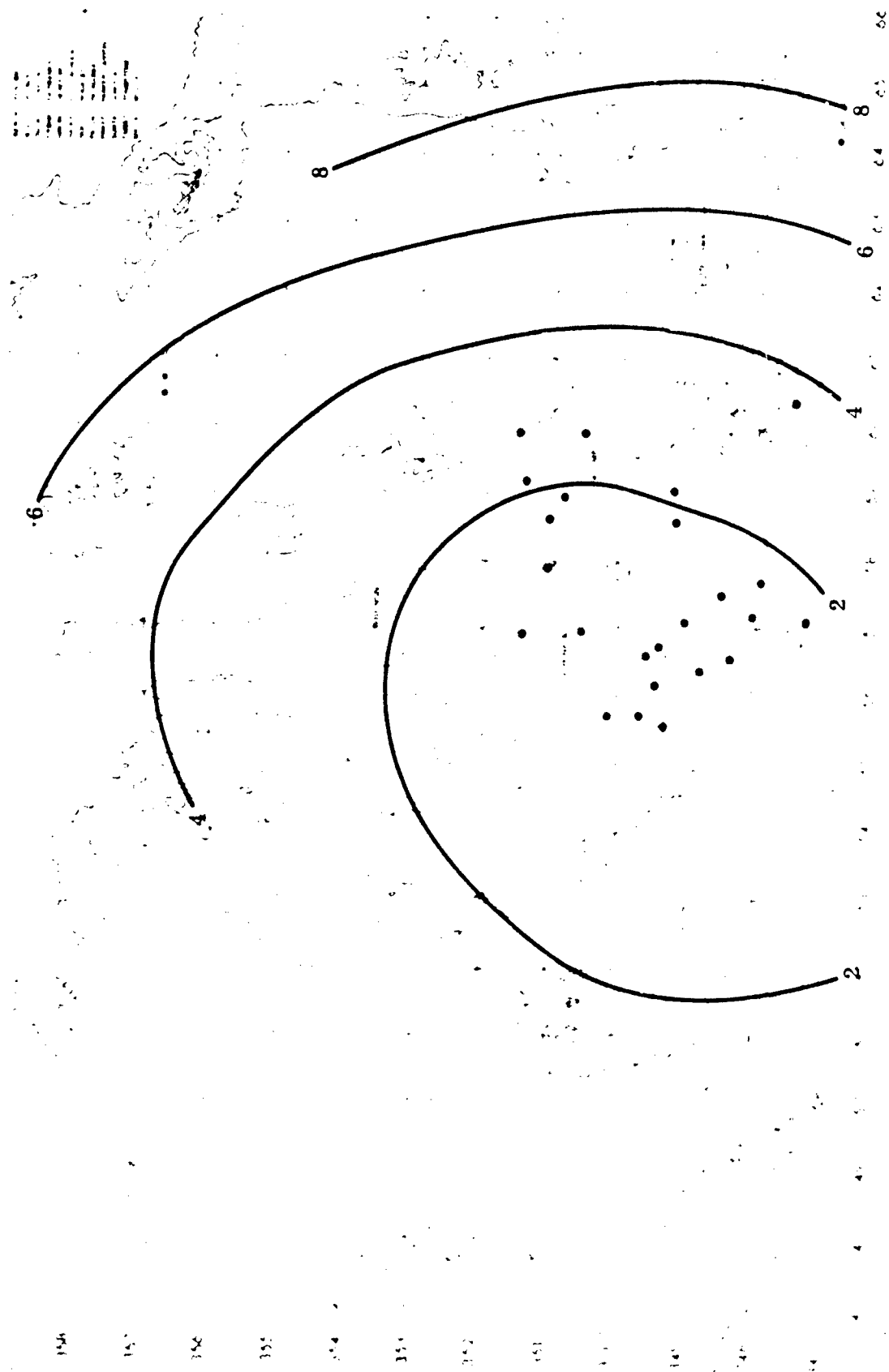


Fig. 6-7. Line-10 rms space differences, u-component (80 cases). "Dots" indicate Zone-10 locations of radio-sondes released from Ft. Huachuca for those cases where the wind had a westerly component and the magnitude of the wind vector exceeded 15 knots.

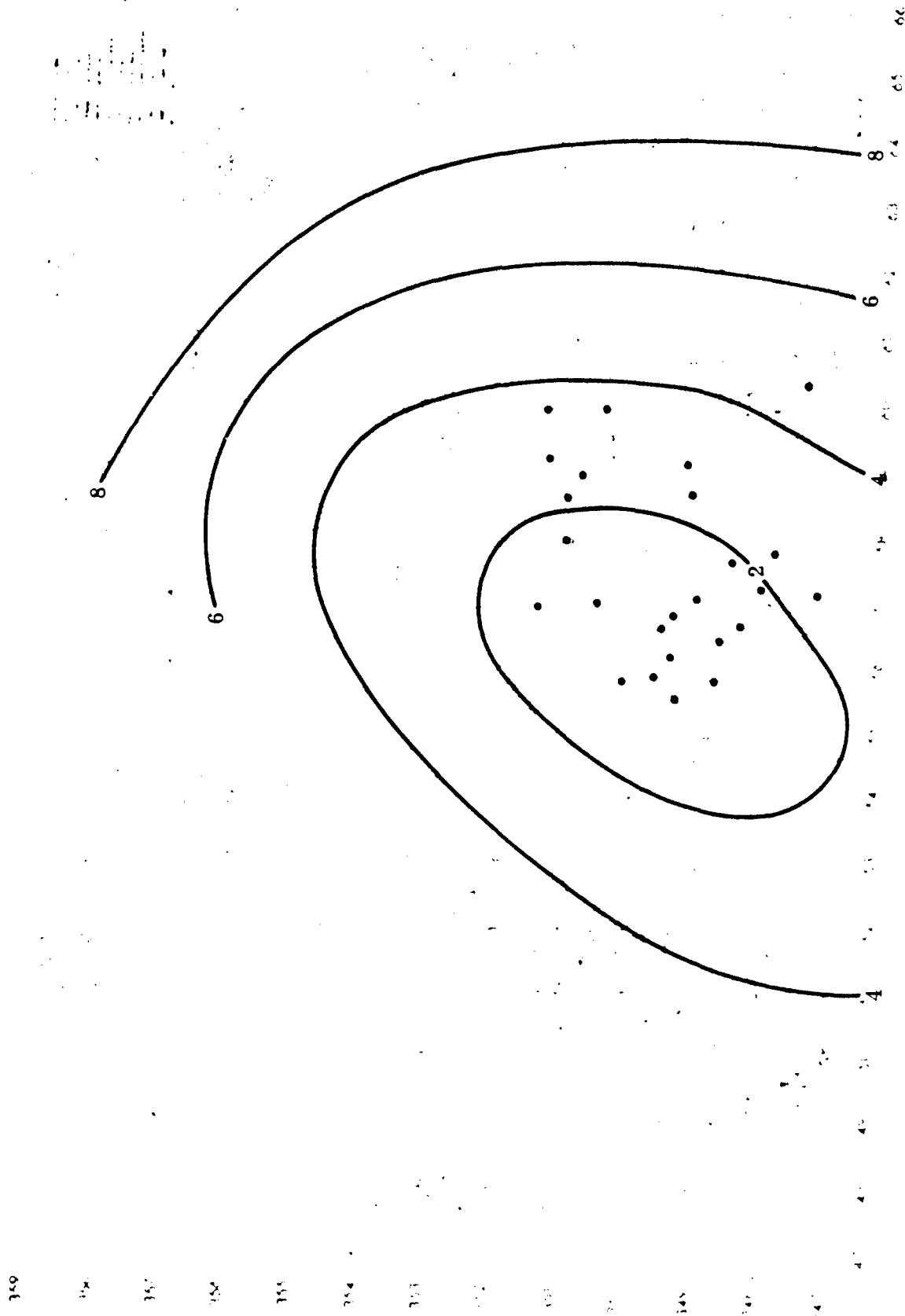


Fig. 6-8. Line-10 rms space differences, v-component (80 cases). "Dots" indicate Zone-10 locations of radio-sondes released from Ft. Huachuca for those cases where the wind had a westerly component and the magnitude of the wind vector exceeded 15 knots.

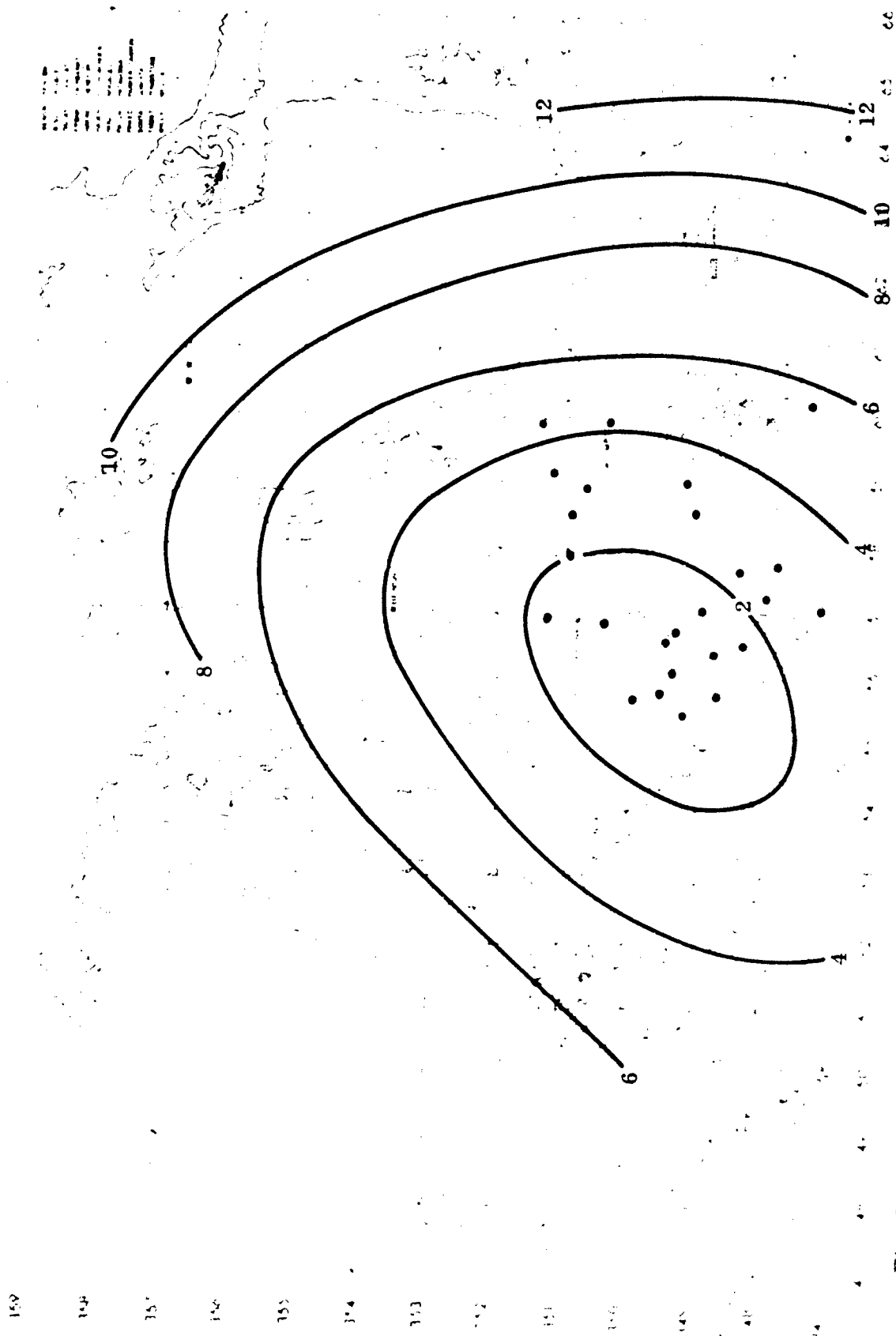


Fig. 6-9. Line-10 rms space differences, vector (80 cases). "Dots" indicate Zone-10 locations of radio-sondes released from Ft. Huachuca for those cases where the wind had a westerly component and the magnitude of the wind vector exceeded 15 knots.

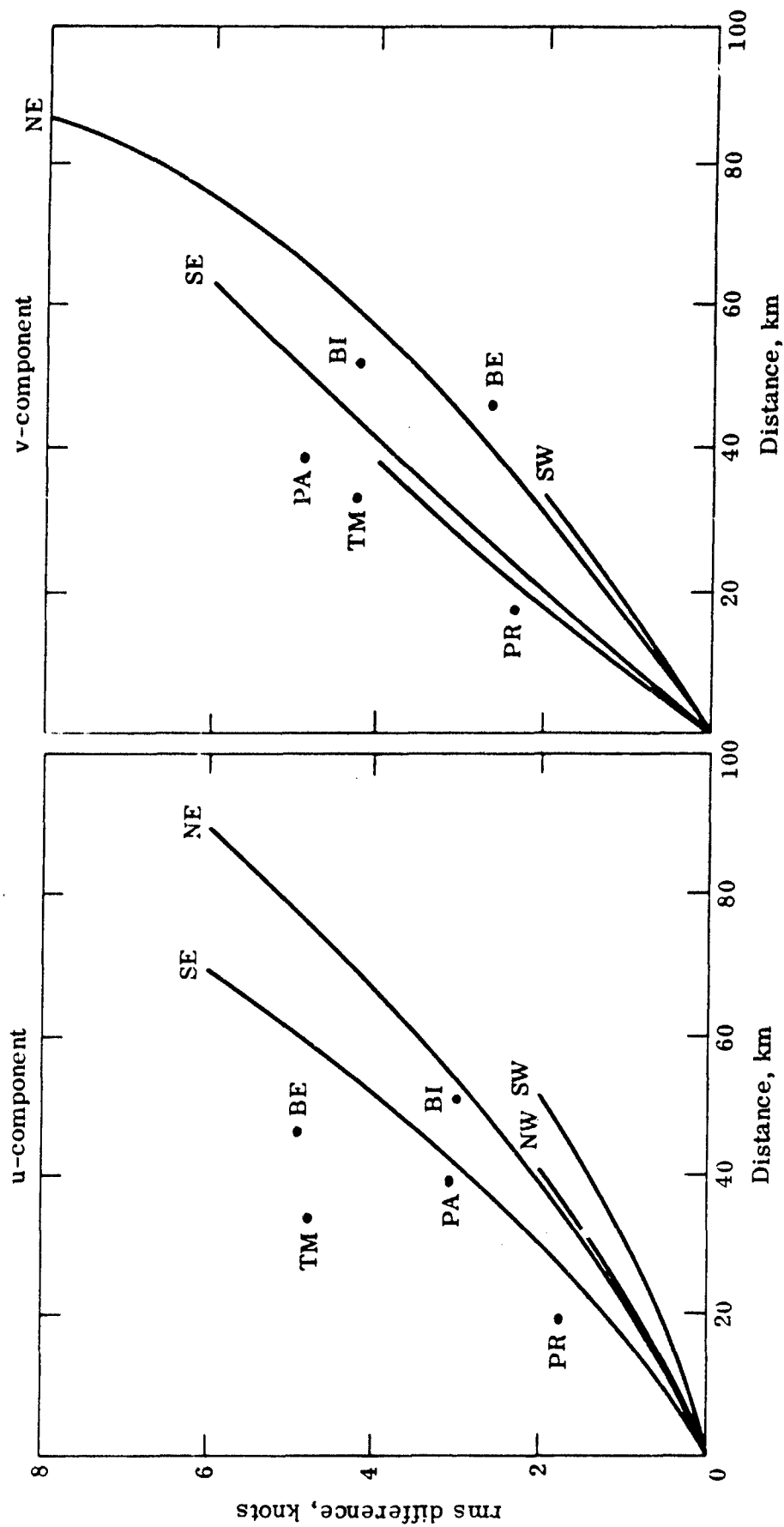


Fig. 6-10. Line-10 rms space differences, u- and v-components.

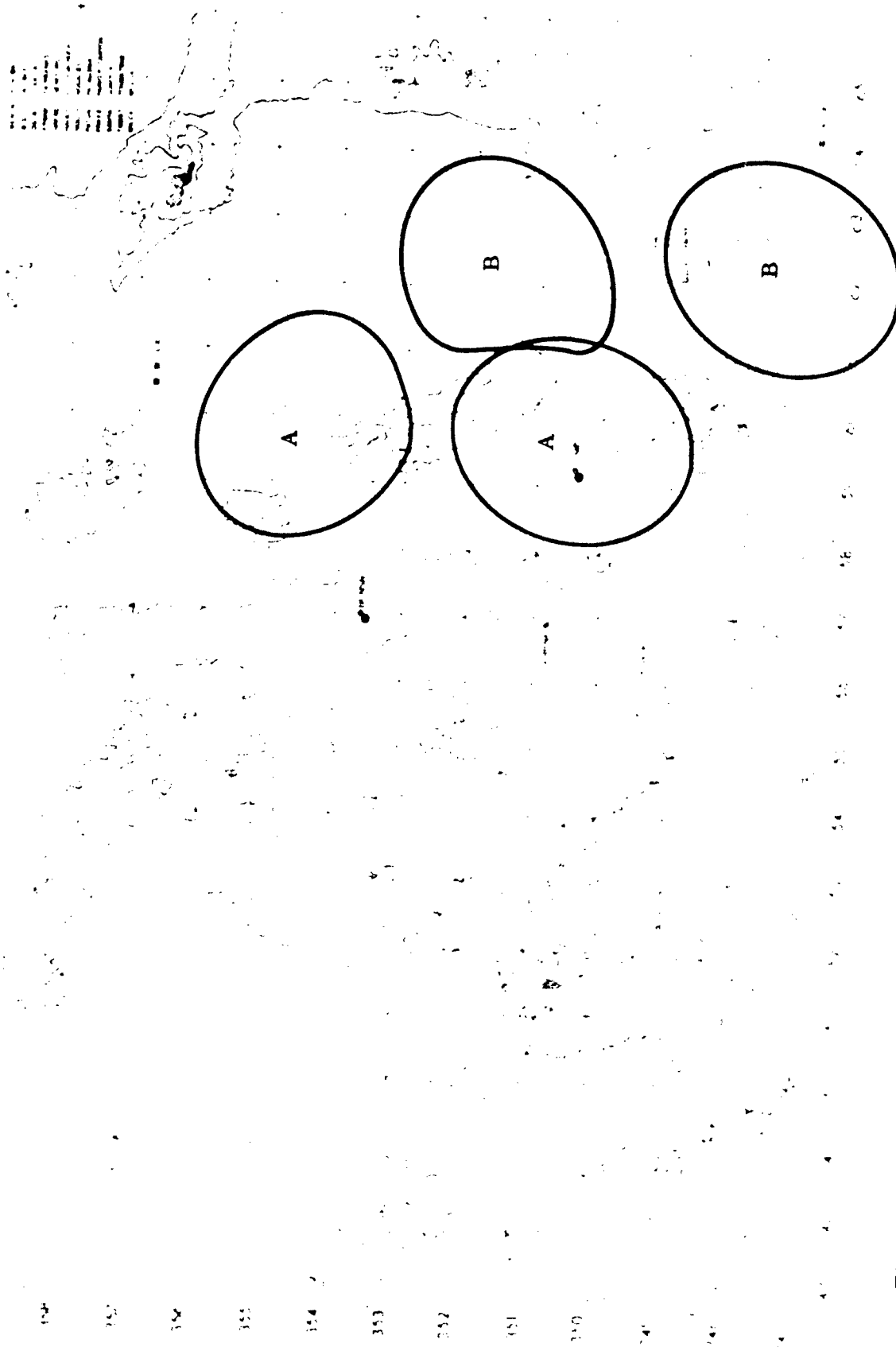


Fig. 6-11. Areas enclosing endpoints of balloon trajectories at Zone 10 for Benson (Areas A) and Tombstone (Areas B).

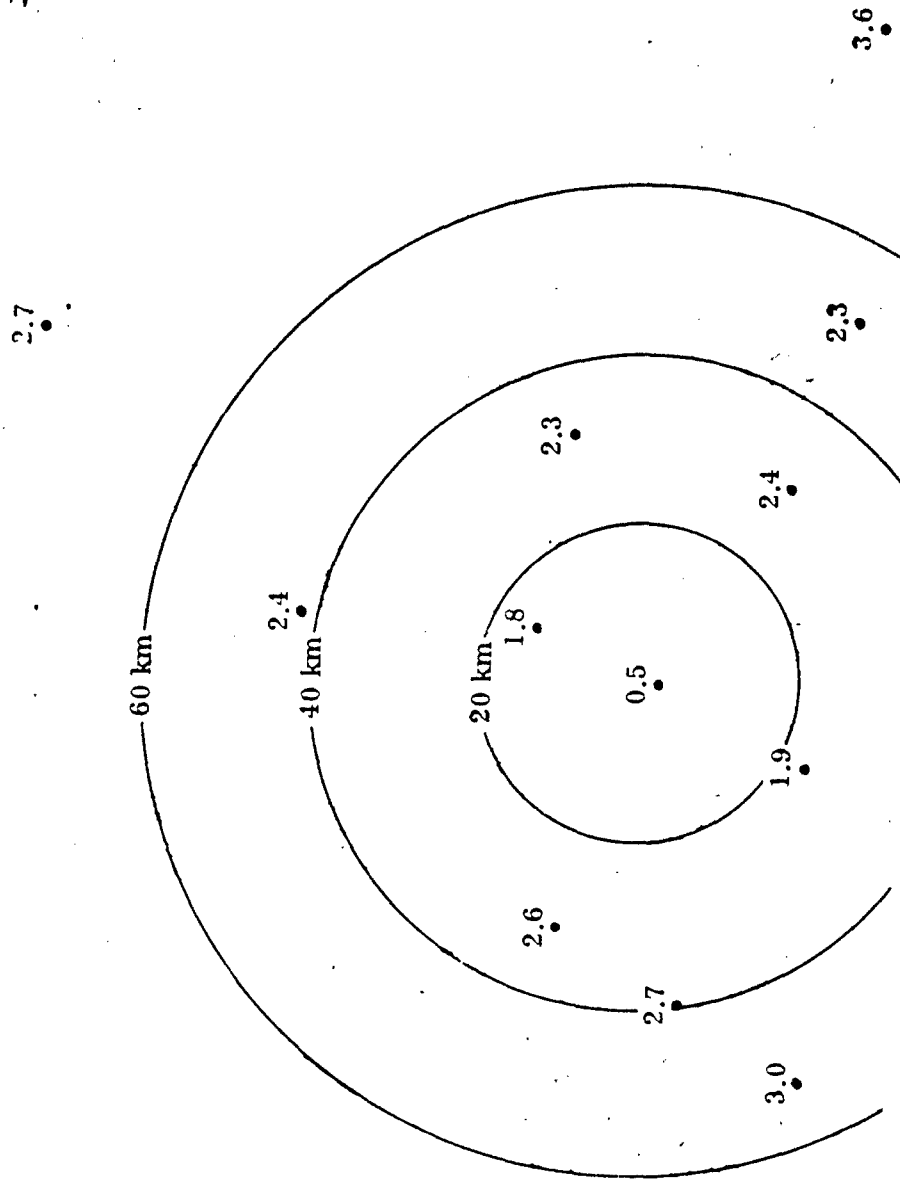


Fig. 6-12. Line-2 rms space differences for selected grid points, u-component (80 cases).

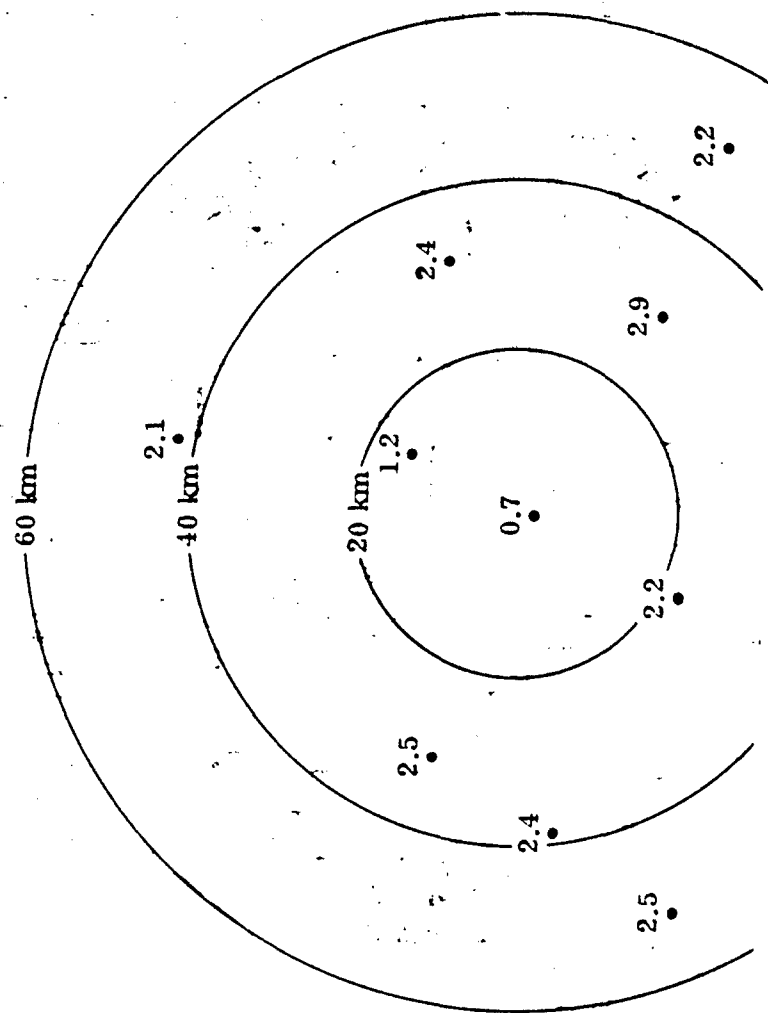


Fig. 6-13. Line-2 ms space differences for selected grid points, v-component (80 cases).

TABLE 7-2
RESIDUAL ERRORS (in Meters) USING INPUT DATA FROM
SINGLE STATION (FT. HUACHUCA) AND CRAM ANALYSES

Date	Case	Single station			CRAM (1/2 Data withheld)			CRAM (All data)		
		Vector	Range*	Deflection	Vector	Range*	Deflection	Vector	Range	Deflection
1/25 AM	17		Missing		535.1	-330.3	421.0	567.9	-345.5	450.7
1/27 AM	21	26.4	-25.4	7.3	34.3	-30.0	-16.6	34.7	-34.7	1.5
1/27 PM	23	83.3	31.4	77.2	67.5	18.6	-64.9	63.5	25.0	-58.4
2/6 AM	37	64.5	32.6	55.7	64.2	56.9	29.8	46.9	33.3	33.0
2/6 PM	39	143.4	114.8	86.0	204.3	188.0	79.9	207.5	186.9	90.1
2/10 AM	41		Missing		175.1	-26.4	173.1	224.2	-54.7	217.4
2/10 PM	43	163.3	-94.3	133.3	147.0	-96.5	110.8	167.2	-68.2	152.7
Average† (5 Cases)		96.2	59.7	71.9	103.5	78.0	60.4	104.0	69.6	67.1
Average† (7 Cases)		-	-	-	175.4	106.7	142.4	187.4	106.9	157.8
rmse error (5 Cases)		108.7	70.4	82.8	120.9	99.2	69.3	125.2	92.2	84.8
rmse error (7 Cases)		-	-	-	236.1	150.7	190.5	253.9	153.5	210.2

*Empirically corrected

†Absolute

As for the question of whether the single station observation alone results in higher residual errors than those given by using values obtained from a CRAM analysis with one-half the data as input, the answer is not readily apparent from the statistics for the five cases where a comparison can be made. The average absolute and rms residual vector error is slightly lower when the Ft. Huachuca data are used as input.

Examination of the individual component error reveals that the range errors are lower using Ft. Huachuca data, but that the deflection errors are lower using the input from the CRAM analysis obtained with half the data. Most of the contribution to the lower vector errors for Ft. Huachuca data is due to the lower range errors. However, these range errors have been empirically corrected (see Section 4.2) and may not be as reliable as the deflection error values.

Although it is difficult to obtain statistical significance with the small number of cases in this sample, the difference in the deflection errors data was subjected to the Student's T-test for paired comparisons (Wadsworth and Bryan, 1963). The result was that there was significance at the 15% level. The value for the level of significance is the same as the probability of the result being due to chance. Thus, there is a relatively low probability that the better result given by the CRAM analyses with half the data is due to chance.

It is concluded that a CRAM analysis which uses data from a network that is half the density of that designed for this study results in the generation of significantly lower residual errors for the deflection component of the error than those provided by data from a single station.

8.0 PREDICTION EXPERIMENTS

To develop an elaborate system to forecast ballistic winds in mountainous terrain is an enormous undertaking. In this study the objective was essentially to assess the magnitude of the problem and to apply a few very modest and straightforward extrapolation procedures.

The data sample used for these experiments consisted of CRAM analyses of ballistic u- and v-wind components for Lines 2, 4, 6, 8, and 10 for the 80 observation times from 0600 MST January 12 through 1400 MST February 12, 1965. The observations, being at two-hourly intervals for a given day, allow consideration of forecast lags (τ) of 2, 4, and 6 hr with valid times of 0800 ($q=2$), 1000 ($q=3$), 1200 ($q=4$), and 1400 ($q=5$).

There were three principal methods used to forecast ballistic winds: trend extrapolation, linear regression, and average value. Persistence was used as a control. All calculations were made at the midpoint of the firing trajectory.

(a) Trend extrapolation There were two types of trends used; a 2-hr trend (2T) that calculated the difference between the two most recent consecutive observations at the trajectory midpoint and extrapolated that difference forward in time, and a 4-hr trend (4T) that used the 0600 and 1000 observations to predict for 1400. The following equations were used:

$$2T: \hat{\phi}(q) = \phi(q-\tau/2) + \frac{\tau}{2} [\phi(q-\tau/2) - \phi(q - \frac{\tau+2}{2})] \quad (8-1)$$

for $\tau = 2, q = 3, 4, 5$

$\tau = 4, q = 4, 5$

$\tau = 6, q = 5$

$$4T: \hat{\phi}(5) = \phi(3) + [\phi(3) - \phi(1)] \quad (8-2)$$

where $\hat{\phi}$ is the extrapolated value of the observation ϕ (either u- or v-wind component).

(b) Linear regression The method of least squares is used to fit the 0600, 0800, and 1000 observations to extrapolate for 1200 and 1400, and the 0600, 0800, 1000, and 1200 to extrapolate for 1400. The equation is

$$\hat{\phi}(q) = a + bq \quad (8-3)$$

for $\tau = 2, q = 4, 5$

$\tau = 4, q = 5$

where a and b are regression coefficients derived from $q = 1, 2, 3$ or $q = 1, 2, 3, 4$.

(c) Averaging The average value of the past and present observations is computed and is extrapolated forward as a constant value.

$$\hat{\phi}(q) = \frac{1}{n} \sum \phi_i \quad (8-4)$$

8.1 Ballistic Wind Prediction

Ballistic wind components (u and v) were forecast using the above techniques. The evaluation measure chosen was the vector rms error. The results are shown in Table 8-1 for individual lines (2, 4, 6, 8, 10), lags (2, 4, 6 hr), and valid times (1000, 1200, and 1400). Pooled results (all hours) are shown for techniques that have comparable data samples. Persistence is indicated by "P" in the method column. The pooled results are also presented in Figs. 8-1 through 8-5. It can be seen that for the lower lines (i.e., 2 and 4) the averaging technique (AVE) generally yields better results than the 2-hr trend extrapolation (2T). The trend extrapolation errors increase with time much more rapidly than do the AVE errors for all lines (see Figs. 8-1 through 8-5), especially Line 2. For Lines 6, 8, 10, the errors associated with 2T are smaller than AVE. The errors associated with linear regression (LR) were roughly comparable to 2T, being slightly better at the low lines and slightly worse at the high lines.

Of interest was the comparison of 2T and 4T, in which 2T represents the forecast for 1400 based on 0800 and 1000 data and 4T represents the forecast for the same time based on 0600 and 1000. For the lower lines (2, 4, 6), the 4T error is smaller than the 2T error, but for Lines 8 and 10 the reverse is true although the differences are small.

Persistence (P) gives the smallest errors for Lines 2 and 4 at all lags, but for the higher lines, 2T is generally slightly superior—the exceptions being Lines 8 and 10 for $\tau = 6$. Figure 8-6 shows a comparison between P and 2T by lag and line. The figure shows that 2T performs best at Lines 4 and 6. This is a contrast to persistence, which shows an increasing rms error with height.

TABLE 8-1
BALLISTIC WIND PREDICTION EXPERIMENT RESULTS
USING CRAM ANALYSES*

(a) Line 2

Lag (hrs)	Method	Valid time			All hours
		1000	1200	1400	
2	P	2.7	3.5	3.3	3.2
	2T	3.8	3.5	4.9	4.1
	LR		3.9	4.3	
	AVE	3.0	4.5	4.2	3.9
4	P		5.1	4.7	4.9
	2T		7.8	7.1	7.5
	4T			6.3	
	LR			6.4	
	AVE		5.2	5.0	5.1
6	P			5.4	5.4
	2T			10.3	10.3
	AVE			5.5	5.5

(b) Line 4

Lag (hrs)	Method	Valid time			All hours
		1000	1200	1400	
2	P	2.9	3.8	3.1	3.3
	2T	2.9	4.1	5.2	4.2
	LR		3.9	3.8	
	AVE	3.8	5.2	4.8	4.6
4	P		5.4	4.7	5.0
	2T		5.9	6.7	6.3
	4T			5.7	
	LR			5.6	
	AVE		6.1	5.9	6.0
6	P			6.0	6.0
	2T			7.6	7.6
	AVE			6.8	6.8

*Values are root-mean-square vector errors in knots. Pooled results (all hours) are shown for techniques which have comparable data samples.

TABLE 8-1 (continued)

(c) Line 6

Lag (hrs)	Method	Valid time			All hours
		1000	1200	1400	
2	P	3.7	4.5	3.2	3.8
	2T	2.3	3.4	4.8	3.6
	LR		3.8	4.2	
	AVE	5.1	7.1	6.9	6.4
4	P		7.5	6.1	6.8
	2T		6.0	6.4	6.2
	4T			6.3	
	LR			6.3	
	AVE		8.6	8.5	8.5
6	P			8.8	8.8
	2T			8.3	8.3
	AVE			9.9	9.9

(d) Line 8

Lag (hrs)	Method	Valid time			All hours
		1000	1200	1400	
2	P	3.9	5.0	3.5	4.2
	2T	2.6	4.4	4.2	3.8
	LR		4.8	4.3	
	AVE	5.5	7.6	8.0	7.0
4	P		7.8	7.6	7.7
	2T		7.1	7.5	7.3
	4T			7.9	
	LR			8.0	
	AVE		9.1	9.8	9.4
6	P			10.1	10.1
	2T			10.8	10.8
	AVE			11.2	11.2

TABLE 8-1 (continued)

(e) Line 10

Lag (hrs)	Method	Valid time			All hours
		1000	1200	1400	
2	P	5.0	5.6	4.1	4.9
	2T	4.1	4.3	3.9	4.1
	LR		5.3	4.8	
	AVE	6.8	9.1	9.9	8.6
4	P		9.8	9.0	9.4
	2T		9.5	8.6	9.0
	4T			8.9	
	LR			9.2	
	AVE		11.1	12.1	11.6
6	P			12.7	12.7
	2T			13.8	13.8
	AVE			13.9	13.9

8.2 Artillery Corrections Based on Ballistic Wind Prediction Experiments

The prediction experiments discussed above were evaluated on the basis of rms errors where the verification was made against the CRAM analysis. The question may be raised, quite properly, as to how well the ballistic wind derived from CRAM represents the "true" ballistic wind. This can be answered to some extent by conducting an evaluation of residual errors from the artillery firings based on forecast values of ballistic winds, temperatures, and density. Because trend extrapolation yielded results as good as any of the other methods tried (at Line 10, which is the only line for which the artillery firings are applicable), it was chosen for evaluation, with persistence used as a control. Forecasts were based on both CRAM analyses and the Ft. Huachuca observation.

Forecasts were valid at 1000 or 1400 MST on days when artillery firings were conducted, provided that the meteorological data were also available.

Two-hour trend forecasts (2T) were made using 0600 and 0800 data for a valid time of 1000, and 1000 and 1200 data for a valid time of 1400. Four-hour trend forecasts were made two ways using 0800 and 1000 data for a valid time of 1400 (2T, $\tau = 2$), and using 0600 and 1000 data for a valid time of 1400 (4T).

Because there was some question as to the validity of the range corrections (see Section 4), the evaluation was based on only deflection errors. Unit effects were employed with the forecast parameters in the same manner as was done in the experiment using concurrent data. Table 8-2 lists the residual deflection errors incurred for various lags using trend extrapolations and persistence based on CRAM and the Ft. Huachuca observation. The summarizations in Table 8-3, based on a limited data sample, indicate the following:

(a) Deflection errors based on persistence are smaller for CRAM than the Ft. Huachuca observations, particularly at 4 and 8 hr. (Analysis of decay with time is not appropriate here, as the various lags involve different data subsets.)

(b) Trend extrapolation is superior to both CRAM and Ft. Huachuca persistence for 2-hr lags, but not for 4-hr lags.

(c) A 4-hr extrapolation based on a 2-hr trend (2T, $\tau=4$) yields smaller errors than a straight 4-hr trend (4T), but not smaller than persistence.

The time decay of residual errors based on persistence of ballistic winds derived from CRAM analyses was examined. Average residual deflection errors were computed for the 12 firings conducted at 1000 MST for 0-, 2-, and 4-hour lags and for the 12 firings conducted at 1400 MST for 0-, 2-, 4-, 6-, and 8-hr lags. The results are plotted in Fig. 8-7. Deviations from values in Table 8-3(a) are due to differences in sample size. The most interesting characteristics of Fig. 8-7 are the reductions in errors for the 4-hr lag in the AM firing cases and for the 8-hr lag in the PM firing cases. In the former, the error decreases from 130.0 meters to 124.2 meters when going from 2 to 4 hr, and in the latter the error decreases from 146.9 meters to 143.2 meters when going from 6 to 8 hr.

TABLE 8-2
RESIDUAL DEFLECTION ERRORS IN METERS USING LINE-10 BALLISTIC WINDS
FOR CRAM AND FT. HUACHUCA PERSISTENCE AND EXTRAPOLATION

Date	Case	Lag (τ)	2T		4T		2T ($\tau = 4$)		Persistence	
			CRAM	HUACH	CRAM	HUACH	CRAM	HUACH	CRAM	HUACH
1/16 AM	1	2 4	0.9	15.5					13.3 25.7	28.2 41.0
1/16 PM	3	4 6 8			6.6	38.5	27.9	68.8	10.4 1.6 14.1	34.1 16.7 29.6
1/18 AM	5	2 4	-52.3	-73.6					-57.2 -62.2	-95.1 -116.5
1/18 PM	7	2 4 6 8	-34.0	-14.0	-79.6	-92.2	-80.4	-93.5	-69.1 -104.3 -116.3 -121.2	-74.0 -134.0 -154.2 -175.7
1/20 AM	9	2 4	-53.6	62.4					-29.4 -5.3	27.4 -7.7
1/20 PM	11	2 4 6 8	19.1	48.2	-114.5	-25.2	-59.0	-42.5	-51.2 -121.5 -152.8 -128.6	-15.0 -78.1 -96.0 -131.1
1/27 AM	21	2							-69.6	-42.4
1/27 PM	23	2 4 6	-23.8	-57.4			69.9	32.8	-48.7 -73.6 -145.4	-62.5 -67.7 -118.0
1/29 AM	25	2 4	21.2	44.2					26.9 32.6	38.2 32.2
1/29 PM	27	2 4 6 8	62.8	40.3	64.1	76.1	75.2	69.8	63.6 64.5 59.1 64.9	55.3 70.3 70.6 64.4
2/02 AM	29	2 4	340.2	464.5					219.9 99.5	259.3 54.2
2/02 PM	31	2 4 6 8	103.6	23.3	431.5	544.0	307.1	328.4	208.9 314.1 317.6 196.8	185.5 347.6 357.3 151.3
2/04 AM	33	2							-84.7	-75.6
2/04 PM	35	2 4 6	21.5	2.4			16.5	73.5	-19.9 -61.4 -100.3	-16.9 -36.3 -91.2
2/06 AM	37	2 4	26.0	83.6					-79.2 -184.4	-86.1 -255.8
2/06 PM	39	2 4 6 8	105.6	136.7	285.2	401.8	292.1	373.9	86.9 68.2 -43.7 -148.7	113.8 90.9 -50.6 -220.0
2/10 AM	41	2 4	218.7	158.6					182.2 145.8	182.2 205.8
2/10 PM	43	2 6 8							156.8 191.1 154.7	153.3 191.1 214.8
2/12 AM	45	4							-4.1	-49.6
2/12 PM	47	4 8			-29.9	-11.6			7.9 45.7	-5.7 0.3

TABLE 8-3
AVERAGE RESIDUAL DEFLECTION ERRORS (meters)
FOR PREDICTION EXPERIMENTS

(a) CRAM persistence vs. Ft. Huachuca persistence

	Lag (τ)				All lags
	2	4	6	8	
CRAM	86.3	81.5	125.3	109.3	95.2
Ft. Huachuca	88.9	95.7	127.3	123.4	103.4
No. of cases	17	17	9	8	51

(b) Trend extrapolation vs. persistence

	$\tau = 2$		$\tau = 4$		$\tau = 4$	
	Extrap. (2T)	Persist.	Extrap. (4T)	Persist.	Extrap. (2T)	Persist.
CRAM	77.4	82.6	144.5	98.7	116.0	102.3
Ft. Huachuca	87.5	88.5	169.9	108.7	135.4	107.4
No. of cases	14	14	7	7	8	8

(c) 2T ($\tau = 4$) vs. 4T

	2T	4T	Persist.
CRAM	140.3	163.6	113.7
Ft. Huachuca	162.8	196.3	125.8
No. of cases	6	6	6

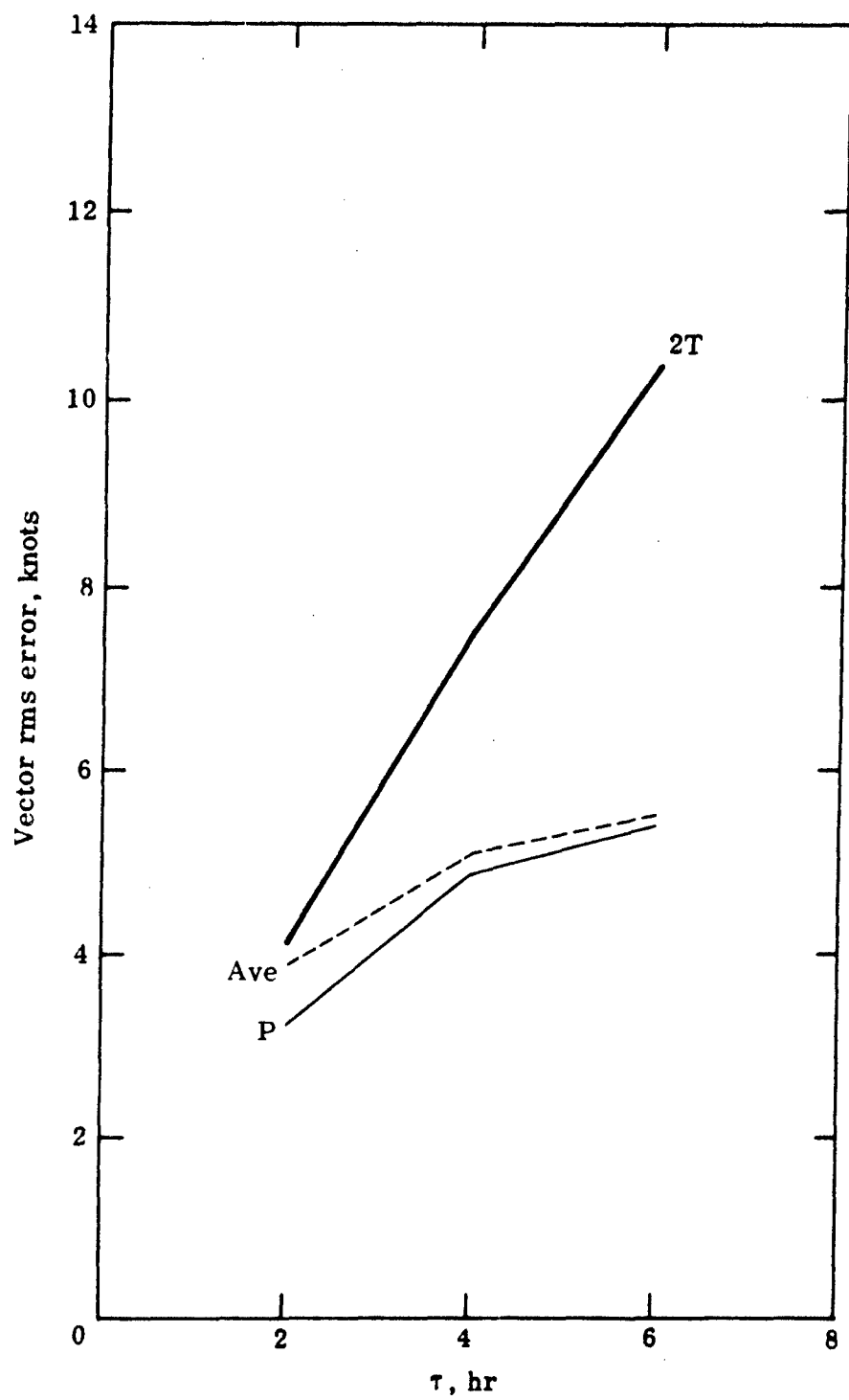


Fig. 8-1. Ballistic wind prediction verification,
Line 2.

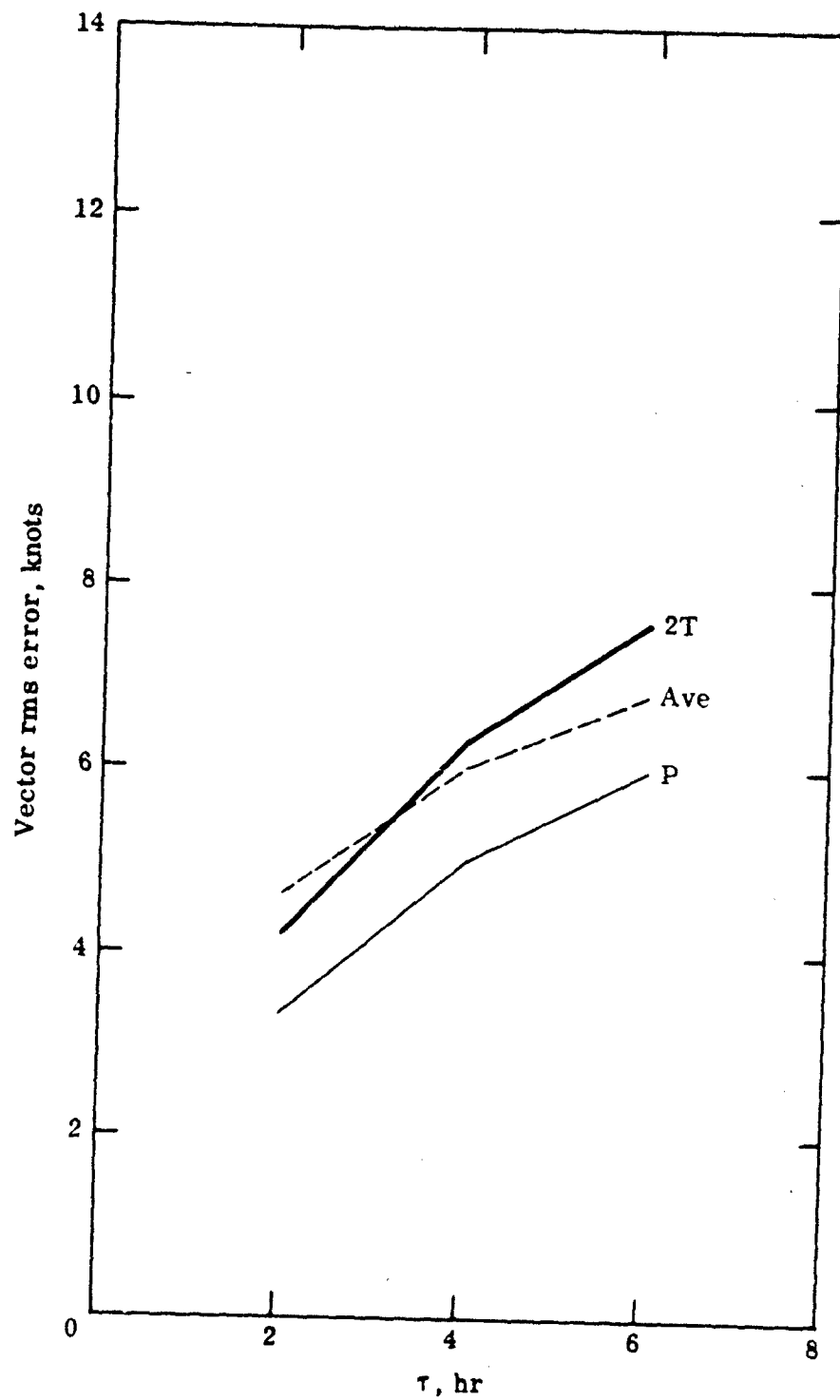


Fig. 8-2. Ballistic wind prediction verification,
Line 4.

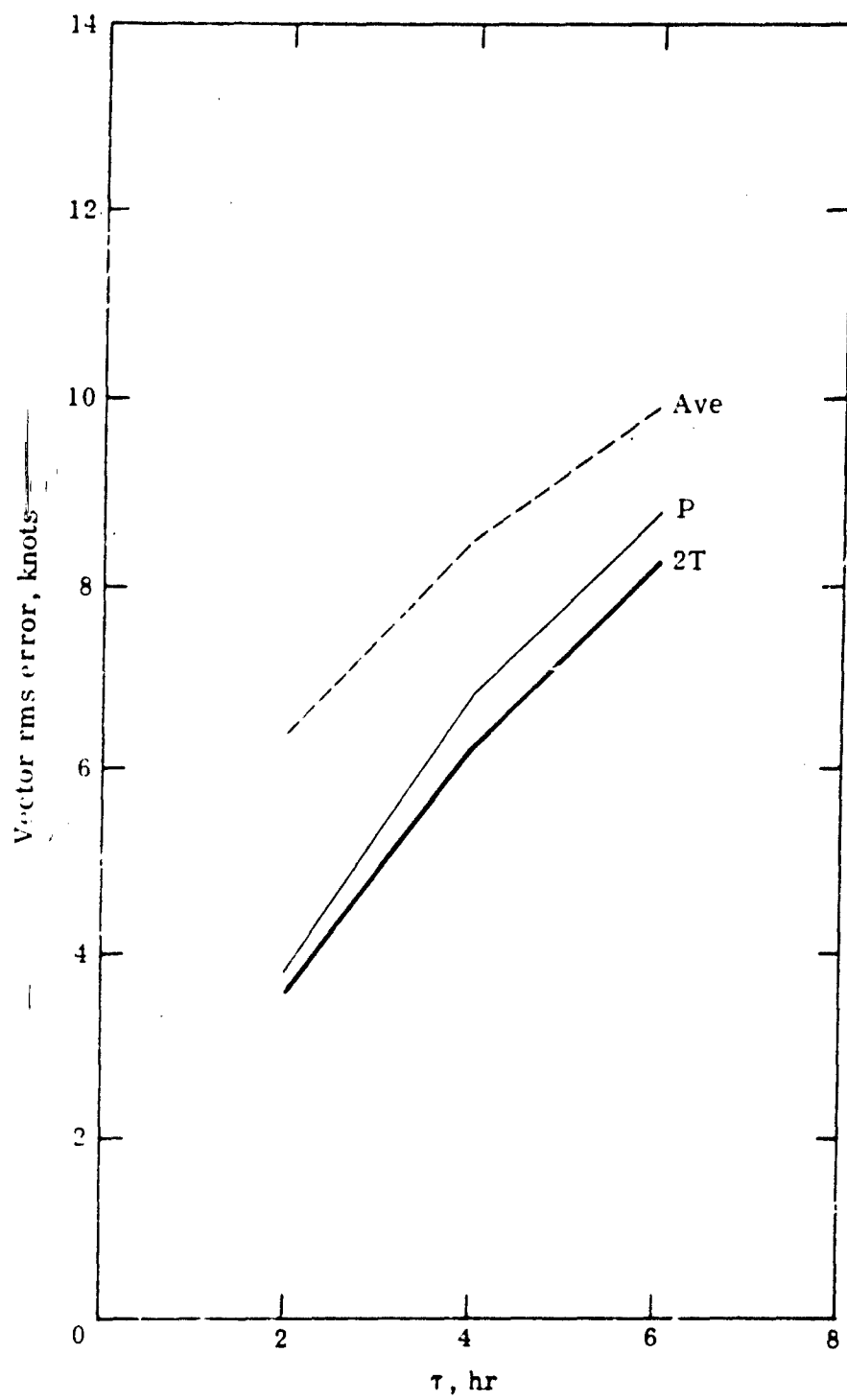


Fig. 8-3. Ballistic wind prediction verification,
Line 6.

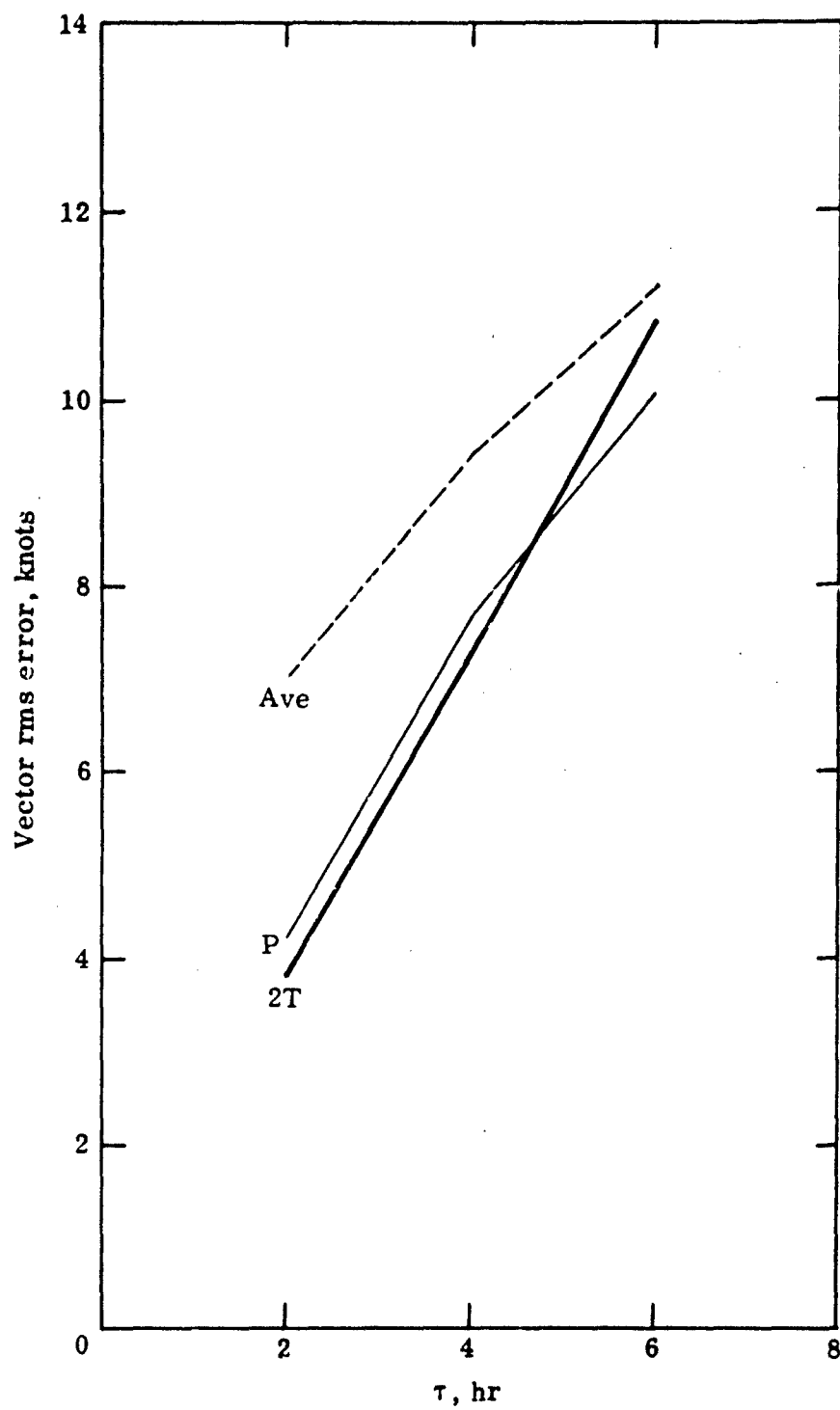


Fig. 8-4. Ballistic wind prediction verification,
Line 8.

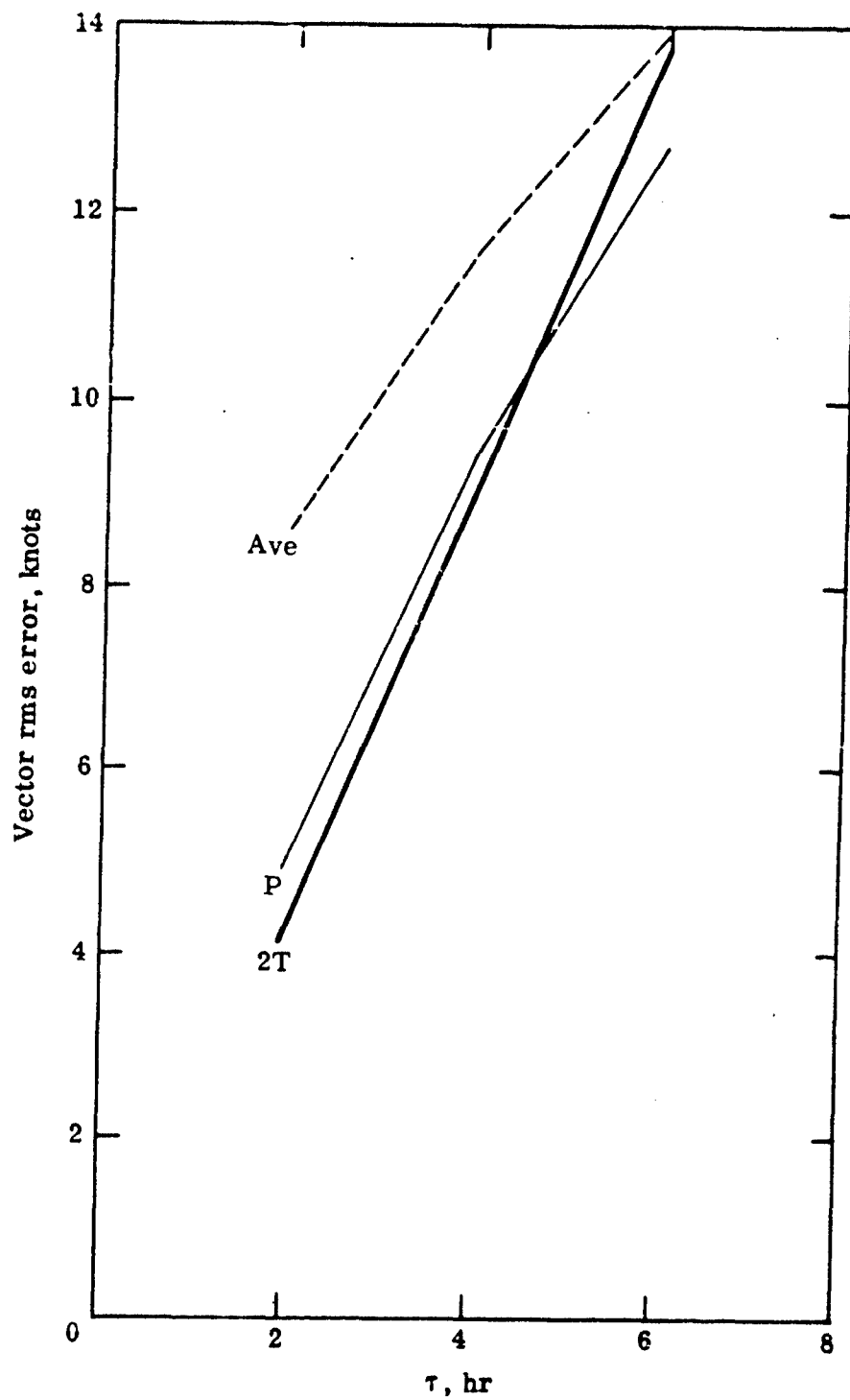


Fig. 8-5. Ballistic wind prediction verification,
Line 10.

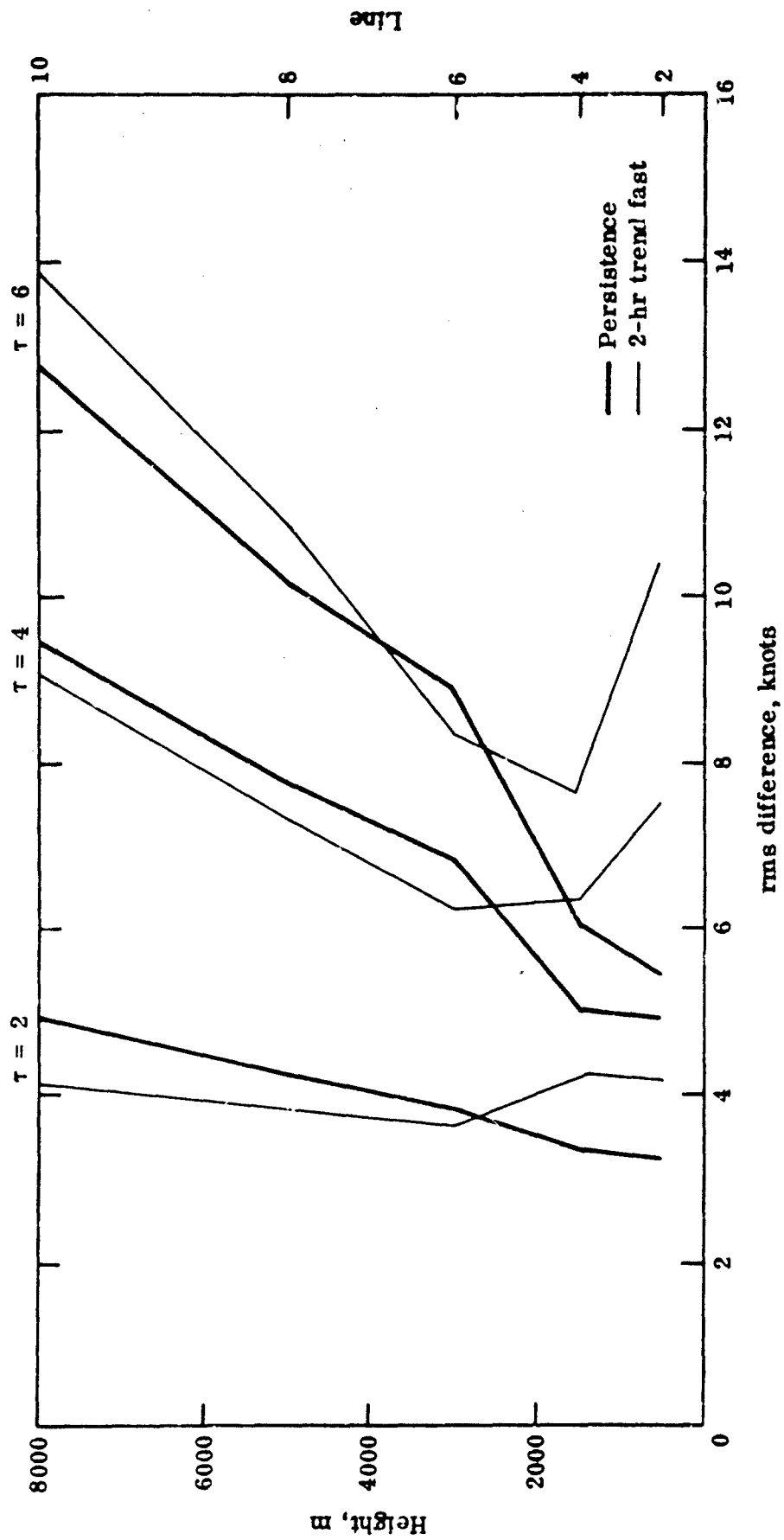


Fig. 8-6. Vertical profile ballistic wind vector errors.

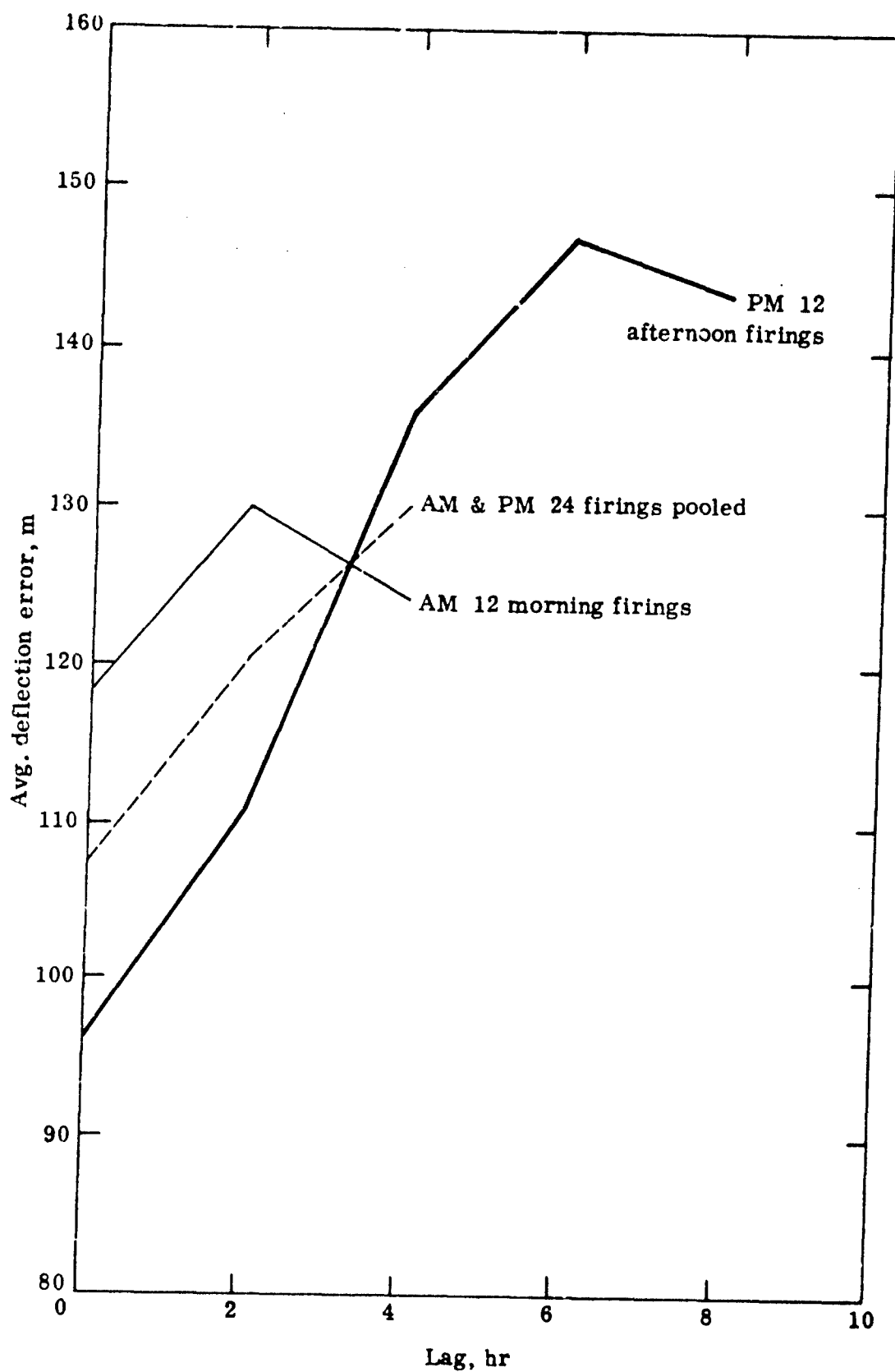


Fig. 8-7. Average residual deflection errors based on CRAM persistence.

9.0 CONCLUSIONS AND RECOMMENDATIONS

The objective analysis technique chosen for this study, CRAM, was well suited for the problem at hand (i.e., development of techniques for correction of artillery firings), and produced analyses which gave a reasonable representation of the wind, temperature, and density fields from a mesonetwork of twelve rawinsonde stations. The analyses that were generated had the desirable characteristics expected of map winds, i.e., relatively smooth contour patterns which varied slowly with time. The application of the method to three dimensions was a straightforward extension of existing two dimensional CRAM programs, with minor modifications.

When applied to the artillery firing situations from the field experiment, meteorological parameters derived from CRAM yielded smaller residual deflection errors on the average than did the parameters from the single-station radiosonde flight (Ft. Huachuca). The average deflection error for CRAM was 75.2 m and for Ft. Huachuca it was 85.1 m, based on 19 firings. The average range error for CRAM was also about 10 m lower than Ft. Huachuca, although the absolute magnitude of the errors was subject to question due to a possible bias in the firing data.

Time and space variability studies were conducted to study the effect of mountainous terrain on the variability of ballistic winds. The time variability studies indicated that the map winds derived by CRAM gave smaller rms time differences than did the single sounding winds. The rms differences at Line 10 using CRAM were as much as two knots less than the Ft. Huachuca single sounding rms differences. The same was generally true for the lower lines. This implies less decay with time of map winds than single sounding winds. The Line 10 rms component differences at the trajectory midpoint increase from about 3-4 knots for 2-hr lags to 10-12 knots for 8-hr lags. This is more rapid than the $\sigma = 2t^{1/2}$ formula would predict. This variation does not appear to be significantly affected by change of sample size with lag. Differences are greater than 5 knots for a 4-hr lag. Line 4 field-average rms components differences increase from about 2 knots at 2-hr lag to about 5-6 knots at 8-hr lag and fit $\sigma = 2t^{1/2}$ well. The horizontal range of time variability is small at Line 10 but is larger at Line 2 and is apparently topographically caused. For a 2-hr lag the spatial range is about 1/2 knot at Line 10 and about one knot at Line 2. The vertical range of the time variability is large. There is a general increase in variability with height, except from Line 2

to 4, that appears to be caused by topography.

The space variability studies suggest that in a situation where several observations are somewhat removed from the firing site and they represent the only available source of ballistic wind information, an objective analysis (i.e., CRAM) will produce a superior ballistic wind estimate than any of the observations considered individually.

It was also noted that there was a significant difference in the u-component of the Line-10 ballistic wind between Benson and Tombstone when the winds were above 15 knots, with the Tombstone u-component averaging 7.7 knots stronger than Benson's. For these situations it was found from the balloon trajectories that the Benson-launched balloons at Zone 10 were located over mountainous terrain while the Tombstone balloons were usually over relatively flat terrain for the same zone. The magnitude of the Line-10 ballistic wind from the Tombstone observation was also 4.5 knots stronger on the average than the Ft. Huachuca observation.

Spatial differences at low levels (i.e., Line 2) were also attributed to terrain. Differences in the v-component toward the northeast were smaller than for the same distances toward the more mountainous terrain south and west of the firing site.

In determining the optimum station placement, consideration should be given, when possible, to the wind climatology of an area. For example, more observing sites upstream from a firing range and fewer downstream would allow for a more favorable spatial distribution of balloons when they reach the higher zones, e.g., Zone 10.

Of particular importance is the question of how accurately and for what duration can map winds be forecast. The predictability experiments demonstrated that a simple trend extrapolation at or near the trajectory midpoint will not, in general, produce ballistic wind superior to that obtained with persistence. However, for a 2-hr lag, the trend extrapolation does give smaller residual deflection errors than persistence. For 14 cases the average residual deflection error was 77.4 m for a 2-hr prediction, while it was 82.6 m using CRAM persistence and 88.5 m using Ft. Huachuca persistence. The comparison between CRAM persistence and Ft. Huachuca persistence showed that the CRAM persistence yielded smaller average residual deflection errors than Ft. Huachuca for all lags tested (2, 4, 6, 8 hr). The time decay characteristics of the deflection errors based on CRAM persistence showed an average error of 107.1 m

for zero lag, 120.4 m for a 2-hr lag, 130.1 m for a 4-hr lag, 146.9 m for a 6-hr lag, and 143.2 m for an 8-hr lag.

Many of the conclusions discussed above are of a tentative nature. There are several areas in which additional investigation should be carried out using the data that have already been edited, error checked, and put on magnetic tape for input to the analysis program. For example, more withheld data experiments could be conducted for much less effort relative to the magnitude of the data editing effort that has been completed.

Some of the various options and parameters associated with the CRAM program should be tested further. Alternate techniques for formulating the all-important initial-guess field, such as use of a prognosis, could lead to significant improvements in determining ballistic winds.

The problem of predictability needs more extensive investigation. A simple approach of trend extrapolation was only successful for a 2-hr lag. The prediction technique described in this report made no distinction among the various zones but rather extrapolated the entire line. Additional experiments could be tried in which the higher zones might be handled differently than the lower ones. The results of the time variability studies showed that the variability in the low levels was much smaller than the high levels.

An alternate method for predicting the higher zone winds could be by incorporation of prognoses from existing mid-tropospheric NWP models. Still another possible approach is to consider both space and time in extrapolating the winds. Consideration was limited to only time extrapolation in the present study.

10.0 REFERENCES

Bellucci, R., 1961: Analysis of ballistic meteorological effects on artillery fire. USASRDL Technical Report 2224, U.S. Army Signal Corps Research and Development Laboratory, Fort Monmouth, N. J.

Carstensen, L. P., 1962: Progress report. Fleet Numerical Weather Facility, U.S. Naval Postgraduate School, Monterey, Calif.

Fujita, T., and H. A. Brown, 1960: Design of a three-dimensional meso-meteorological network. Fourth Quarterly Technical Report, Signal Corps Contract No. DA-36-039 SC-78901, Department of Meteorology, University of Chicago.

Lowenthal, M. J., 1953: Use of map winds for artillery purposes, Part I. Technical Memorandum No. M-1535, U.S. Army Signal Corps Engineering Laboratories, Fort Monmouth, N. J.

—, 1957: Use of map winds for artillery purposes, Part II. Technical Memorandum No. M-1901, U.S. Army Signal Corps Engineering Laboratories, Fort Monmouth, N. J.

Thomasell, A., and J. G. Welsh, 1963: Studies of techniques for the analysis and prediction of temperature in the ocean, Part I: The objective analysis of sea-surface temperature Technical Report 7046-70, The Travelers Research Center, Inc.

Wadsworth, G. P., and J. G. Bryan, 1960: Introduction to probability and random variables. pp. 255f, McGraw Hill, New York, N. Y.

APPENDIX

SYNOPTIC SITUATIONS FOR
DAYS OF BALLISTIC WIND ANALYSES

APPENDIX. SYNOPTIC SITUATIONS FOR DAYS OF BALLISTIC WIND ANALYSES

Jan. 12, 1965

At sea level, a large nearly stationary high located over eastern Oregon influenced the surface winds and sky cover in southeastern Arizona. At 0500 MST, one hour prior to the first radiosonde flight for the small network of stations in southeastern Arizona, there were only scattered clouds, light southeasterly winds and temperatures in the low 40's (°F). Temperatures warmed to the low 60's by 1400 under partly cloudy skies and nearly calm surface winds. At upper levels, a weak trough was oriented northeast-southwest from southern Nevada to off the south California coast at 0600, resulting in west to southwest winds aloft with speeds about 30 knots at the 500-mb level.

Jan. 14, 1965

The sea-level pressure pattern changed little from that of Jan. 12. The high over eastern Oregon moved very slowly to northern Nevada and strengthened. At 0500 MST the surface temperature was 37°F at Ft. Huachuca, with considerable high cloudiness and no wind. The temperature climbed to the middle 60's by early afternoon and conditions remained nearly calm under high clouds that allowed sunshine through (some occasional very light winds from the east-southeast were reported). In the lower and mid troposphere, a ridge line was located on a northwest-southeast line from a high center off the Oregon coast to southeastern Arizona. Thus, the winds were very light and variable from the surface to the mid troposphere (20,000 ft) and only increased slightly at the 30,000-ft level.

Jan. 16, 1965

The high pressure system over the western states on the 12th and 14th remained strong and moved only to Idaho on the 16th. Gradient flow in the low levels over southeast Arizona was generally from the east, but a north-northeast wind at 10 knots was reported at Ft. Huachuca at 0500 MST with a temperature of 45°F under cloudy skies (high clouds). Afternoon temperatures rose to the mid 60's near Ft. Huachuca, but farther west, near Tucson, temperatures were around 75°F.

At upper levels, a strong high was centered almost directly over the sea-level high in Idaho with a ridge line southeastward over southeastern Arizona causing light

and variable winds at all levels to 30,000 ft.

Jan. 18, 1965

The western U.S. continued to be dominated by a large high-pressure system centered in Idaho, resulting in generally fair skies over south-eastern Arizona all day. Winds at the surface remained nearly calm at Ft. Huachuca for both the 1000 and 1400 firings, while temperatures climbed rapidly from the mid 30's at 0600 and 0800 to the mid 70's by the 1400 firing.

At upper levels, a ridge line was noted from western Montana southward to central Arizona, this ridge caused relatively light north to northwesterly winds over the firing area during the early morning. The winds gradually backed to more westerly as a weak trough moved eastward across the west central states during the day.

Jan. 20, 1965

The high pressure system centered over Idaho for 5 days was still there, but had weakened considerably and a trough formed from central Arizona northwestward. Some showers and thunderstorms occurred along the trough line but none was observed at Ft. Huachuca through the day to the 1400 firing time. Temperatures ranged from the upper 40's to around 60°F under mostly cloudy skies, and surface winds were south-southwest around 10 mph after a period of calm from about 0500 to 0800.

At upper levels a weak low was moving southeastward along the California/Arizona border during the day, causing southwesterly winds about 20 knots at 18,000 ft by 1400 MST.

Jan. 22, 1965

Southeastern Arizona was under the influence of a high-pressure system located over Idaho and Nevada. Once again surface winds were very light or calm and skies were only partly cloudy. Temperatures in the low 30's at 0600 rose to the mid 50's by the 1400 firing time.

At levels above the surface a deepening trough located over eastern New Mexico and western Texas caused northwesterly winds over southeastern Arizona that increased from 20—30 knots at about 10,000 ft above sea level to 50—60 knots at 18,000 ft and probably higher at 30,000 ft.

At 850 mb (just above the surface of the firing site) the winds were west-northwest at 5—15 knots.

Jan. 25, 1965

Southeastern Arizona was dominated by the circulation around an intense developing low in the southern plains states and a large high-pressure system off the California coast. Surface winds at Ft. Huachuca which were light at 0500 MST increased by 0800 and the sky was obscured by blowing sand at that time. Temperatures ranged from an early morning low around 35 to a high of about 50 at the 1400 firing time. Skies were mostly clear after the 0800 sand storm.

At upper levels, a strong trough was located east of the region and was moving eastward at about 25 knots. This trough caused strong northwesterly winds above the Ft. Huachuca area that were around 100 knots at the 30,000-ft level and nearly 100 knots as low as 20,000 ft at 0500 MST.

Jan. 27, 1965

A strong high-pressure system moved in from the Pacific Ocean and was centered over the eastern Arizona/Utah border during the day, dominating the weather over southeastern Arizona with clear skies and calm, or occasionally light easterly surface winds. Temperatures ranged from around 25°F at 0800 MST to the low 40's by the 1400 firing time.

A trough was located from Central Oklahoma to northern Mexico at upper levels resulting in north-northwesterly winds that increased with elevation to around 40 knots at 18,000 ft and probably stronger at 25—30 thousand ft at 0500 MST. The winds diminished somewhat toward mid-afternoon as the trough moved farther from the area.

Jan. 29, 1965

A ridge of high pressure extended southeastward from a high center in western Nevada to the Ft. Huachuca area. The influence of ridge conditions resulted in clear to partly cloudy skies, calm wind conditions, and a wide temperature range from 24°F at 0800 MST to 65°F at 1400 MST.

At upper levels, southeastern Arizona was in a "col" area with generally light winds mostly from a northerly direction.

Jan. 31, 1965

A very weak high system was centered over Arizona causing partly cloudy to clear sky conditions, little or no wind at the surface, and a temperature range from the low 30's at the time of the 0600 and 0800 radiosonde flights to near 70°F by 1400 MST.

At upper levels, westerly winds increased with increasing height and were gradually shifting to more northwesterly through the day and strengthening. Speeds were about 25 to 35 knots at 0500 MST at about 18,00 ft and had increased to 40 knots at the level by 1700 MST.

Feb. 2, 1965

Throughout the day a stationary front lay in an east-west line across Northern Arizona with only a weak pressure gradient over southeastern Arizona. Thus, winds were light and variable at the surface and skies were generally cloudy due to the proximity of the front. The temperature range was rather small from around 50°F at 0500 to the low 60's by the 1400 firing time.

At upper levels a weak low was centered southwest of Arizona just off the south Pacific coast of North America and a ridge was located over California. Winds were quite light at levels up to about 20,000 ft.

Feb. 4, 1965

Ridge conditions at both the surface and aloft prevailed over Arizona all day, with winds generally calm at the surface and light northeasterly aloft. Temperatures ranged from near 30°F at 0800 MST to the mid 60's by 1400 MST.

Feb. 6, 1965

During the day, a developing low-pressure system was moving southward through eastern Nevada with an active cold front extending southward from the low center through southeastern California and off the Pacific coast. Showers along the front were advancing eastward across Arizona, but had not yet reached the Ft. Huachuca area by the 1400 firing time. Skies were mostly cloudy through the day near Ft. Huachuca and surface winds were increasing from the south. The temperature ranged from the upper 40's at 0600 MST to the upper 50's in the early afternoon.

At 0500 MST an upper-level trough extended southward from central Oregon to off

the central California coast. This trough progressed slowly eastward during the day and caused upper-level winds over southern Arizona to be from the west-southwest, and later to be from the southwest with increasing speed. Speeds at about 18,000 ft ranged from 40 knots at 0500 MST to about 60 knots during the afternoon. Very likely the winds increased with elevation above 18,000 ft.

Feb. 8, 1965

A high centered over Nevada dominated the weather over the southwestern U.S. Winds at the surface were light and variable or calm all day and skies were partly cloudy. Temperatures ranged from a low around freezing at 0500 MST to near 50°F in the early afternoon.

At upper levels a closed low was centered just north of Tucson at 0500 MST, moving slowly eastward during the day. Winds were probably from the southwest ahead of the low during the morning, but were in the process of shifting during the day as the low passed just to the north of Ft. Huachuca. Speeds ranged from 20–35 knots at the 18,000-ft level.

Feb. 10, 1965

A large sprawling trough of low pressure with several centers was located to the north and east of the Ft. Huachuca area over Utah and New Mexico during most of the day. In the morning hours, 0600 to 1200, the surface winds were northerly at 5–10 knots, but backed to west-southwest in the afternoon and increased to 15–20 knots. Temperature range during the day was from 28°F at 0500 MST to the low 40's during the afternoon.

An intense upper-level low had moved south-southeastward into northern Arizona by 0500, but it then turned east-northeastward during the next 12 hours. As a result, winds were quite strong (80–90 knots at about 18,000 ft) throughout the day, generally from a westerly direction. Wind speeds undoubtedly increased with elevation and were probably around 100 knots near the 30,000-ft level.

Feb. 12, 1965

A large ridge of high pressure dominated the entire western quarter of the U.S. (including Arizona) through the day. Skies were nearly clear over the Ft. Huachuca

area and calm conditions at 0600 and 0800 gave way to west-northwest surface winds of 5—10 knots for the 1000 and 1400 firings. Temperatures ranged from a low of 15°F at 0600 and 0800 to the low 40's by 1400.

At levels above the surface, a rather strong ridge of high pressure that extended in an arc from western Canada to off the central California coast resulted in north-westerly flow over the Ft. Huachuca area. Speeds increased with elevation to 35—45 knots at 18,000 ft and probably continued increasing to the 30,000-ft level.

Security Classification

DOCUMENT CONTROL DATA - R&D

(Security classification of title, body of abstract and indexing annotation must be entered when the overall report is classified)

1 ORIGINATING ACTIVITY (Corporate author) The Travelers Research Center, Inc. 250 Constitution Plaza Hartford, Connecticut 06103		2a. REPORT SECURITY CLASSIFICATION Unclassified
		2b. GROUP n/a
3 REPORT TITLE BALLISTIC WINDS STUDY		
4 DESCRIPTIVE NOTES (Type of report and inclusive dates) Final Report No. 4. 1 June 1965 to 30 June 1966		
5 AUTHOR(S) (Last name, first name, initial) Ostby, Frederick P. Veigas, Keith W. Pandolfo, Joseph P. Spiegler, David B.		
6 REPORT DATE October 1966	7a. TOTAL NO. OF PAGES 153	7b. NO. OF REFS 7
8a. CONTRACT OR GRANT NO. DA 28-043 AMC-01377(E)	9a. ORIGINATOR'S REPORT NUMBER(S) 7472-225	
b. PROJECT NO. 1VO-25001-A-126-01	9b. OTHER REPORT NO(S) (Any other numbers that may be assigned this report) ECOM-01377-F	
10. AVAILABILITY/LIMITATION NOTICES Distribution of this Document is unlimited.		
11. SUPPLEMENTARY NOTES None	12. SPONSORING MILITARY ACTIVITY U.S. Army Electronics Command, AMSEL-BL-AP Fort Monmouth, New Jersey 07703	
13 ABSTRACT <p>A three-dimensional objective analysis technique known as CRAM (Conditional Relaxation Analysis Method) was applied to investigate various properties of ballistic winds on a mesoscale in mountainous regions. From a 12-day sample of upper-air soundings taken 5 times a day at 2-hr intervals for 12 rawinsonde stations in the Ft. Huachuca region of southeastern Arizona, and artillery firings taken twice a day, CRAM analyses of temperature, density, and winds were performed for 10 atmospheric zones between the surface and 8,000 m using an IBM-7094.</p> <p>It was determined that the CRAM technique produced fields which had the desirable features of map winds, i.e., the contour patterns were relatively smooth and varied slowly with time. The residual deflection errors which resulted were smaller for CRAM (75.2 m) than for a single station (Ft. Huachuca) near the firing range (85.1 m). It was also found that the time decay of ballistic winds in the firing area was smaller using CRAM than using the Ft. Huachuca observation, which implies that CRAM is a better tool with which to make a persistence forecast than a single station.</p>		

24

KEY WORDS

LINK A

LINK ID

LINK C

ROLE

AC, E

WT

ROLE

WT

Ballistic Winds
Forecasting Technique
Mapping Technique

INSTRUCTIONS

1. **ORIGINATING ACTIVITY:** Enter the name and address of the contractor, subcontractor, grantee, Department of Defense activity or other organization (*corporate author*) issuing the report.

- 2a. **REPORT SECURITY CLASSIFICATION:** Enter the overall security classification of the report. Indicate whether "Restricted Data" is included. Marking is to be in accordance with appropriate security regulations.

- 2b. GROUP: Automatic downgrading is specified in DoD Directive 5200.10 and Armed Forces Industrial Manual. Enter the group number. Also, when applicable, show that optional markings have been used for Group 3 and Group 4 as authorized.

2. **REPORT TITLE:** Enter the complete report title in all capital letters. Titles in all cases should be unclassified. If a meaningful title cannot be selected without classification, show title classification in all capitals in parenthesis immediately following the title.

4. **DESCRIPTIVE NOTES:** If appropriate, enter the type of report, e.g., interim, progress, summary, annual, or final. Give the inclusive dates when a specific reporting period is covered.

3. **AUTHOR(S):** Enter the name(s) of author(s) as shown on r in the report. Enter last name, first name, middle initial. If military, show rank and branch of service. The name of the principal author is an absolute minimum requirement.

- REPORT DATE:** Enter the date of the report as day, month, year, or month, year. If more than one date appears in the report, use date of publication.

- a. **TOTAL NUMBER OF PAGES:** The total page count should follow normal pagination procedures, i.e., enter the number of pages containing information.

5. NUMBER OF REFERENCES: Enter the total number of references cited in the report.

3. **CONTRACT OR GRANT NUMBER:** If appropriate, enter the applicable number of the contract or grant under which the report was written.

- 7, 8c, & 8d. **PROJECT NUMBER:** Enter the appropriate military department identification, such as project number, subproject number, system numbers, task number, etc.

1. **ORIGINATOR'S REPORT NUMBER(S):** Enter the official report number by which the document will be identified and controlled by the originating activity. This number must be unique to this report.

5. OTHER REPORT NUMBER(S): If the report has been assigned any other report numbers (either by the originator or by the sponsor), also enter this number(s).

10. AVAILABILITY/LIMITATION NOTICES: Enter any limitations on further dissemination of the report, other than those imposed by security classification, using standard statements such as:

- (1) "Qualified requesters may obtain copies of this report from DDC."
- (2) "Foreign announcement and dissemination of this report by DDC is not authorized."
- (3) "U. S. Government agencies may obtain copies of this report directly from DDC. Other qualified DDC users shall request through _____."
- (4) "U. S. military agencies may obtain copies of this report directly from DDC. Other qualified users shall request through _____."
- (5) "All distribution of this report is controlled. Qualified DDC users shall request through _____."

If the report has been furnished to the Office of Technical Services, Department of Commerce, for sale to the public, indicate this fact and enter the price, if known.

11. SUPPLEMENTARY NOTES: Use for additional explanatory notes.

12. **SPONSORING MILITARY ACTIVITY:** Enter the name of the departmental project office or laboratory sponsoring (paying for) the research and development. Include address.

13. **ABSTRACT:** Enter an abstract giving a brief and factual summary of the document indicative of the report, even though it may also appear elsewhere in the body of the technical report. If additional space is required, a continuation sheet shall be attached.

It is highly desirable that the abstract of classified reports be unclassified. Each paragraph of the abstract shall end with an indication of the military security classification of the information in the paragraph, represented as (TS), (S), (C), or (U).

There is no limitation on the length of the abstract. However, the suggested length is from 150 to 225 words.

- 14. KEY WORDS.** Key words are technically meaningful terms or short phrases that characterize a report and may be used as index entries for cataloging the report. Key words must be selected so that no security classification is required. Identifiers, such as equipment model designation, trade name, military project code name, geographic location, may be used as key words but will be followed by an indication of technical context. The assignment of links, rules, and weights is optional.